AD-A034 217 NAVAL WEAPONS CENTER CHINA LAKE CALIF F/G 1/3
BASELINE DATA FROM AN A-4 COCKPIT IN SIMULATED CARRIER DECK FIR--ETC(U)
AUG 76 A SAN MIGUEL
UNCLASSIFIED NWC-TP-5812 NL

1 OF 2
AD
A034217

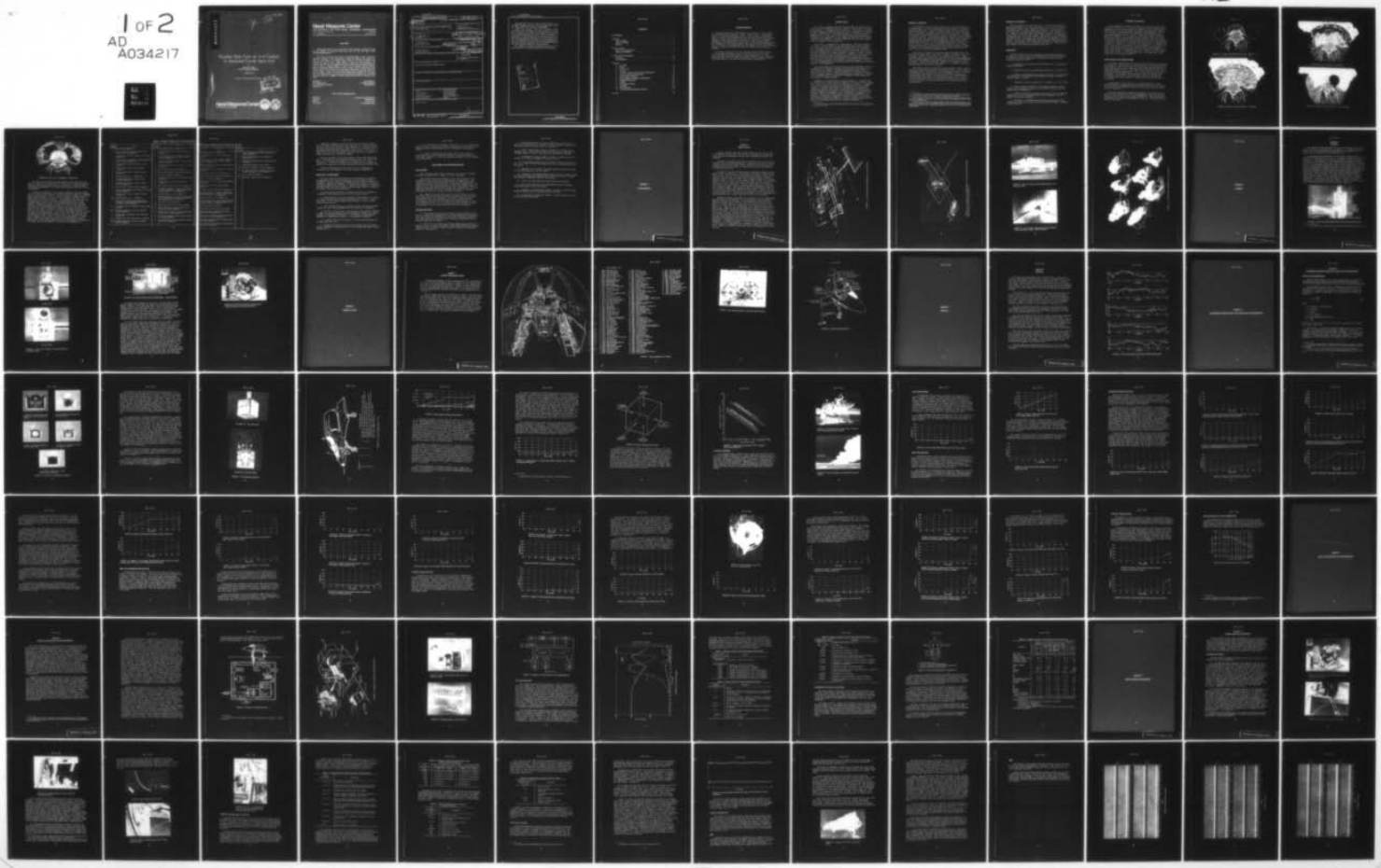

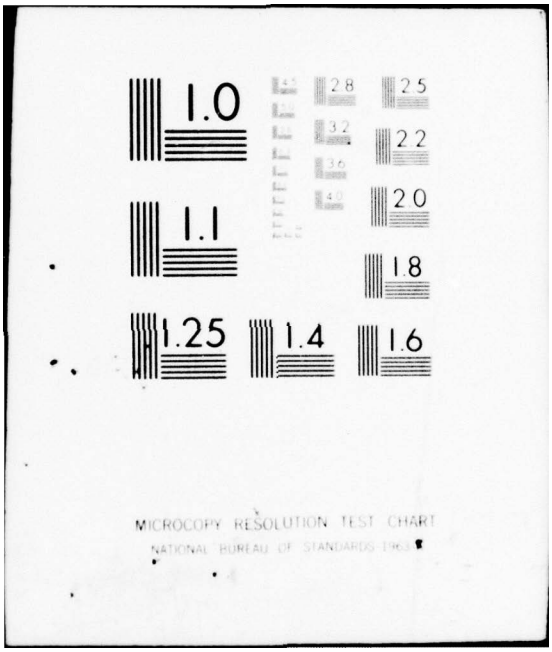
1.0
1.1
1.25
1.4
1.6
2.8
2.5
3.2
2.2
3.6
2.0
4.0
1.8
MICROCOPY RESOLUTION TEST CHART
NATIONAL BUREAU OF STANDARDS 1963

NWC TP 5812

12

Baseline Data From an A-4 Cockpit in Simulated Carrier Deck Fire

by
Anthony San Miguel
Systems Development Department

AUGUST 1976

Naval Weapons Center
CHINA LAKE, CALIFORNIA 93555

Naval Weapons Center

AN ACTIVITY OF THE NAVAL MATERIAL COMMAND

R. G. Freeman, III, RAdm., USN ..... Commander
G. L. Hollingsworth ..... Technical Director

FOREWORD

Baseline response behavior of an unarmed Navy A-4 cockpit engulfed by a simulated carrier deck fire was acquired and characterized during fiscal years 1975 and 1976 under AirTask A03P-03Pa/008c/6WSL33-001.

Draft copies of this report were reviewed by the following people: Dr. John A. Parker, Dr. Domenick E. Cagliostro, and Dr. Narcinda Lerner of NASA, Ames Research Center, Moffett Field, Calif.; Dr. Alfred Buchler of the National Research Council; Dr. Wei Young of California State University, San Jose; Dr. Carlos J. Hilado, Kathleen Y. Smouse, and Colette Slattengren of the University of San Francisco; Dr. Stan Martin and Ray Algers of Stanford Research Institute, Menlo Park, Calif.; Dr. Robert F. Landel and Clifford D. Coulbert of the Jet Propulsion Laboratory, California Institute of Technology, Pasadena; Richard W. Bricker of NASA, Lyndon B. Johnson Space Center, Houston, Texas; Dr. Irvin N. Einhorn of the Flammability Research Center, University of Utah, Salt Lake City; CDR L. J. Jenkins of the Naval Medical Research Institute, Bethesda, Md.; and Thomas Horeff and William McGuire of the Federal Aviation Administration, Washington, D.C. Their highly constructive comments and suggestions are greatly appreciated and have been incorporated into the report.

Released by
M. M. ROGERS, *Head*
Systems Development Department
28 July 1976

Under authority of
G. L. HOLLINGSWORTH
Technical Director

NWC Technical Publication 5812

Published by ..... Technical Information Department
Manuscript 5362/MS 76-133
Collation ..... Cover, 82 leaves
First printing ..... 115 unnumbered copies

UNCLASSIFIED

SECURITY CLASSIFICATION OF THIS PAGE (When Data Entered)

REPORT DOCUMENTATION PAGE

READ INSTRUCTIONS BEFORE COMPLETING FORM

1. REPORT NUMBER: NWC-TP-5812	2. GOVT ACCESSION NO.
3. RECIPIENT'S CATALOG NUMBER	
4. TITLE (and Subtitle): BASELINE DATA FROM AN A-4 COCKPIT IN SIMULATED CARRIER DECK FIRE	5. TYPE OF REPORT & PERIOD COVERED: Carrier fire study; Fiscal years 1975–1976
	6. PERFORMING ORG. REPORT NUMBER
7. AUTHOR(s): Anthony San Miguel	8. CONTRACT OR GRANT NUMBER(s): Technical publication FY 1975-1976,
9. PERFORMING ORGANIZATION NAME AND ADDRESS: Naval Weapons Center, China Lake, Calif. 93555	10. PROGRAM ELEMENT, PROJECT, TASK AREA & WORK UNIT NUMBERS: AirTask A03P-03Pa/008c/6WSL33001
11. CONTROLLING OFFICE NAME AND ADDRESS: Naval Weapons Center, China Lake, Calif. 93555	12. REPORT DATE: August 1976
	13. NUMBER OF PAGES: ~~162~~ 12 145p.
14. MONITORING AGENCY NAME & ADDRESS (if different from Controlling Office)	15. SECURITY CLASS. (of this report): UNCLASSIFIED
	15a. DECLASSIFICATION/DOWNGRADING SCHEDULE

16. DISTRIBUTION STATEMENT (of this Report)

Approved for public release; distribution unlimited.

17. DISTRIBUTION STATEMENT (of the abstract entered in Block 20, if different from Report)

18. SUPPLEMENTARY NOTES

19. KEY WORDS (Continue on reverse side if necessary and identify by block number)

Pool fire	Test animal behavior
Carrier deck fuel fire	Toxicity measurement
A-4 cockpit fire	Smoke measurement
Temperature measurement	A-4 structural degradation
Heat flux measurement	Manikin

20. ABSTRACT (Continue on reverse side if necessary and identify by block number)

See back of form.

DD FORM 1 JAN 73 1473 EDITION OF 1 NOV 65 IS OBSOLETE S/N 0102-014-6601

UNCLASSIFIED

SECURITY CLASSIFICATION OF THIS PAGE (When Data Entered)

(U) *Baseline Data From an A-4 Cockpit in Simulated Carrier Deck Fire*, by Anthony San Miguel. China Lake, Calif., Naval Weapons Center, August 1976. 162 pp. (NWC TP 5812, publication UNCLASSIFIED.)

(U) This report describes a study that was designed to gather fundamental data on the survivability of an aircraft cockpit in a carrier deck fire, on the characteristics of cockpit structural degradation in the fire, and on various interacting mechanisms that reduce a pilot's functionability. An unarmed Navy A-4 cockpit was subjected to a simulated carrier deck pool fire. The cockpit was instrumented with transducers to measure temperature, heat, smoke, toxic gases, light, shock, sound, pressure, and physiological behavior of rats and mice. A number of appendixes to the report give detailed descriptions of the various measuring systems and the data they produced.

(U) In addition to providing much immediately useful data, the test yielded a good base of data on which to design future tests of this kind.

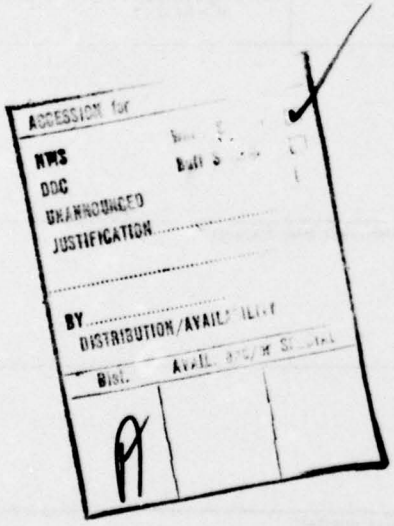

CONTENTS

ACKNOWLEDGMENT

The author gratefully acknowledges the assistance of the following Naval Weapons Center personnel: James L. Rieger, Larry L. Rollingson, and Jon A. Schmidt who designed and built the telemetry equipment and aided in the data acquisition; Marion D. Williams, Virgil R. Christenson, Joseph H. Winter, Gerald Rogers, and Eugene J. Dibble, who prepared transducers, instrumentation, and the test aircraft; Thomas Griffith, Jr., who designed and constructed glassware and helped make gas measurements; Don P. Phillips, who designed and machined modules; and Dr. Arnold Adicoff, Joseph H. Johnson, and Gerald Whitnack, who advised on chemical gas analyses.

He is also indebted to Dr. Steve Packham and Dr. Kenneth Vorhees of the Flammability Research Center, University of Utah, for their assistance with the animal and toxic gas measurements, and to Capt. D. D. Hicks and CDR R. Gibson of NAVAIR Code 03PAF, the consecutive cognizant sponsoring officers, who gave continuing guidance and support.

INTRODUCTION

This report complements NWC motion picture TMP 413[1] and describes a single baseline data-gathering test in which an unarmed Navy A-4 cockpit was subjected to a simulated carrier deck fire. The study was designed to gather fundamental and baseline data on the survivability of a manned cockpit in such a fire, on the characteristics of cockpit structural degradation in the fire, and on the various interacting mechanisms contributing to the degradation of the cockpit and hence directly reducing a pilot's functionability. The word "baseline" is used in the context of best available current information.

This report is organized for a dual purpose. The first purpose is to present a concise review of the significant study elements pursued, with appropriate reference to detailed information in the appendixes. This is accomplished by discussing the problem addressed, the methodological approach used to solve the problem, and the objectives required to be met to quantify the stated problem. A summary of results follows, substantiated by an artist's conception of significant events within the test item and a table listing the chronology of significant events measured by various types of transducers. These events and measurements are discussed at length in the various referenced appendixes. Conclusions and recommendations are then given, which are based on the extensive material in the appendixes.

The second purpose of the report is to present information that will be sufficient to eventually develop a baseline analytical model with long-term utility capable of identifying component problem areas. It should also be of use to aircraft designers in the context of survivability trade-off studies. Therefore, extensive information is provided in the appendixes with the objective of helping to better define the gray areas of a complex problem.

Appendix A is a description of the fire facility. A manikin that was placed in the pilot's position during the fire is described in Appendix B, and the A-4 cockpit layout is depicted in Appendix C. Appendix D explains the sequence of events that transpired as the fire test was conducted. Detailed descriptions of the individual data-gathering systems and the data they acquired and some analyses of the data are given in Appendixes E through K. An explanation of the techniques and equipment used to extinguish the fire is contained in Appendix L. An analysis of structural failure based on post-test examination of the aircraft is discussed in Appendix M. Finally, a report on the piggyback materials experiment conducted by the California Institute of Technology Jet Propulsion Laboratory is included as Appendix N.

---

[1] Naval Weapons Center. *Aircraft Fire Survivability*. China Lake, Calif., NWC, 1976. (Technical motion picture 413, 10-1/2 min., color, sound.)

PROBLEM ADDRESSED

A catastrophic aircraft carrier deck fire[1] can be described in the following manner. Aircraft loaded with fuel and ordnance are parked on a crowded flight deck. Some are tied down, while others are awaiting launch instructions. A weapon of either friendly or enemy origin penetrates an aircraft, starting a fuel fire on the carrier deck. Burning fuel spreads, and heat from the fire causes other weapons on the damaged aircraft to cookoff.[2] These weapons penetrate adjacent aircraft, spreading destruction over and below the flight deck. Deck crews attempt to contain the fire and keep it from spreading to other aircraft and to compartments below deck. If not contained within some 5 minutes, the fire is likely to incapacitate the strike capability of the carrier. Pilots in the aircraft are faced with split-second decisions of whether to abandon their weapon-laden aircraft, which would further feed the fire, or try to taxi them to possible safety.

This scene is typical of accidental carrier deck fires that have occurred in recent years on the U.S.S. *Oriskany* (in 1966), on the U.S.S. *Forrestal* (in 1967), and on the U.S.S. *Enterprise* (in 1969). These accidents killed 204, injured 185, destroyed 42 aircraft and damaged even more, and caused damage to the carriers that cost more than $70,000,000 to repair.[3] History also provides a number of vivid examples of the destruction caused by such fires in combat (e.g., Japanese and American carrier losses in the battle of Midway).

The armed aircraft is the primary fire propagator. Hence, data is required to quantitatively define its behavior in fire in the context of understanding how to decrease its fire-propagating potential. Although this goal can be attained in any or all of a number of ways (e.g., firefighting), this study is focused specifically on quantitatively characterizing the problems of a pilot and aircraft in such a fire.[4] The underlying goal is that the information attained in the study be useful for design trade-offs between functional performance and fire survivability.

---

[2] Naval Weapons Center. *Shrike and Sparrow Missile Baseline Cookoff Tests*, by Anthony San Miguel and P. McQuaide. China Lake, Calif., NWC, October 1974. (NWC TP 5672, publication UNCLASSIFIED.)

[3] Naval Air Systems Command. *Study of Technology Requirements for the Containment of Shipboard Aviation Fire Hazard*. Washington, D.C., NAVAIR, 1972. (Exotech Report TRSR-70-15, also available from DDC as AD 884 422, publication UNCLASSIFIED.)

[4] Anthony San Miguel. "Rocket Motor Design Considerations to Meet Fast Cookoff Requirements," in *JANAF Operational Serviceability and Structures and Mechanical Behavior Working Groups Combined Annual Meeting*. Silver Spring, Md., Johns Hopkins University, Applied Physics Laboratory, May 1975. Pp. 399-415. (CPIA publication 264, UNCLASSIFIED.)

APPROACH TO PROBLEM

The basic approach in this study was to take precision laboratory measuring equipment to the field and apply it to a full-scale burn test. This approach differs from traditional "laboratory" tests in that no attempt was made to isolate significant variables. The interior of an A-4 cockpit was instrumented with transducers to measure temperature, heat, smoke, toxic gases, light shock, sound, pressure, and the physiological behavior of a rat and a mouse. The exterior of the cockpit was instrumented with temperature- and heat-measuring transducers. Directly below the cockpit in an underground tunnel were instruments and control animals. The interior cockpit data were redundantly transmitted via RF and hard-wire telemetry to a receiving van at the site. Data acquired were organized for subsequent analytical modeling.

OBJECTIVES

The main objective of this study was to obtain baseline data on mechanical, thermal, chemical, and animal behavior events occurring in an unarmed A-4 cockpit subjected to a simulated carrier deck fire. Secondary objectives were to:

1. Determine the occurrence and concentrations of toxic gases and oxygen deficiencies.

2. Appraise the use of an underground laboratory in a field test.

3. Evaluate the feasibility of using rats and mice in an uncontrolled environment to determine the physiological response of humans to various aspects of a fire.

4. Evaluate the use of telemetry for obtaining data in such fires.

5. Record on movie film what a pilot might experience visually during a fire, limited of course by the distinction between film and human vision discrimination.

6. Study the effects of stopping a large pool fire at a predetermined point in a test to preserve the vehicle, equipment, and test animals for post-test analysis.

7. Evaluate the problems associated with measuring heat flux, temperature, smoke, toxic gases, and animal behavior during a simulated carrier deck fire.

SUMMARY OF RESULTS

An instrumented A-4 cockpit was heated by a simulated carrier deck pool fire. On the basis of post-test inspection of the dissected cockpit (Appendix M), film coverage within the cockpit during the test (Appendixes B and L), and heat and smoke transducer data (Appendixes E and H), it is possible to reconstruct the significant events leading to the structural degradation of the cockpit. Figure 1(a) depicts conditions before fire ignition. At 11 seconds after ignition, external fire was building up on the starboard side as shown in Figure 1(b). This situation in which fire builds up faster on one side of the aircraft represents a realistic condition for a fire developing on the deck of a carrier that is under way. Figure 1(c) illustrates the conditions at 71 seconds; the cockpit was filled with smoke and fire was spreading to the exterior port side. Between 192 seconds and the time that light water applied by firemen was observed by the camera in the cockpit at 232 seconds, flames were in the cockpit, as shown in Figure 1(d). Figure 1(e) shows conditions after the test. A chronological list of the significant events during the fire is given in Table 1.

MAJOR EVENTS AND OBSERVATIONS

The cockpit heated faster on the starboard side due to the prevailing wind direction. First flicks of flame were seen in the cockpit at about 192 seconds. By about 222 seconds, the canopy had completely failed, and flames engulfed the cockpit. Calorimeter data indicated that the first significant heating in the cockpit came from the direction of the canopy at about 203 seconds (Appendix E). Next, a relatively hot burst came from below at 208 seconds. The entire region where the directional calorimeter was located was heated between 213 and 232 seconds. By 232 seconds, light water applied by firemen had cooled the interior of the cockpit.

Thermocouples in the vicinity of the canopy showed only a very gradual increase in temperature until near the end of the test (at about the time flames were breaking through the canopy) when there were sharp increases (Appendix E).

Toxic gas measurements (Appendix F) appeared to correlate with the behavior of test animals and with carboxyhemoglobin levels in post-test samples of blood from the test animals (Appendix G). There was significant depletion of oxygen and development of CO, CO_2, Cl^-, and CN^- but not enough to be lethal.

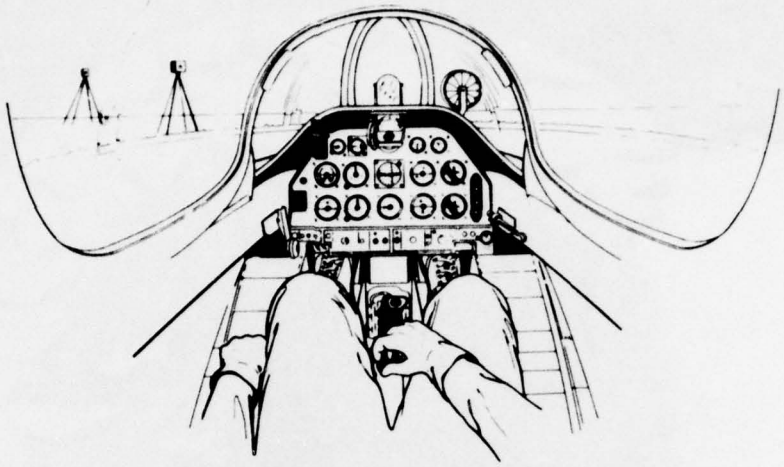

FIGURE 1(a). Conditions That Would Be Seen by Pilot at Ignition (t = 0).

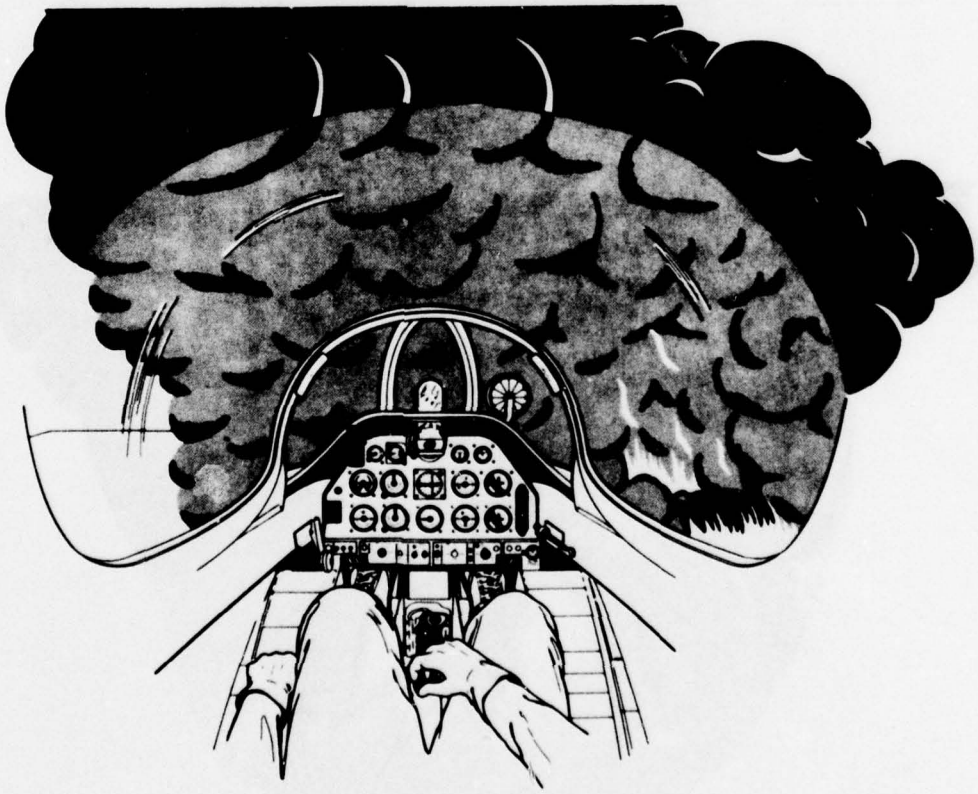

FIGURE 1(b). Eleven Seconds After Ignition (t = 11 Seconds).

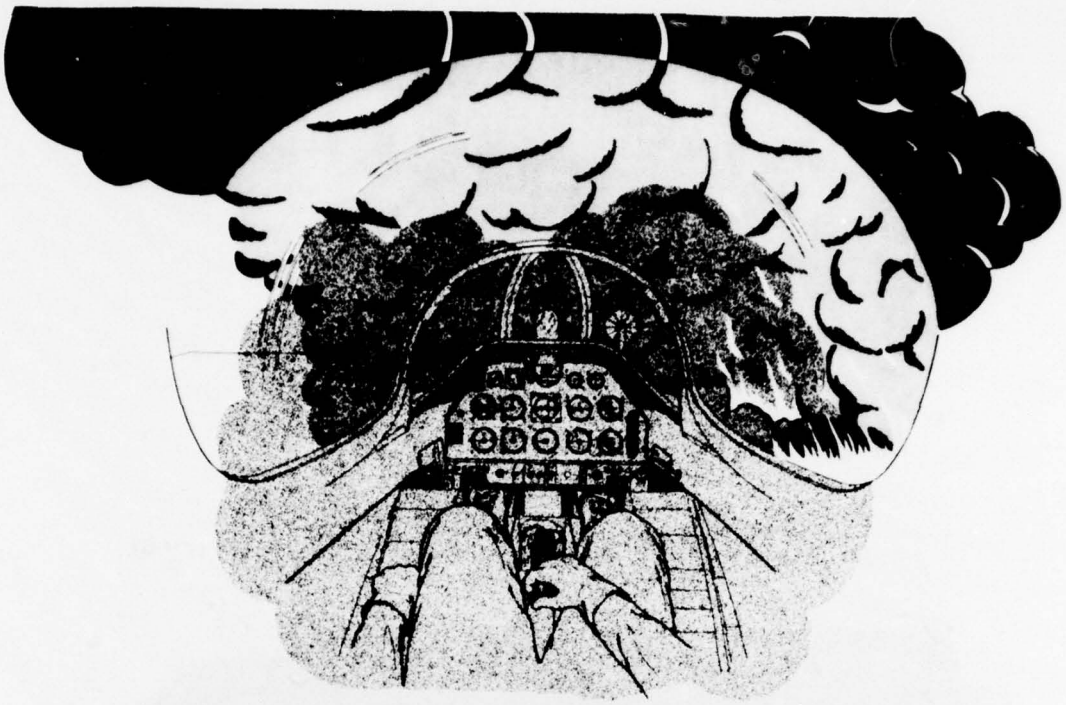

FIGURE 1(c). After 71 Seconds (t = 71 Seconds).

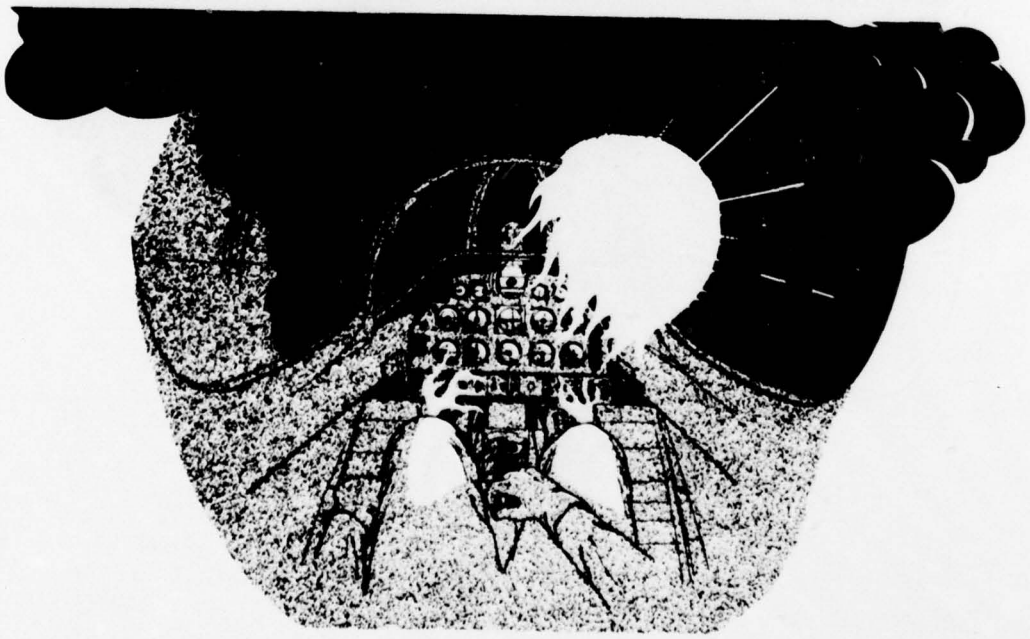

FIGURE 1(d). Between 192 and 232 Seconds (t = 192–232 Seconds).

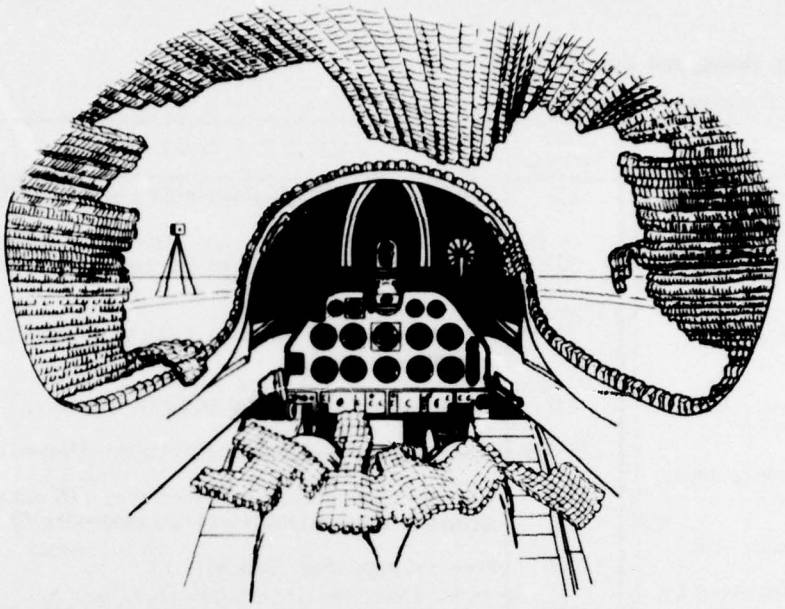

FIGURE 1(e). After Fire was Extinguished (t = 243 Seconds).

The output of the smoke transducer indicated that there were two periods (from 30 to 70 seconds and from 120 to 140 seconds) during which there was significant smoke production (Appendix H). Complete smoke obscuration was measured at 155 seconds and continued until the fire was extinguished.

A mouse on a treadmill in the cockpit perished in the fire (Appendix G), but the cockpit camera recorded the animal running for 71 seconds after the beginning of the test. An instrumented rat inside the pilot's helmet atop the manikin survived the fire, though it suffered third-degree burns over much of its body. A blood sample taken from that rat 30 minutes after the test showed a carboxyhemoglobin level of 49%. (Concentrations between 40 and 50% in humans typically cause severe headaches, weakness, dizziness, dimness of vision, nausea, vomiting, fainting, and increased pulse and respiratory rates.) By contrast, a control rat in the instrumentation bunker, which had breathed air piped down from the cockpit, was able to perform an avoidance response to electric shock after the test. A post-test blood sample from the control rat showed a carboxyhemoglobin level of 43%. Two control mice in the instrumentation bunker, also breathing cockpit air, survived the test with no apparent toxic effects. One was mated subsequently, and both lived normally while under observation for 6 months after the test. Subjective electroencephalographic and electrocardiographic responses for the cockpit rat were recorded for the entire test (Appendix G).

TABLE 1. Chronology of Significant Events Occurring During A-4 Bur

References in parentheses indicate where event is discussed in app

Time, seconds	Event	Time, seconds	Event
0	Fuel ignition (Appendix D)	109	EEG amplitude decreases (Appendix G)
7.4	Initial temperature change recorded on inside bottom of nose cone (Appendix E)	113	Starboard fuselage skin reaches steady state (Appendix E)
11	Initial heat recorded on starboard side of cockpit (Appendix E)	120	Flux transducers indicate asymmetric heating of cockpit (Appendix E); EKG reference voltage stabilizes (Appendix G)
21	Initial heat flux recorded on bulkhead between nose cone and cockpit (Appendix E)	123	Steady-state heating reached on starboard side of cockpit (Appendix G)
27	Initial heat recorded on port side of cockpit (Appendix E)	126	Maximum depletion of O_2, production of CO and CO_2 (Appendix F)
30	Initial smoke recorded by smoke transducer (Appendix H)	128	EKG reference increases again (Appendix G)
34	EKG amplitude reduction, frequency increase (Appendix G)	131	EEG reference drops, lower amplitude (Appendix G)
37	Smoke measurement, D_S = 16 (Appendix H)	132	Initial Cl^- production (Appendix F)
41	EEG amplitude decreases, spindle incidence decreases (Appendix G)	133	EEG postictal activity, EKG low voltage amplitude (Appendix G)
51	EKG amplitude increases, reference shifting initiated (Appendix G)	134	Initial heat flux through canopy recorded (Appendix E)
59	Initial heating of lower pilot seat (Appendix E)	150	EEG signal indicates animal revival (Appendix G)
63	Initial oxygen depletion and presence of CO and CO_2 measured (Appendix F)	153	O_2 returns to normal, CO returns to normal, CO_2 decreases (Appendix H), partial recovery of EEG and EKG signals off scale (Appendix G)
69	EKG amplitude stabilizes, frequency increases (Appendix G)	155	Smoke measurement, D_S = 200 (Appendix H)
71-120	Smoke measurement, D_S = 71 (Appendix H)	161	Animal hyperexcitability ends, EEG and EKG signals off scale (Appendix G); possible destruction or detachment of nose cone (Appendix E)
93	EKG reference voltage increases dramatically (Appendix G); EEG amplitude increases, spindle incidence increases (Appendix G)	171	End of gas sampling (Appendix F)
95	Fire enters nose cone, impinges on forward cockpit bulkhead	192	Camera records initial fire flick in cockpit
96-161	Exothermic behavior in vicinity of starboard armrest (Appendix G)	203	Top of directional calorimeter senses initial heating from canopy (Appendix E)
97	EKG reference voltage peaks, starts decreasing (Appendix G)	205	Camera and flux transducers facing canopy record initial fire in cockpit (Appendix E)
103	Camera records total initial darkness in cockpit	208	Directional calorimeter measures initial heating from bottom (Appendix E)
104-135	Exothermic behavior in vicinity of starboard armrest (Appendix G)	210	Flux transducer records significant heat entering through floor (Appendix E)

1. Chronology of Significant Events Occurring During A-4 Burn Test.

s in parentheses indicate where event is discussed in appendixes.

Event	Time, seconds	Event
EEG amplitude decreases (Appendix G)	221	Side of directional calorimeter senses initial heating (Appendix E)
Starboard fuselage skin reaches steady state (Appendix E)	222	Cockpit thermocouples record sustained fire (Appendix E)
Flux transducers indicate asymmetric heating of cockpit (Appendix E); EKG reference voltage stabilizes (Appendix G)	224	Fire trucks take position and firefighting begins (Appendix L)
Steady-state heating reached on starboard side of cockpit (Appendix G)	232	Light water observed by cockpit camera
Maximum depletion of O_2, production of CO and CO_2 (Appendix F)	231-232	Cooling of directional calorimeter (Appendix E)
EKG reference increases again (Appendix G)	238	EKG amplitude lowers to reference, EEG activity suggests that animal is alive (Appendix G)
EEG reference drops, lower amplitude (Appendix G)	240	Fire extinguished (Appendix L)
Initial Cl^- production (Appendix F)	243	Recording equipment turned off (Appendix D)
EEG postictal activity, EKG low voltage amplitude (Appendix G)		
Initial heat flux through canopy recorded (Appendix E)		
EEG signal indicates animal revival (Appendix G)		
O_2 returns to normal, CO returns to normal, CO_2 decreases (Appendix H); partial recovery of EEG and EKG signals off scale (Appendix G)		
Smoke measurement, D_S = 200 (Appendix H)		
Animal hyperexcitability ends, EEG and EKG signals off scale (Appendix G); possible destruction or detachment of nose cone (Appendix E)		
End of gas sampling (Appendix F)		
Camera records initial fire flick in cockpit		
Top of directional calorimeter senses initial heating from canopy (Appendix E)		
Camera and flux transducers facing canopy record initial fire in cockpit (Appendix E)		
Directional calorimeter measures initial heating from bottom (Appendix E)		
Flux transducer records significant heat entering through floor (Appendix E)		

2

Significant structural failure occurred in the canopy, the nose cone, the sheet aluminum on both sides and under the floorboard station housing electrical and hydraulic lines (Appendix M). Buckling and melting caused separations that could admit flames at the juncture of the floorboard and the forward bulkhead and under the seat. The rubber fuel tank full of JP-5 fuel just behind the cockpit was directly exposed to flames from below, but suffered no damage.

Records were made of the sound produced in the cockpit during the fire, of the pressure differential between the cockpit and the outside, and of the acceleration experienced by the manikin in the cockpit (Appendix I). All three of these records showed either no significant events or no response, but as such they did provide useful baseline data.

Firemen extinguished the fire within seconds, preserving the evidence of the fire damage for post-test inspection (Appendix L).

OBJECTIVES ACCOMPLISHED

All the study objectives were met and are discussed at length in the appendixes. The main study objective to obtain baseline data on mechanical, thermal, chemical, and animal behavior events occuring in an unarmed A-4 cockpit was achieved. The quality and quantity of the baseline data collected was sufficient to initiate the elements of a realistic analytical model that may be used to perform design trade-off studies in the context of pool fire survivability.

In the following discussion, secondary objectives are numbered to correspond to the items in the list in the previous section.

1. Determination of the occurrence and concentrations of toxic gas and oxygen deficiencies are given in Appendixes F, G, and H. It was found that, for the cockpit studied, heat was more critical to pilot survival than toxicity.

2. The experimental results reported could not have been obtained without the use of the underground facility described in Appendix A.

3. The use of rats and mice to determine the physiological response of humans to various aspects of cockpit degradation proved to be indispensable, as discussed in Appendix G. The animal as a physiological transducer is significantly superior to any man-made transducer.

4. Telemetry was shown in Appendix J to be an excellent means for attaining pool fire data.

5. Appendix K discusses motion picture coverage that was used to obtain data useful to characterize what a pilot would experience visually during a fire.

6. The feasibility of stopping a large pool fire at a predetermined point in a test to preserve the vehicle, equipment, and test animals for post-test analysis was demonstrated and is discussed in Appendixes L and M.

7. Finally, problems were identified and solutions found for measuring heat flux and temperature (Appendix E), smoke (Appendix H), toxic gases (Appendix F), and animal behavior (Appendix G) in a simulated carrier deck fire.

CONCLUSIONS AND RECOMMENDATIONS

CONCLUSIONS

The conclusions which follow are made in the context of baseline information obtained from a single full-scale experiment.

Heat transfer mechanisms (Appendix E) are more critical to pilot survivability than those of toxic gas production (Appendix F). The influence of smoke in reducing visibility for the pilot and thereby jeopardizing his chances for survival is significant (Appendix H). The levels of toxic gases measured during the test are not great enough to produce serious short-term effects in the pilot (Appendix F). It is not known what influence the pilot's clothing, parachute, or extraneous paraphernalia would have on these baseline conclusions.

The cockpit did not get "hot" until the canopy failed. At that time flame effluent penetrated through the cockpit from the holes (from melted aluminum) in the floorboard. The time to canopy failure was 192 seconds. This time would have been shorter had the pool fire developed more quickly, as in an unrealistic no-wind condition. Under ideal conditions a pool fire can develop fully in 20 seconds. Thus it is conceivable that the canopy could have failed at 110 seconds.

RECOMMENDATIONS

1. Fire-hardened canopy concepts should be tested using an insulated A-4 cockpit hull suspended at the proper height within a pool fire. Such tests should be instrumented so that heat and light are measured. Such data could then be used to specify realistic requirements for the physical properties of canopies.

2. Pool fire tests should be performed emphasizing the baseline behavior of the A-4 wing and fuselage. Dummy weapons should be suspended under the wings. Retrofit concepts should be evaluated to harden the cockpit at the same time.

3. Aluminum skins melt in the fire environment. The use of a steel film or other active or passive (nontoxic) inorganic materials as fire walls within the cavity should be considered.

4. Doors to wheel wells should be designed to be closed at all possible times. They should be opened only during maintenance when an attendant requires access to the electrical and hydraulic systems.

5. An emergency fireproof ladder is needed to enable the pilot to escape and to allow fire fighters to reach the pilot.

6. A fire-sensing signal could be provided to warn the pilot of a pool fire so that he could take appropriate action (abandon aircraft or taxi away).

7. Modeling of the cockpit structural degradation behavior should be initiated using data from this report.

8. Transducers (including animals) identified in this report should be further developed and standards established for their use in future fire-testing of components and full-scale items.

9. A pool fire characterization model should be developed.

10. The cockpit test (after fire-hardening) should be repeated, using armed devices within the cockpit.

11. Lifetime of electronic gear needed to control critical aircraft functions during fuel fire buildup should be evaluated.

12. A statistically significant number of animals should be used in future data-gathering studies.

Appendix A

FIRE FACILITY

Appendix A
FIRE FACILITY

The main elements that were brought together at the test facility to accomplish the test were an A-4 cockpit including the fuselage fuel tank, various data-gathering systems, and firefighting personnel and equipment.

A survey of existing test facilities revealed that no facility was available that could both accommodate a simulated carrier deck fire and provide the quality and amount of data required by the task objectives. Consequently, a fire facility was designed and partially completed at the Naval Weapons Center.

A sketch of the test facility that was originally designed and proposed is shown in Figure A-1. This design incorporated a concrete pad and fire pan. An A-4 aircraft cockpit section is shown situated at the center of the fire pan. A 3-inch (76-mm) inside diameter insulated umbilical connects the test item to the instrument bunker in the tunnel directly below. A 7-foot (2.1-m) diameter tunnel connects the instrument bunker to the fire control barricade on one side and to an emergency exit and air vent on the other. Electric power lines, data lines, and water lines are routed from the control barricade through the tunnel to the instrument bunker. The initial design also incorporated a built-in fire protection system with hydrants at each corner. A dam at one end of the fire pan would allow the pan to hold water on which fuel would be floated during a test. The dam would be opened to let the remaining fuel and water drain into a nearby dump after the test was concluded.

Because of funding constraints on the program, only the underground part was completed as proposed. For the remainder of the facility a temporary fire pan was bulldozed in the earth and lined with plastic. Figure A-2 shows a sketch of the actual facility that was used. The Navy A-4 aircraft used as the test item is pictured on the fire pan in Figure A-3. Figure A-4 is a photograph of the completed 220-foot (66-m) long tunnel, looking toward the instrumentation bunker from the fire control barricade. A blower in the barricade provided a positive pressure to move fresh air through the tunnel and instrumentation bunker and out through an exhaust port at the other end of the tunnel, thus protecting test personnel from possible accumulation of toxic gases. No permanent instrumentation was installed in the facility. Instead, the particular instrumentation that is required will be installed for each experiment. At present the facility has both flexibility and vast potential for further development. A variety of possible applications of the facility is suggested by the drawings in Figure A-5, which illustrate a number of different items that could be accommodated for future testing.

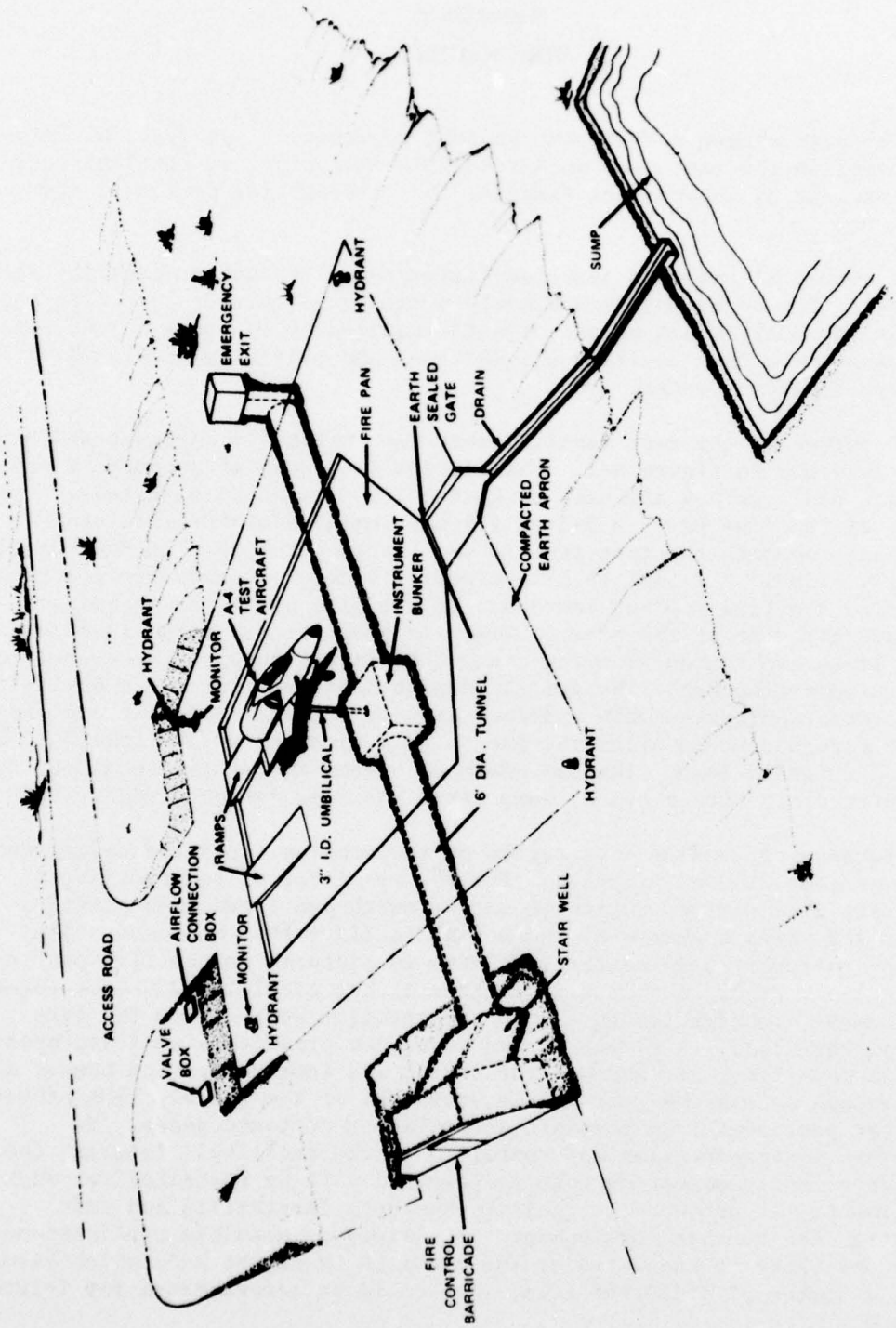

FIGURE A-1. Artist's Conception of Proposed Design for Fire Test Facility.

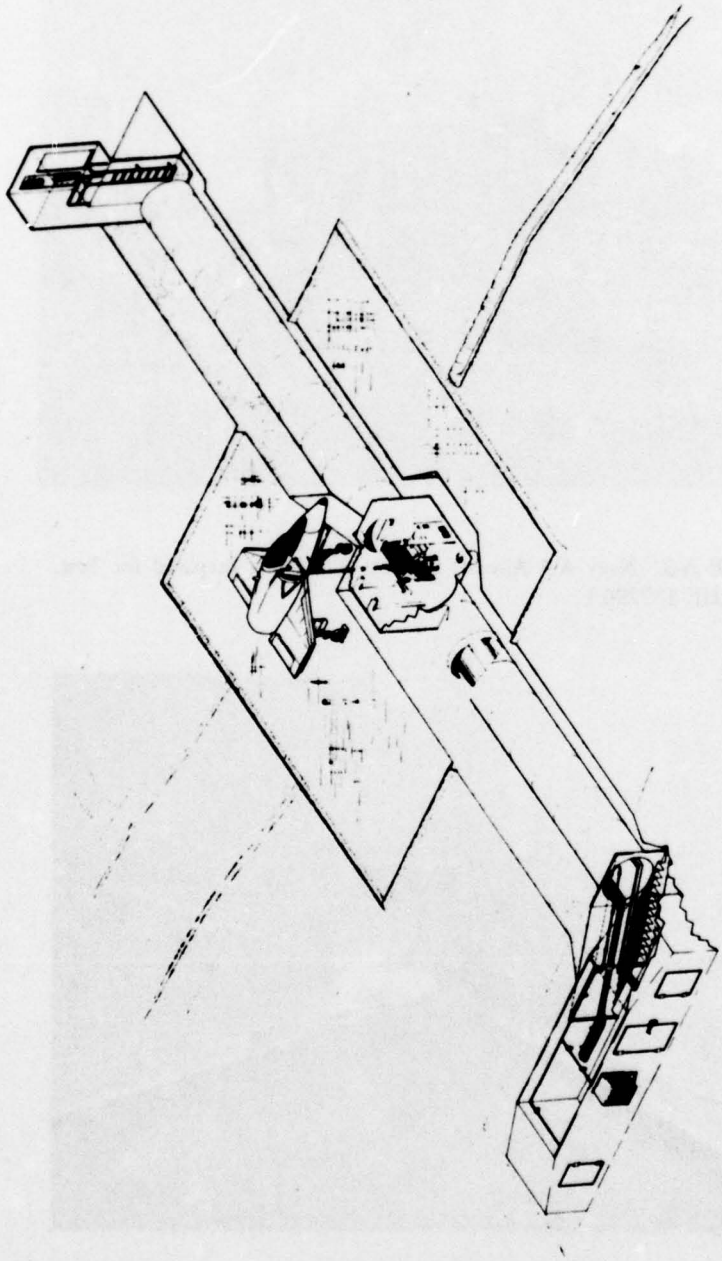

FIGURE A-2. Artist's Sketch of Test Facility Utilized. (In actual test aircraft was oriented about 60 degrees clockwise from position shown.)

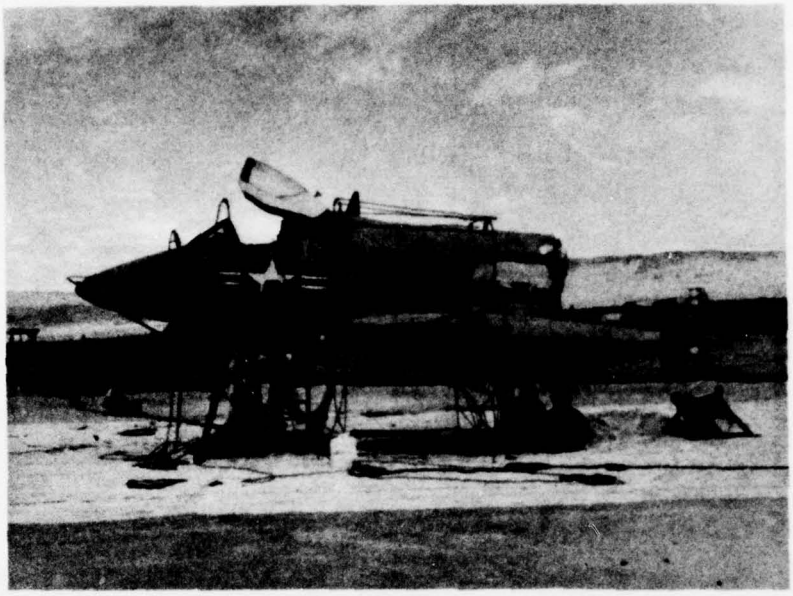

FIGURE A-3. Navy A-4 Aircraft on Test Site Being Prepared for Test. (Neg. LHL 187296)

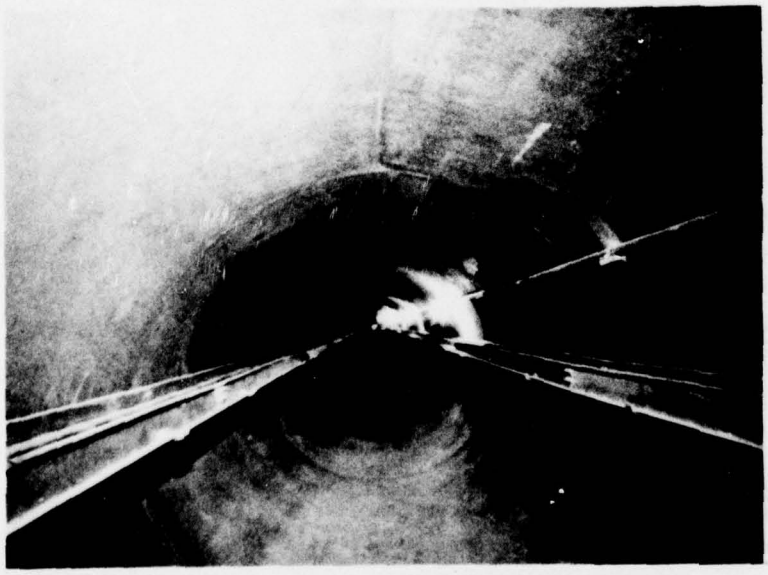

FIGURE A-4. View of Tunnel Looking From Fire Control Barricade Toward Instrumentation Bunker. (Neg. LHL 186988)

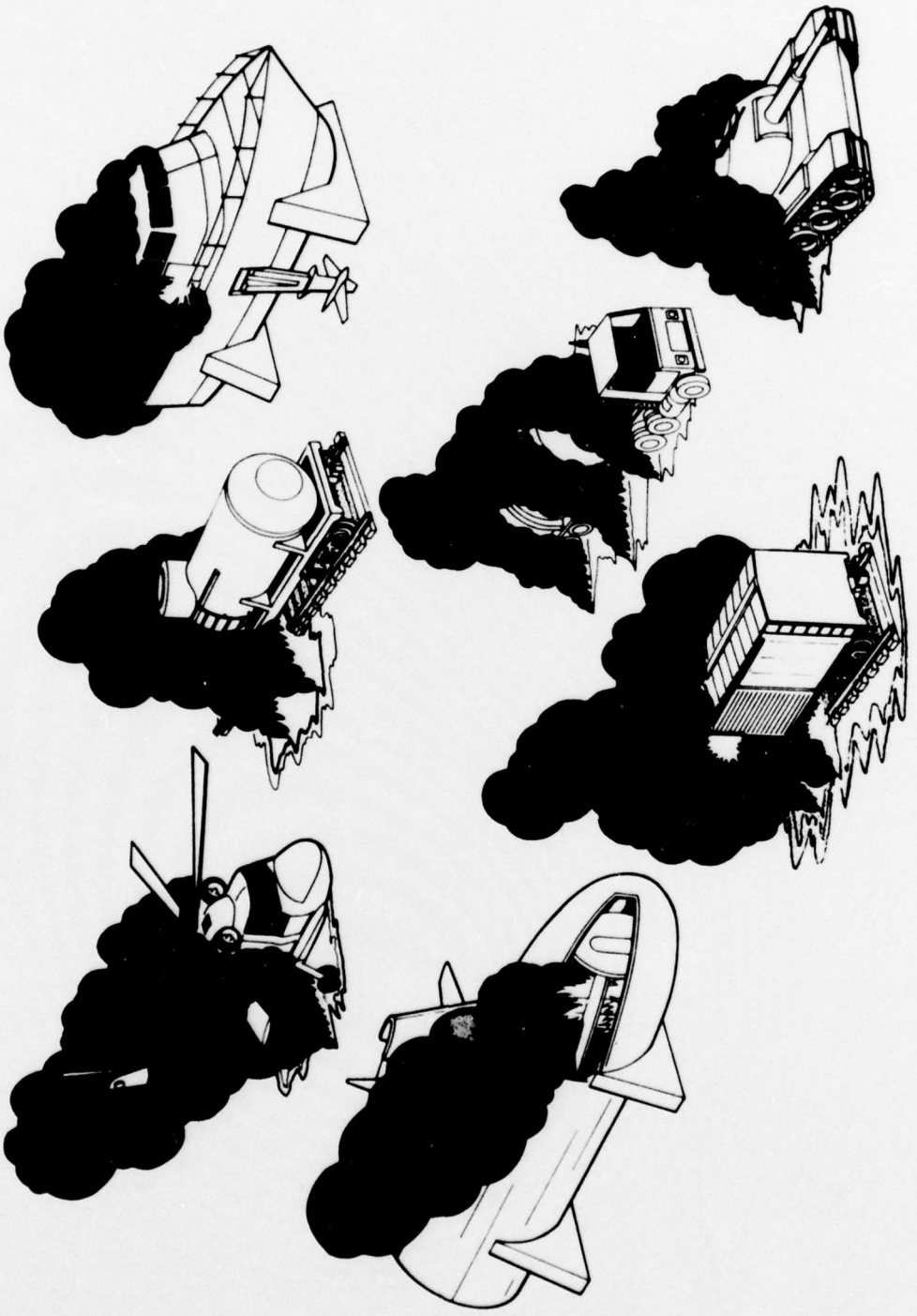

FIGURE A-5. Composite Sketch of Possible Uses of Fire Test Facility.

Appendix B

MANIKIN

Appendix B
MANIKIN

Instrumented lifelike manikins that can be used for fire work exist and are useful for evaluating pilot clothing, etc.[5] However, since the cockpit test objectives emphasized degradation, the expense of such a manikin was not warranted for this baseline test.

A sheetmetal [0.62-inch-thick (15.7-mm-thick) stainless steel] manikin was constructed for this test to represent a pilot in the cockpit (Figure B-1). The small box on the rod extending out from the lower front part of the manikin is a three-dimensional calorimeter to measure the amount of heat contained in the cockpit and the direction of the heat source. Also extending out from the front of the lower section is an ice bath for thermocouples. Redundant signals from the sensors are sent via an RF transmitter and through a land line to the telemetry receiving van. A detailed description of the calorimeter system is given in Appendix E. Figure B-2 provides interior views of the upper and lower sections of the manikin. The top section contained a water-jacketed cylinder to house a motion picture camera. The lower section contained a second water-jacketed cylinder to house encoding electronics and a telemetry transmitter. A microphone was also housed in the lower section to record what a pilot would hear in the cockpit. Figure B-3 shows the two water-jacketed cylinders, the camera, and the camera lens.

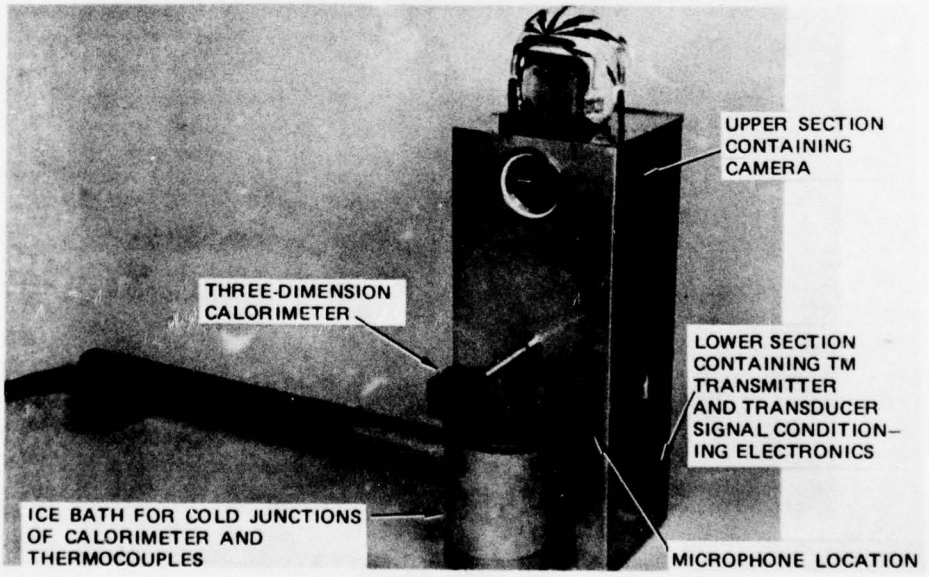

FIGURE B-1. Exterior View of Manikin Before It Was Put Into Cockpit. (Neg. LHL 185687)

[5] G. Tichner and R. Bendler. "Thermo Man Tester," *Instruments and Control Systems*, June 1974, pp. 39-42.

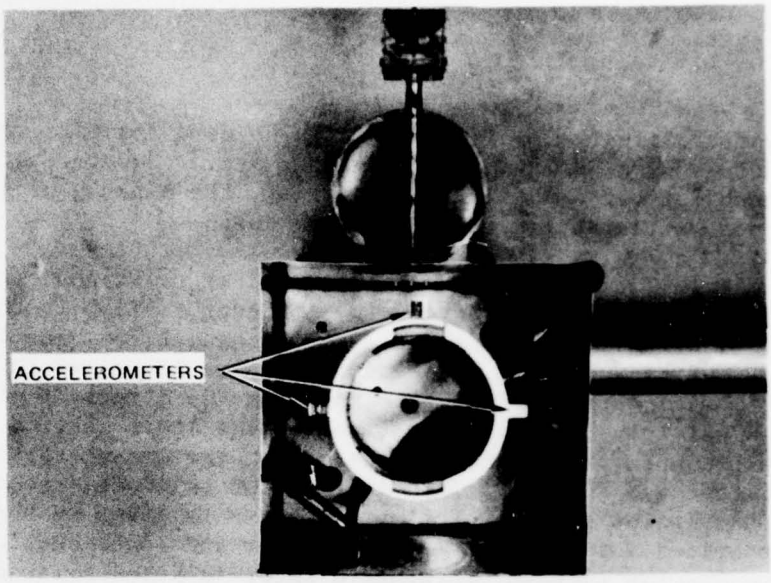

(a) Upper Section

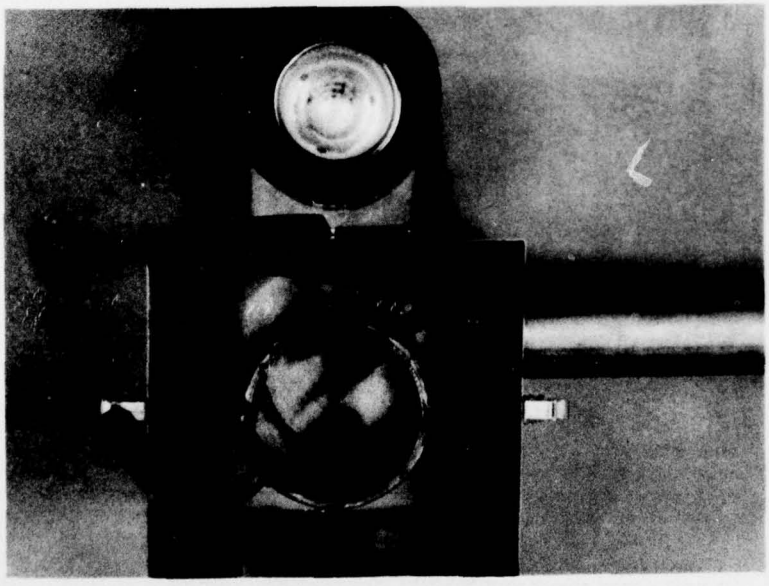

(b) Lower Section

FIGURE B-2. Interior Views of Manikin. (Neg. LHL 185690 [top] and 185686 [bottom])

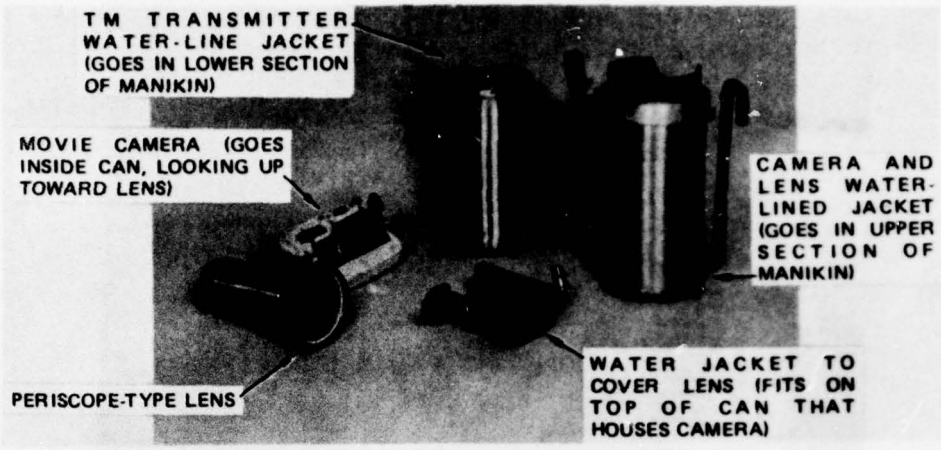

FIGURE B-3. Lens, Camera, and Water Jackets Used Inside Manikin. (Neg. LHL 185685)

The quartz glass window near the top of the front plate of the manikin (Figure B-1) provides an opening for a 16-mm motion picture camera utilizing a 3-mm wide-angle lens. During the test the camera recorded what a pilot might see in such a fire. In particular it recorded the occurrence of smoke, the entry of the fire into the cockpit, and the activity of a mouse on a ferris-wheel-type treadmill. The treadmill was put near the starboard windshield within view of the camera, where the mouse would be exposed to heat, toxic gas, and other physiological stimuli that occur in the fire. It is noted that the response of a single animal is not statistically significant.

In still another experiment associated with the manikin, a rat was placed in the pilot's helmet atop the manikin (Figure B-4). The rat, which had EEG and EKG electrodes implanted in its head and chest, was strapped into a sling. Leads from the electrodes were connected to amplifying circuits in the helmet. Signals from the electrodes were transmitted to recording instruments in the telemetry van via the transmitter in the manikin to record the brain and heart activity of the rat during the fire. Cockpit air, containing potentially toxic gas, breathed by the cockpit rat was also circulated to a control rat in the instrument bunker below. A 0.25-inch (6.3-mm) diameter stainless steel tube (some 20 feet--6 m--long) with its open end just in front of the nose of the cockpit rat passed through the umbilical down to the instrument bunker. There it provided the air the control rat breathed during the test. It is unknown how much of the toxic products are absorbed in such a tube. Further details on the rat and mice experiments and the movie camera mounted in the manikin are given in Appendixes G and K. After the camera and instrumentation were put into place for the test, the remaining space between the inner cylinders and the outer shell were filled with diatomaceous earth to insulate the inner items from heat and fire damage.

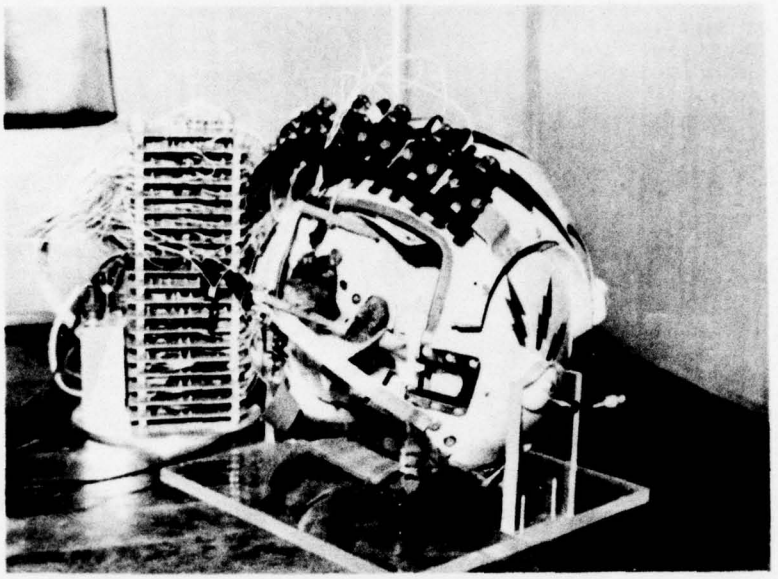

FIGURE B-4. Rat With EEG and EKG Electrodes Connected to Telemetry Transmitter (At Left). (Neg. LHL 187263)

Appendix C

COCKPIT LAYOUT

Appendix C
COCKPIT INSTRUMENTATION

A diagram and numbered callouts showing the interior arrangement of one version of an A-4 cockpit is given in Figure C-1 for general reference only. The cockpit tested (shown in Figure C-2) was significantly different from that shown in Figure C-1. Because of Navy procurement practice and continuous component upgrading, it is unlikely that the chemical composition of the items illustrated can be labeled with any confidence.

The A-4 cockpit interior was equipped with sensors to measure heat, temperature, smoke, toxic gas, shock, pressure, light, sound, and animal brain and heart activity. Heat- and temperature-measuring transducers were also attached to the outside of the cockpit. In addition, three mutually perpendicular accelerometers were mounted inside the manikin to measure acceleration in case of an explosion, a sound microphone was installed in the manikin to record what a pilot would hear in a fire, and a differential pressure transducer was installed inside the cockpit with an extension tube to the outside to measure any pressure differential that might occur. The various systems are shown in Figure C-3.

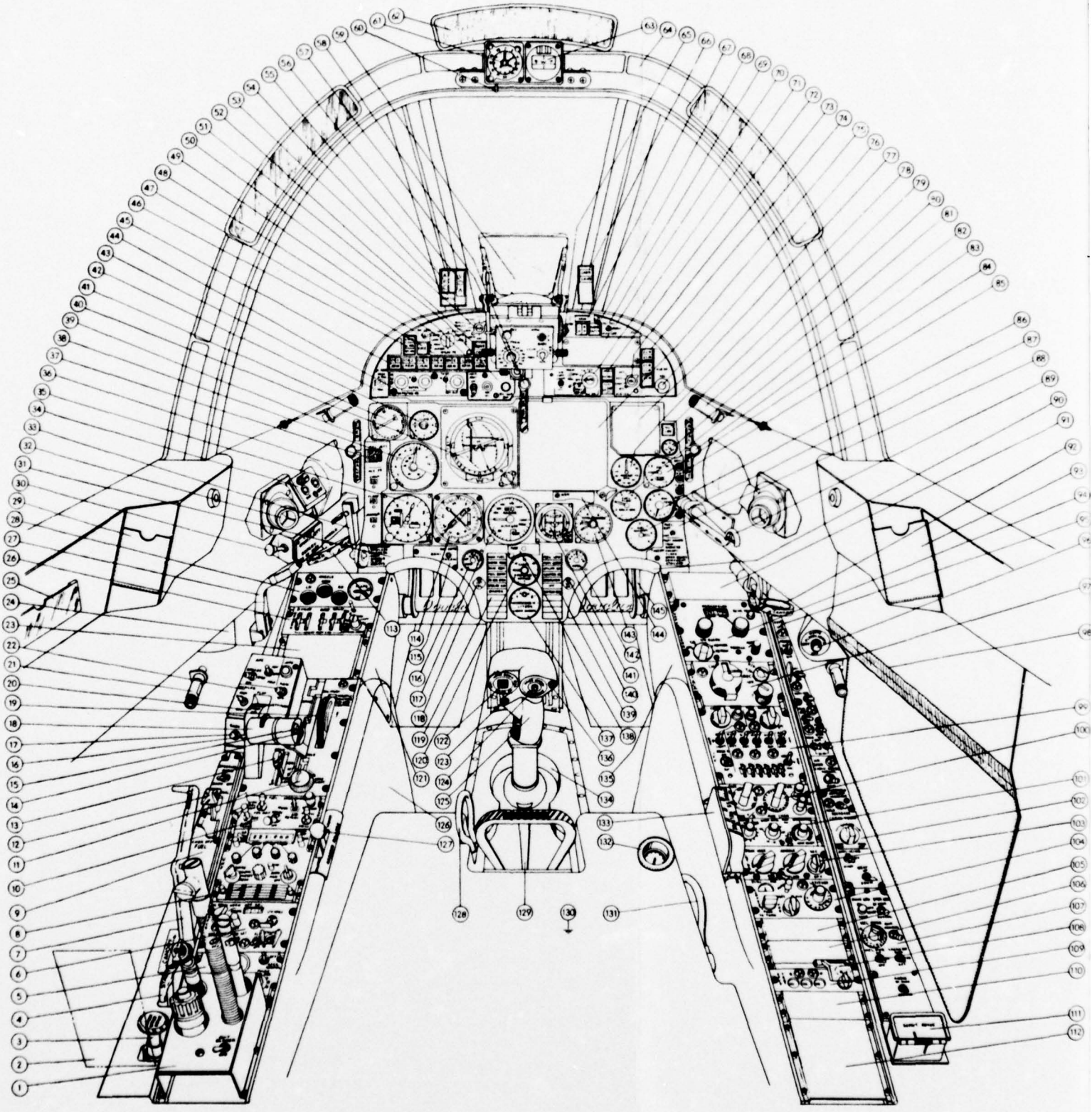

A-4M COCKPIT ARRANGEMENT (ECP #1120)

1. 5827049 AIRCREW SERVICES (6-3/8)
2. 5827999 PILOT RELIEF BAG CONTAINER
3. 5813765 EMERGENCY SPEED BRAKE CONTROL
4. 5577989 STARTER ACTUATING HANDLE
5. 5829941 GROUND CONTROL BOMBING SYSTEM (3)
6. 5560804 AUTOMATIC FLIGHT CONTROL SYSTEM (3-3/8)
7. 5446749 CANOPY CONTROL HANDLE
8. 7660781 AN/ARC-159(V) UHF RADIO (4-7/8)
9. 5826639 EMERGENCY FUEL/NOSE STEERING
10. 5825210 ENGINE CONTROL (2-1/4)
11. 5814051 RUDDER TRIM CONTROL
12. 5544744 MANUAL FUEL SHUTOFF CONTROL
13. 5813630 HORIZ. STAB TRIM MANUAL OVERRIDE CONTROL
14. 5814051 SPEED BRAKE SWITCH
15. 5814051 COMMUNICATION RADIO MIKE BUTTON
16. 5814051 EXTERIOR LIGHTS MASTER SWITCH
17. 5824090 RAIN REPELLENT
18. 5814051 THROTTLE CONTROL LEVER/MANUAL RANGE CONTROL
19. 5814051 THROTTLE FRICTION CONTROL
20. 5813630 FLAPS CONTROL
21. 5818395 CONSOLE RED FLOODLIGHTS (6 PLCS)
22. 5824090 SPOILER, JATO & APC CONTROL ASSY.
23. BLANK PANEL (PROVISIONS FOR ALTERNATE EQUIPMENT (3)
24. 5818395 COCKPIT WHITE FLOODLIGHTS (2 PLCS)
25. 4446206 AIRSPEED CORRECTION CARD HOLDER
26. 5820678 WEAPON CONTROL ASSY. (1-7/8)
27. 4817817 CATAPULT HAND GRIP
28. 3451981 WHEELS & FLAPS (2-1/4)
29. 5828472 SPARE CARD HOLDER
30. 5578845 DRAG CHUTE DEPLOYMENT SWITCH
31. 7660820 LANDING CHECK LIST
32. 5829858 AIR CONDITION EYEBALL DIFFUSERS
33. 5445388 LANDING GEAR CONTROL LEVER
34. 5578877 UHF & VHF TRANSMIT SELECTOR
35. 7660781 ALTIMETER
36. 5578872 HIGH INTENSITY WHITE FLOODLIGHTS (2 PLCS)
37. 7660820 ALE-39 COUNTERS & SELECT JETTISON SWITCH
38. 7660781 AIRSPEED INDICATOR
39. 5660818 EMERGENCY SALVO HANDLE
40. 7660781 ALL ATTITUDE INDICATOR
41. 7660781 ANGLE OF ATTACK INDICATOR
42. 7660781 RATE OF CLIMB INDICATOR
43. 5579552 STORES ARM SWITCH
44. 5579552 PILOT'S CONTROL UNIT (PCU)
45. 5579552 STATION SELECT SWITCHES
46. 5579552 CP 741 ADVISORY LIGHTS
47. 5579552 FIRE WARNING LIGHT
48. 5579552 SIDEWINDER COOLANT SWITCH
49. 5579552 ARMAMENT MODE SELECT
50. 5579552 L.H. & R.H. GUN ARM SWITCHES
51. 5579552 MASTER ARMT. SW., ADI SEL. & STA/GUN DIMMER
52. 5579552 GUNS CHARGE SWITCH
53. 5579552 WALLEYE & SHRIKE SWITCH
54. 5579559 WHEELS INDICATOR LIGHT
55. 5579559 APPROACH POWER COMPENSATOR WARNING LIGHT
56. 5579559 ANGLE OF ATTACK INDEXER
57. 5578558 KNEEBOARD FLOODLIGHT
58. 5660818 EMERGENCY GENERATOR RELEASE HANDLE
59. 5579570 PILOT'S DISPLAY UNIT (PDU)
60. 5828474 COMPASS/CLOCK LIGHT SWITCH
61. 7660781 ELAPSED TIME CLOCK
62. 5828484 REAR VIEW MIRRORS (3 PLCS)
63. 7660781 STANDBY COMPASS
64. 5829442 CANOPY ASSY.
65. 5579553 ALQ-126 CIRCUIT BREAKER
66. 5579559 LABS, LAWS WARNING LIGHTS
67. 5579553 GCBS L.H., R.H., ARM LIGHT
68. 5579553 MASTER CAUTION LIGHT
69. 5579553 CORRELATION SWITCH
70. 5579553 COVER PLATE (ALR-45 TDU PROVISIONS)
71. 5579553 ALE-39 SELECT SWITCHES
72. 5579553 ECM WARNING LIGHTS (ALQ-126)
73. 5579553 ALQ-126 SWITCHES
74. 5579553 ECM LIGHTS (ALR-45/ALR-50)
75. 3828710 COVER PLATE (RADAR PROVISIONS)
76. 5579553 ALR-50 VOLUME CONTROL
77. 4829187 COVER PLATE (ALR-45 INDICATOR PROVISIONS)
78. 7660781 TACHOMETER
79. 7660820 OIL LOW CAUTION LIGHT
80. 5579552, 5579553 INSTR. PANEL RED FLOODLIGHTS (2 PLCS)
81. 7660781 OIL PRESSURE INDICATOR
82. 7660781 FUEL FLOW INDICATOR
83. 5660818 MANUAL FLIGHT CONTROL HANDLE
84. 7660781 ENGINE PRESSURE RATIO INDICATOR
85. 7660820 VARIABLE RESISTORS (PRIMARY FLT. INSTRUMENTS LIGHTING)
86. 7660781 EXHAUST TEMPERATURE INDICATOR
87. 7660781 FUEL QUANTITY
88. 7660820 FUEL QUANTITY SW. & TAKE OFF CHECK LIST
89. 5445039 ARRESTING HOOK CONTROL LEVER
90. 9579599 KNEE PADS
91. 7660822 BLANK PANEL(PROVISIONS FOR LST CONTROL)(1-7/8)
92. 3818389 CANOPY JETTISON HANDLE
93. 5828472 COMPASS CORRECTION CARD HOLDER
94. 7660822 VHF/FM COMMUNICATION ARC-114(4-1/8)
95. 5669493 EXTERIOR LIGHT CONTROLS
96. 5818395 EMERGENCY WHITE FLOODLIGHTS CONTROL
97. 7660781 TACAN PANEL (3)
98. 5817559 DATA CASE
99. 7660822 FAA BEACON APX-72 (5-1/4)
100. 7660822 AUX. RECEIVER ARR-6) (2-1/4)
101. 7660822 UNIVERSAL WEAPON CONTROL (1-7/8)
102. 5669493 AIR CONDITIONING & ANTI-ICING CONTROLS
103. 5828825 INTERIOR LIGHTS CONTROL (2 1/4)
104. 7660822 COMPASS CONTROL (2 5/8)
105. 7660822 BLANK PANEL(PROVISIONS FOR JULIET C-8057/ARC)(1-1/2)
106. 7660822 BLANK PANEL(PROVISIONS FOR JULIET C-8057/ARC)(1-1/2)
107. 5579583 MISC. SWITCHES CONSOLE
108. 4812066 AFCS GUARD ASSEMBLY (3/8)
109. 5660804 AFCS PRE-FLIGHT TEST (1-1/2)
110. S4386543 C17 BLANK PANEL (1-7/8)
111. 5579583 SPARE LAMPS CONTAINERS
112. S4386543 C52 BLANK PANEL (5-1/4)
113. 5660818 EMERGENCY LANDING GEAR HANDLE
114. 7660781 BEARING, DISTANCE & HEADING INDICATOR
115. 7660820 BDHI SWITCH
116. 7660781 NOSE TRIM INDICATOR (UP-DOWN)
117. 7660781 RADAR ALTIMETER
118. 7660820 LST BORESIGHT POTENTIOMETER(ELEVATION)
119. 3579573 CAUTION & ADVISORY ANNUNCIATOR PANEL
120. 7660781 CABIN PRESSURE ALTIMETER
121. 9667118 L.H. CONSOLE STRUCTURE
122. 4664450 NOSE TRIM SWITCH
123. 4664450 BOMB RELEASE SWITCH
124. 4664450 NOSE WHEEL STEERING SWITCH
125. 4664450 CONTROL STICK GRIP WITH GUN/ROCKET TRIGGER
126. 5822131 ROCKET EJECTION SEAT
127. 5822131 HARNESS INERTIA REEL CONTROL
128. 283000 BAILOUT OXYGEN RELEASE RING
129. 5822131 SEAT LOWER EJECTION HANDLE
130. RSSK-GB-1 RIGID SEAT SURVIVAL KIT
131. RSSK-GB-1 SURVIVAL KIT RELEASE HANDLE
132. RSSK-GB-1 BAILOUT OXYGEN PRESSURE GAGE
133. 3579527 HARNESS RELEASE HANDLE
134. 5660817 CONTROL COLUMN
135. 9667119 R.H. CONSOLE STRUCTURE
136. 4664480 AFCS DISENGAGE SWITCH
137. 7660781 LIQUID OXYGEN QUANTITY INDICATOR
138. 7660820 MASTER PRESS TO TEST SWITCH
139. 3579573 CAUTION ANNUNCIATOR PANEL
140. 7660820 LST BORESIGHT POTENTIOMETER (AZIMUTH)
141. 7660781 STANDBY ATTITUDE INDICATOR
142. 7660781 NOSE TRIM INDICATOR (LEFT-RIGHT)
143. 7660781 ACCELEROMETER
144. 7660820 NAVY SERIAL NUMBER PLATE
145. 5442548 RUDDER PEDALS AND BRAKES

FIGURE C-1. Interior Arrangement of A-4 Cockpit.

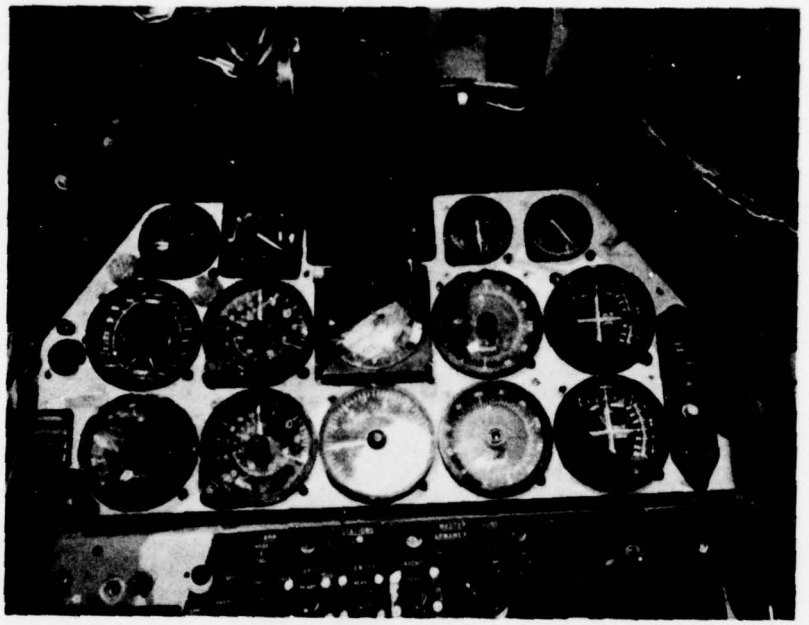

FIGURE C-2. View of Instrument Panel of A-4 Test Item. (Neg. LHL 186977)

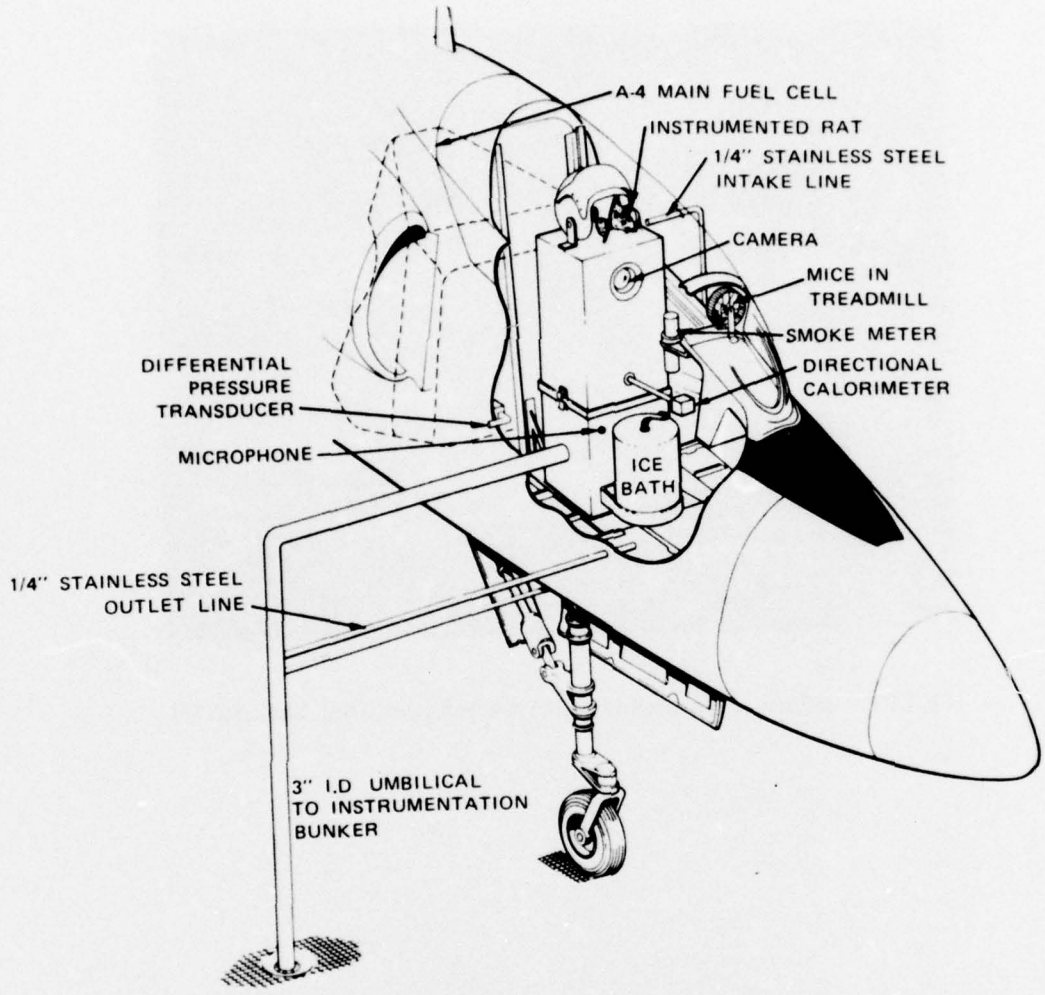

FIGURE C-3. Cockpit Instrumentation Systems.

Appendix D

TEST LOG

Appendix D
TEST LOG

The test was started about 0715 on 16 April 1975. Early in the morning 7,000 gallons (26,500 liters) of water were dumped into the fire pan, while the animals were being made ready for the test. About an hour before the test started, a rat and a mouse were put into place in the cockpit, and a control rat and two mice were placed in the instrumentation bunker. After the cockpit canopy was closed, EEG and EKG readings from both rats were checked to see that the instrumentation systems were working.

One 20-gallon (75.7-liter) gasoline half-drum was placed below the front of the A-4 and another below the rear. The half-drums were on pivots so they could be remotely dumped. Five flares were arranged so as to ignite the fuel evenly around the cockpit. JP-5 fuel was poured onto about 5 inches (127 mm) of water in the 75-foot (22.5-m) diameter fire pan. Figure D-1 shows a plot of wind velocity made by Stanford Research Institute personnel in their trailer at the test site.

The data recording systems were started, the two gasoline drums were dumped, and the five flares were initiated. Only two of the five flares ignited, and consequently the fire developed unevenly, burning more on the starboard than on the port.

The fire was allowed to burn until a cockpit thermocouple registered a temperature that indicated the fire had penetrated the cockpit. At this point the test director signaled the firefighting crew to extinguish the fire to preserve as much information from the test as possible. An earthen bank at one side of the test site prevented the firefighting crew from approaching the fire from upwind, as would have been optimal. Nevertheless, despite having to attack the fire crosswind, they extinguished it within 16 seconds. The total time of the test was 243 seconds.

When the fire was out, the firemen entered the cockpit and retrieved the rat, which, though badly burned, was found to be still alive upon being examined by Dr. Steve Packham of the University of Utah. The mouse in the cockpit had perished. Two firemen with gas masks then went into the tunnel to check for toxic gas. No toxic gas was detected, as indicated by the fact that two canaries, which had been placed in the instrumentation bunker, were alive and well.

The data-gathering systems were turned off, the fresh air blowers were turned on, and test personnel began checking the data that had been recorded.

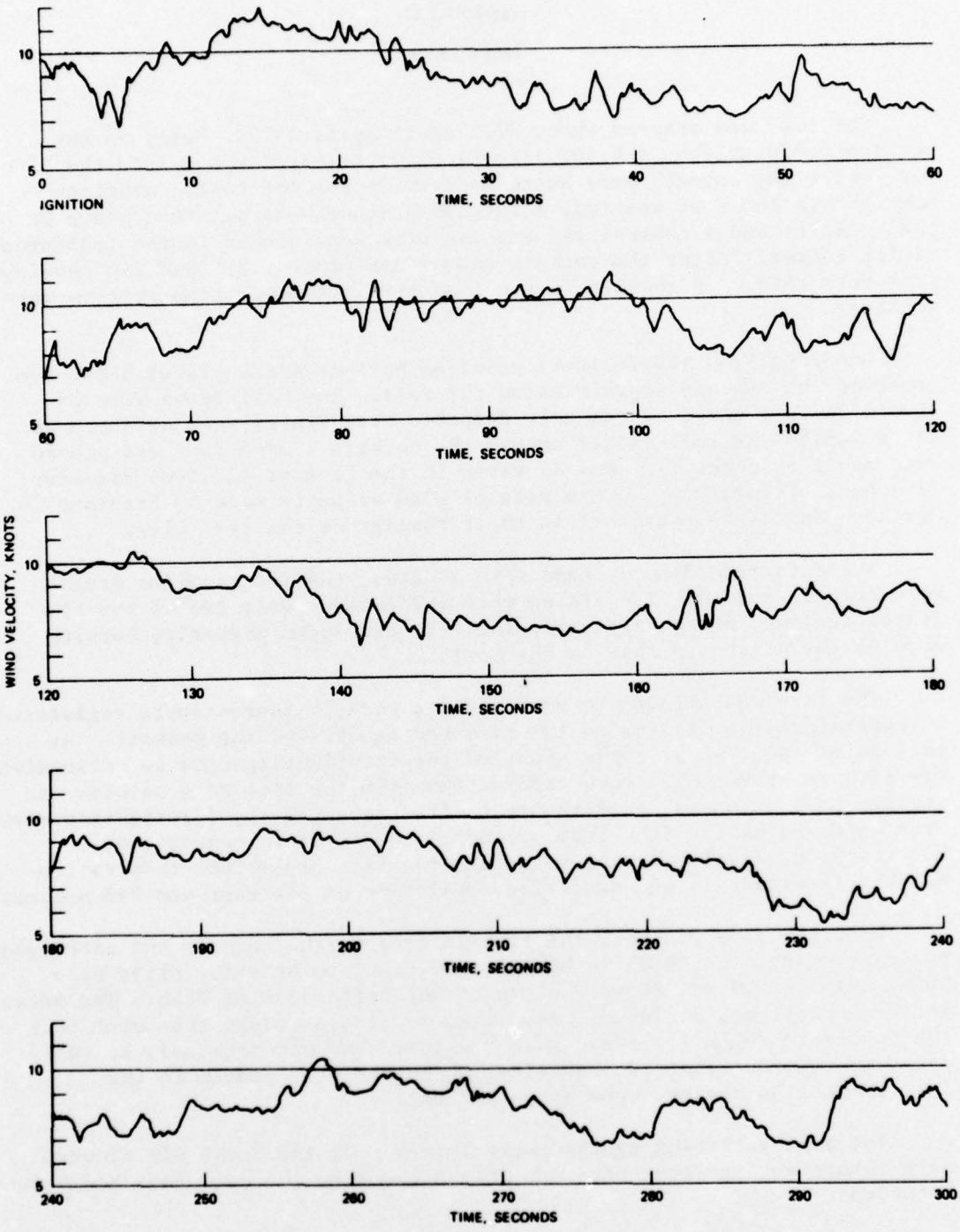

FIGURE D-1. Wind Velocity During Test as Recorded by Stanford Research Institute.

Appendix E

CALORIMETER CONSTRUCTION AND COCKPIT HEAT MEASUREMENTS

APPENDIX E
CALORIMETER CONSTRUCTION AND COCKPIT HEAT MEASUREMENTS

HEAT FLUX MEASUREMENTS

Heat flux measurements[6] must be made independently of temperature measurements during transient non-steady-state burning experiments, because thermal energy conversion processes cannot be otherwise quantified.

Slug calorimeters can be used as transducers to estimate the heat flux available for heating a test item.[7,8] The principle of such a transducer is to measure the amount of heat stored during a given time, utilizing the thermal storage capacity of a known mass. The modeling equation is

$$q = \rho c L \frac{dT_m}{dt} \qquad \text{(E-1)}$$

where

q = a measure of the heat flux

L = thickness

ρ = density

c = heat capacity

T_m = mean temperature of the mass

t = time

Equation E-1 can be used only as a first-order approximation for measuring transient heat flux.

Two versions of a thick-film slug calorimeter were used to estimate transient heat flux within the A-4 cockpit. The first version was designed to approximate a one-dimensional transducer. Its construction is shown in Figure E-1(a), (b), (c), (d), (e). Figure E-1(a) shows the backside of the machined element, made of Armco iron sheet. Its overall dimensions are 0.0625 by 0.75 by 0.75 inches (1.6 by 19 by 19 mm).

---

[6] Naval Ordnance Laboratory, White Oak. *A Mobile Field Laboratory for Fires of Opportunity*, by R. S. Alger and J. R. Nichols. Silver Spring, Md., NOL, 10 October 1973. P. 118. (Report No. NOLTR-73-87, publication UNCLASSIFIED.)

[7] H. Grober, S. Erk, and U. Grigull. *Fundamentals of Heat Transfer*. New York, McGraw-Hill, 1961. P. 5.

[8] D. J. Gaines. "Selecting Unsteady Heat Flux Sensors," *Instruments and Controls Systems*, May 1972. Pp. 80–83.

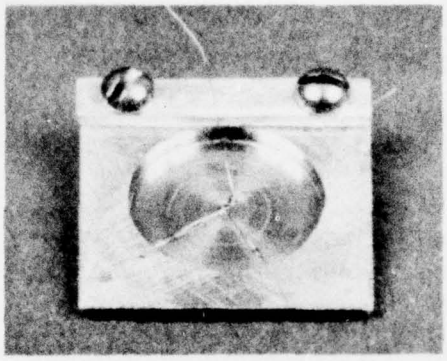

(a) Backside of machined element with thermocouple welded to disk. (Neg. LHL 192306)

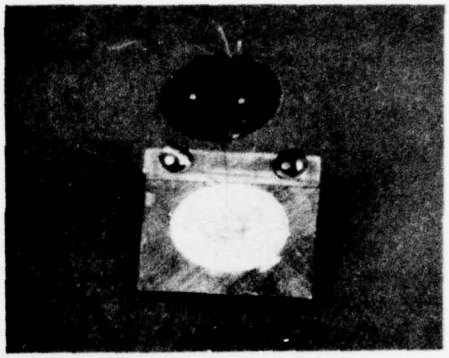

(b) Cavity filled with diatomaceous earth. (Neg. LHL 192307)

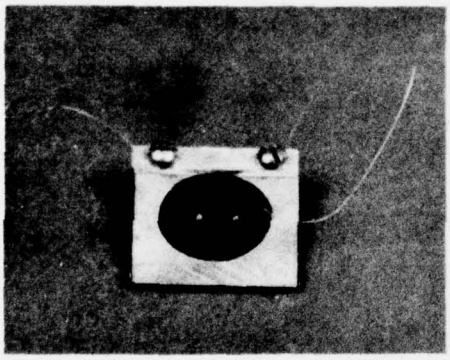

(c) Mica cover plate over diatomaceous earth. (Neg. LHL 192303)

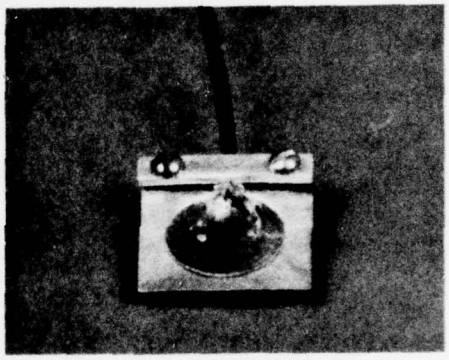

(d) Junction of thermocouple and lead wire. (Neg. LHL 192304)

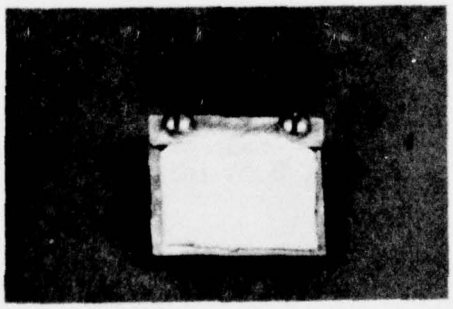

(e) Ceramic coating over entire transducer. (Neg. LHL 192305)

FIGURE E-1. Construction of One-Dimensional Transducer.

The diameter of disk (the circular section remaining after the cylindrical recess was machined out) is 0.50 inch (12.7 mm); its thickness is 0.005 ± 0.0005 inch (0.127 ± 0.013 mm). A 0.001-inch (0.025-mm) (AGW-50) chromel-alumel thermocouple is shown welded to the disk. The functional junction is near the center of the disk. Figure E-1(b) shows the cavity full of diatomaceous earth. Figure E-1(c) shows a 0.001-inch (0.025-mm) mica cover sheet in place, used to retain the diatomaceous earth. Figure E-1(d) shows a junction where the 0.001-inch (0.025-mm) thermocouple is spliced to 0.010-inch (0.25-mm) wire. The larger wire is anchored to the basic element by two setscrews. In Figure E-1(e) is shown a protective coating of ceramic. This transducer is positioned on the test item so that its face is toward the direction of the oncoming heat.

The second version of the slug calorimeter was designed to approximate a three-dimensional transducer (Figure E-2(a), (b)). Figure E-2(a) shows an interior view of the transducer. It is made of six Armco iron plates, each 3 by 3 by 0.0625 inches (76.2 by 76.2 by 1.6 mm), that are thermally insulated from each other. Two thick-film disks were machined in each of the six plates. One disk was 0.030 inch (0.762 mm) thick and the other was 0.010 inch (0.254 mm). The diameter of each disk was 0.75 inch (19 mm). The construction of this slug calorimeter differed from that in Figure E-1 in that a glass container of silicone oil was placed in the cavity instead of diatomaceous earth. A second 0.001-inch (0.025 mm) thermocouple was placed in the silicone oil in each element. A splice similar to that shown in Figure E-1 can be seen in Figure E-2(a). The entire cavity inside the transducer (inside the box) was filled with diatomaceous earth. Figure E-2(b) shows the assembled transducer. Ceramic caulking was used to seal the seams. In principle, each of the five exposed faces provided an independent measurement of transient heat flux along the principal axes.

Figure E-3 shows the placement of seven one-dimensional transducers (F1 through F7) in the A-4 cockpit. The three-dimensional transducer was mounted on the manikin, which was placed in the pilot's position in the cockpit (see Figure C-3).

Figure E-4 shows the outputs from the seven one-dimensional transducers. The outputs are derived from the thermocouples attached to the slug calorimeters (Figure E-1(a)). By assuming that this temperature is T_m, then estimates of q can be made using Equation E-1.

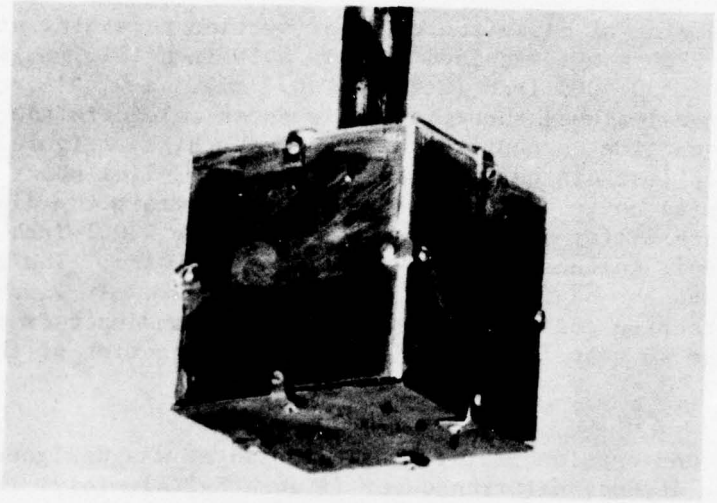

(b) Outside view. (Neg. LHL 186392)

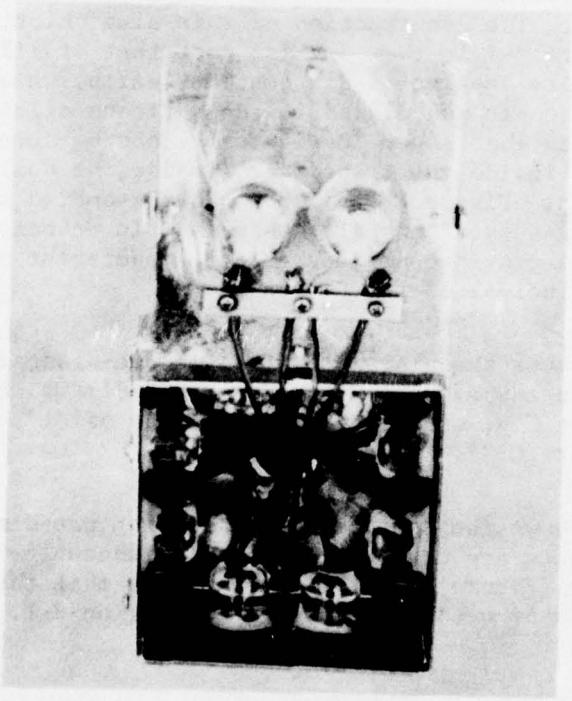

(a) Interior view. (Neg. LHL 186391)

FIGURE E-2. Three-Dimensional Calorimeter.

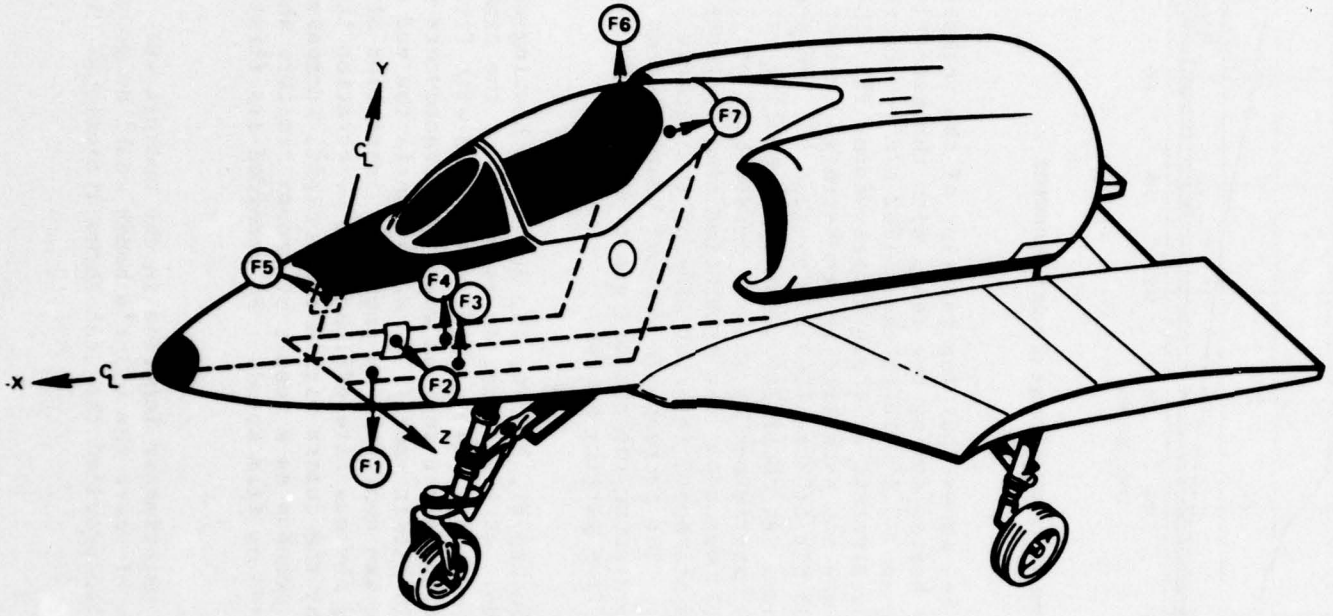

TRANSDUCER	X	Y	Z	LOCATION DESCRIPTION
F1	8	0	7	PORT SIDE A/C. ON TOP OF COCK PIT FLOOR MAT, FACING DOWN.
F2	15	8	5	PORT SIDE A/C. ON BACK SIDE OF COCK PIT ACCESS DOOR, FACING OUT.
F3	7	0	22	PORT SIDE A/C. ON TOP OF METAL FLOOR, FACING UP.
F4	7	0	-22	STARBORD SIDE A/C. ON TOP OF METAL COCKPIT FLOOR, FACING UP.
F5	15	8	-5	STARBORD SIDE A/C. ON BACK SIDE OF CUT ACCESS DOOR, FACING OUT.
F6				TOP OF SEAT FRAME, FACING SKY THROUGH CANOPY
F7				BACK OF SEAT FRAME, FACING AFT

FIGURE E-3. Locations of Slug Calorimeters on A-4.

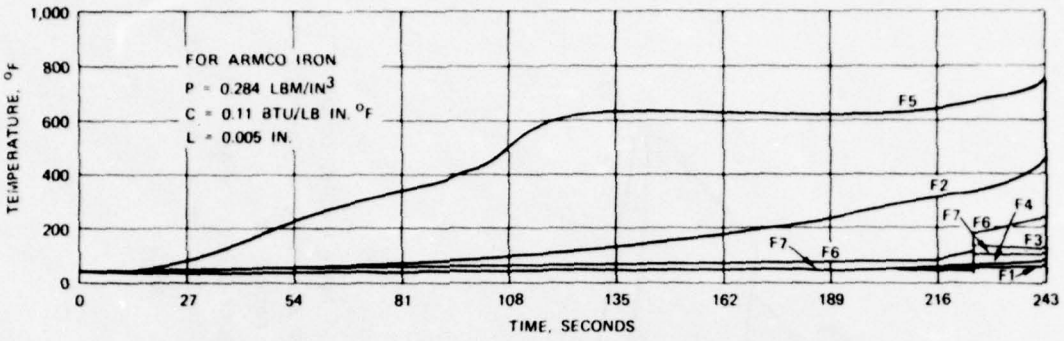

FIGURE E-4. Mean Temperature Change of Slug Calorimeters.

An overview of Figure E-4 shows that the interior of the cockpit was not being significantly heated during the test, with the exception of F5. The maximum heating--q < 0.15 BTU/ft^2-sec (1702 W/m^2)--occurred on the starboard side of the aircraft as shown by transducer F5. That the heating of the cockpit was not symmetric is demonstrated in that F2 heated more slowly--q < 0.05 BTU/ft^2-sec (567 W/m^2)--than F5. F2 sensed initial heating at 59 seconds. At about 185 seconds the heating rate increased to that initially experienced by F5. F5 sensed heat at 11 seconds and was saturated at 123 seconds. The saturation time suggests steady-state heating of the starboard interior side of the cockpit between 123 and 210 seconds. The increase in cockpit heating after 210 seconds is due to heat entering the cockpit via cracks in the cockpit and not because of the fire getting hotter.

The response of transducers F1, F3, F4, F6, and F7 to heating were negligible until 224 seconds. At this time, as confirmed by the camera within the cockpit (at 222 seconds), the cockpit was filled with fire effluent gas. Cockpit heating in the regions where the transducers were located was modest--q < 0.15 BTU/ft^2-sec (1702 W/m^2)--until the end of the test. This observation was confirmed by post-test inspection of the cockpit interior. Prior to obvious fire effluent gas penetration into the cockpit, as confirmed by the camera within the cockpit, increased heating of F6 began at 214 seconds as a result of canopy fracture which started at 205 seconds (based on film speed). F6 recorded its first rise at 134 seconds.

The three-dimensional calorimeter location in the cockpit was chosen to be representative of where the pilot's hands would be most of the time. That position also provided the best three-dimensional view of the cockpit interior.

The typical response of a thermocouple sensing the temperature rise of all slugs in the three-dimensional transducer is shown in Figure E-5. The essential feature is that no significant heat is observed until about 205 seconds. The face of the transducer viewing the forward instrument panel sensed a heat rate of 0.46 BTU/ft^2-sec (5221 W/m^2) between 213 and 222 seconds. The port and starboard faces recorded only about 0.022 BTU/ft^2-sec (250 W/m^2) between 211 and 231 seconds. The bottom face measured about 0.94 BTU/ft^2-sec (10,700 W/m^2) between 208 and 232 seconds and the top face measured about 0.32 BTU/ft^2-sec (3600 W/m^2) between 203 and 232 seconds. These data are summarized in Figure E-6. They suggest that initial significant heating came from the canopy region first (203 seconds). Next a relatively hot burst came from below at 208 seconds. The entire region where the three-dimensional transducer was located was heated during the period from 213 to 232 seconds. By 232 seconds, light water from the firefighting equipment had cooled the interior of the cockpit.

The significance of the levels of heat flux measured within the cockpit is indicated by Figure E-7. This graph indicates the pain threshold for humans. For example, the 0.94 BTU/ft^2-sec (10,700 W/m^2) measured in the cockpit between 208 and 232 seconds represents unbearable pain after some 3 seconds of exposure time. This and additional data relating heat flux to human survival time can be found in an article published in the *Journal of the American Medical Association*.[9]

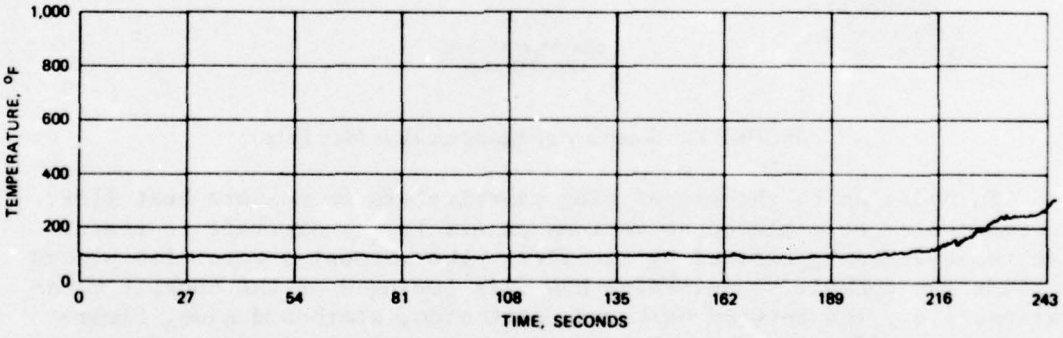

FIGURE E-5. Typical Response of Thermocouple Sensing Temperature Rise of Slugs in Three-Dimensional Transducer.

[9] K. Buettner, "Effects of Extreme Heat on Man," *Amer. Med. Ass. J.*, 28 October 1950, pp. 732-38

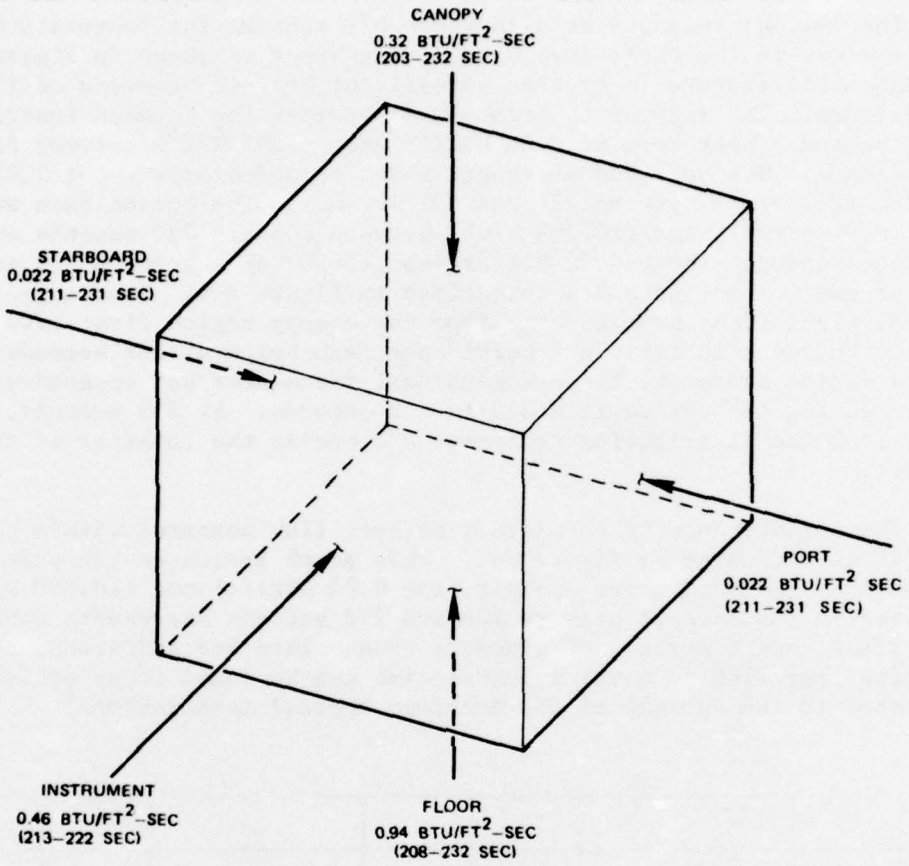

FIGURE E-6. Summary of Maximum Heat Flux Data.

In addition to the use of slug calorimeters to measure heat flux, thermocouples were placed at various points in the aircraft to measure the temperatures generated by the fire. Thermocouples were also placed outside the cockpit to determine how fire impinged on the cockpit boundaries, i.e., the forward bulkhead, port side, starboard side, floorboard, back side, and top. External thermocouple leads were adequately insulated (for a sustained 1700°F or 925°C environment) and attached to the steel re-bar cage around the aircraft as shown in Figure E-8. Internal thermocouple leads (0.005 inch or 0.122 mm in diameter) were used that were electrically insulated for temperatures to 500°F (260°C). Such insulation was deemed adequate since temperatures to 200°F (93°C) would be presumed intolerable for the pilot.

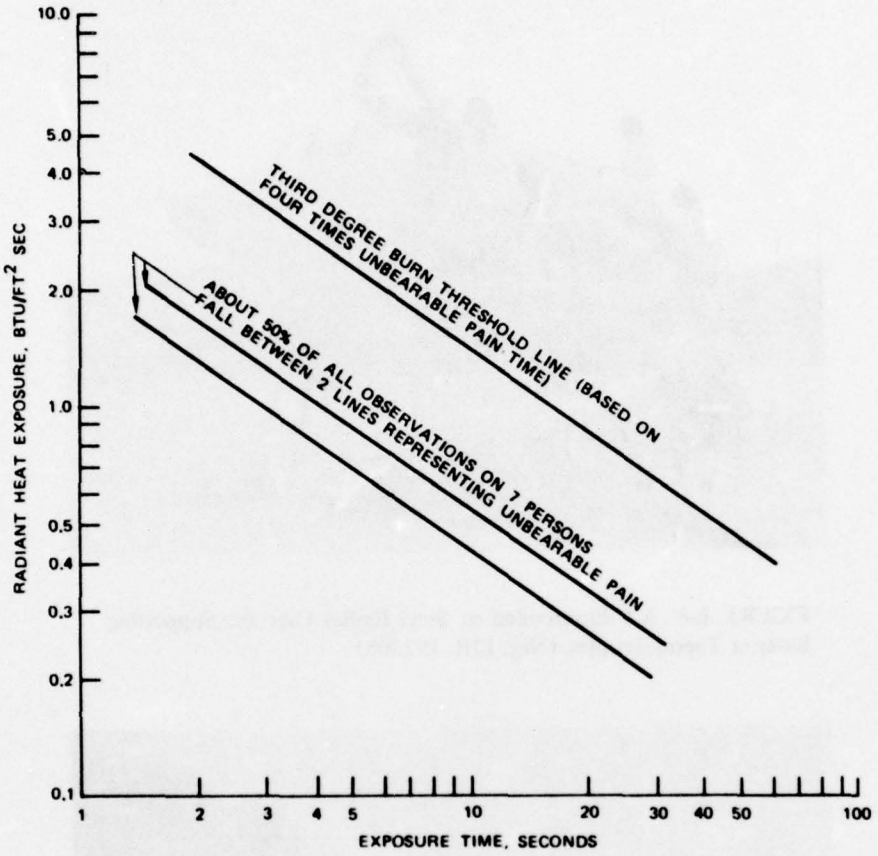

FIGURE E-7. Radiant Heat Versus Exposure Time for Unbearable Pain and Third-Degree Burns.

EXTERNAL HEATING

As discussed earlier, wind and gusts caused the fire plume to be deflected as shown in Figure E-9. These conditions, together with the protective effect of the wings, prevented the pool fire from heating the insulated aft portion of the aircraft. Fortunately, conditions were such that the cockpit section was engulfed by fire, as confirmed by the movie camera within the manikin. Unfortunately, the external thermocouple data was lost (due to recorder power failure), and hence flame characterization could not be evaluated since there was no telemetry backup.

FIGURE E-8. A-4 Enshrouded in Steel Re-Bar Cage for Supporting Exterior Thermocouples. (Neg. LHL 192308)

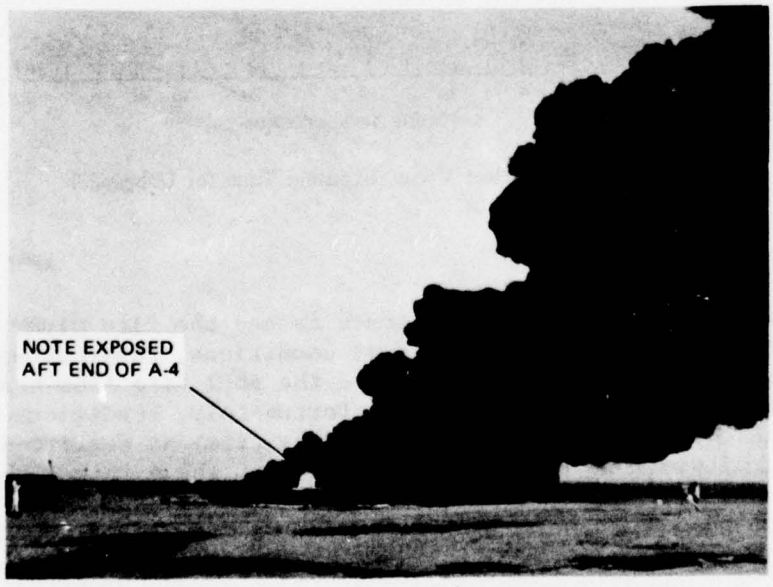

FIGURE E-9. A-4 Pool Fire Deflected by Prevailing Wind. (Neg. LHL 187354)

BACK SIDE HEATING

A thermocouple rake was placed within the fuselage fuel tank directly behind the cockpit. The data from these thermocouples were lost. However, post-test inspection revealed that the rubber fuel bladder suffered no damage, even though the bottom of the bladder was directly exposed to fire after the bottom aluminum skin melted through. No damage was suffered because the bladder being full of fuel acted as a heat sink protecting the rear of the cockpit. The consequence was that the fuselage fuel tank actually protected the rear of the cockpit from the fire. Post-test inspection, confirmed by gas analysis, showed no evidence of fuel leaking into the cockpit during the test.

A slug calorimeter was placed on the back of the seat facing aft to detect potential heating from the fuselage fuel tank. Its output is shown in Figure E-10. No appreciable heating was recorded before the canopy failed.

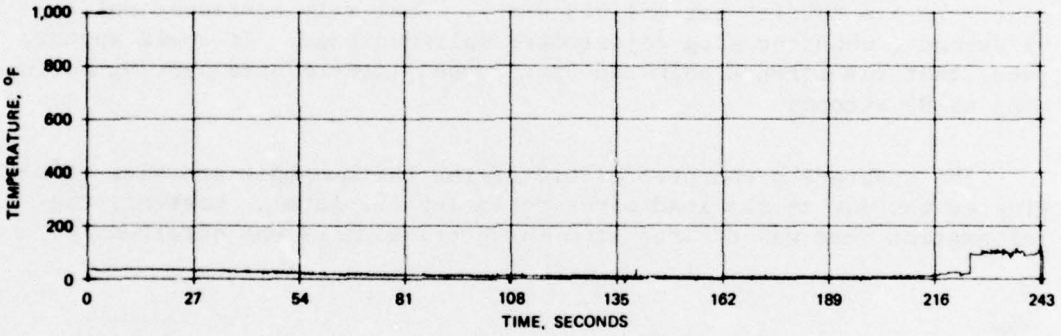

FIGURE E-10. Output of Slug Calorimeter Placed on Back of Pilot's Seat, Facing Aft.

NOSE CONE HEATING

A thermocouple and a slug calorimeter were placed inside the fiberglass nose cone, which houses the radar and a radio filter screen, to measure the development of heat in that section. The thermocouple was placed on the inner lower surface of the fiberglass about 1 ft (0.3 m) in front of the cockpit bulkhead hinge. The slug calorimeter was placed on the radio filter screen on the outer surface of the forward cockpit bulkhead, facing the interior of the cone.

The response of the thermocouple is shown in Figure E-11. Initial heating was detected at 7.4 seconds after ignition. Heating remained relatively uniform until 162 seconds, at which time the thermocouple failed, perhaps suggesting that the nose cone was destroyed by fire or mechanically detached.

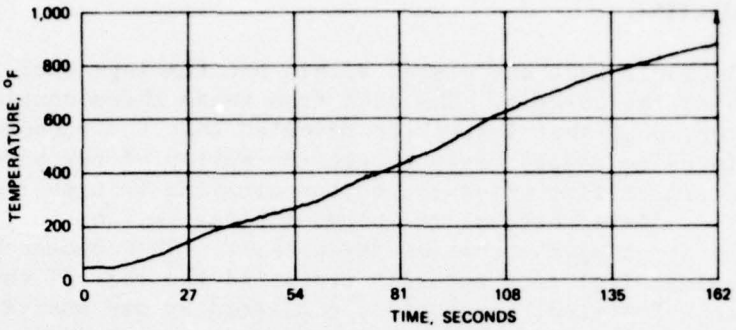

FIGURE E-11. Output of Thermocouple Located 1 Foot (0.3 m) in Front of Bulkhead Hinge in Nose Cone.

The slug calorimeter response is shown in Figure E-12. Initial heating was detected at 21 seconds. The heating rate was about 0.05 BTU/ft^2-sec (567 W/m^2). At 95 seconds the heating rate increased significantly to 4.5 BTU/ft^2-sec (51,048 W/m^2). That rate continued until 99 seconds, when the slug calorimeter malfunctioned. It would appear, then, that the forward bulkhead experienced fire-related heating beginning at 95 seconds.

The apparent premature failure of the thermocouple and slug calorimeter was due to the lead wires not being insulated. However, the information that was desired from these transducers was obtained.

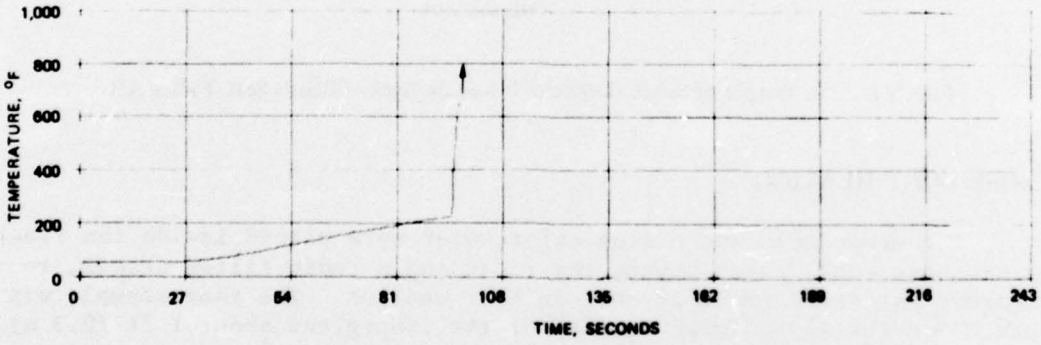

FIGURE E-12. Output of Slug Calorimeter Placed on Radio Access Filter Screen in Nose Cone.

FORWARD BULKHEAD HEATING

The forward bulkhead served as an efficient thermal barrier. This was confirmed by a thermocouple attached by a screw to the back side of the bulkhead (facing the interior of the cockpit), as shown in Figure E-13. Note that no appreciable heating was measured until about 236 seconds and that heating was registered after the fire in the cockpit was put out by the firefighters at 232 seconds.

Heating of the air in the forward port region of the cockpit is indicated from the data in Figures E-14 through E-19. The response of a thermocouple attached by a screw to the metal wear plate on top of the floor covering is shown in Figure E-14. The location of this thermocouple was about 8 inches (203 mm) from the centerline, 4 inches (102 mm) behind the forward bulkhead, directly on the cockpit floor. No significant heating was indicated until after 222 seconds. The light water cooling was never detected. This lack of heating was confirmed by a slug calorimeter facing the floor covering in the proximity of the thermocouple. The heating of the slug calorimeter was negligible, as shown in Figure E-15. It would appear, then, that the air in the vicinity of the port floorboard was nearly ambient during the test. This observation was confirmed by post-test inspection in that no significant discoloration, deformation, or melting of plastics was observed.

Access doors were constructed on both the port and starboard sides of the cockpit to provide access to locate thermocouples and slug calorimeters in the forward inner region of the cockpit. The doors were located 5 inches (127 mm) behind the forward bulkhead and 8 inches (203 mm) above the floorboard. The doors consisted of the original fuselage skins with reinforced edges. On the inner faces of these doors a thermocouple and a slug calorimeter were attached to estimate skin temperature and heat flux available to the interior of the cockpit.

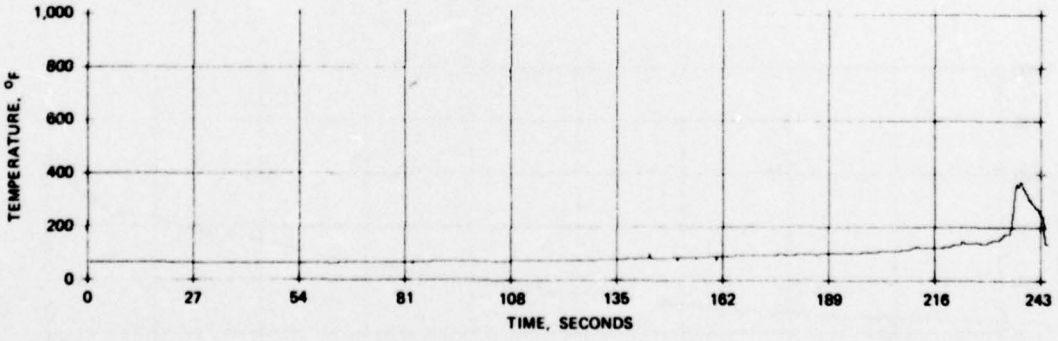

FIGURE E-13. Output of Thermocouple Attached to Screw on Back Side of Cockpit Bulkhead (Inside Cockpit).

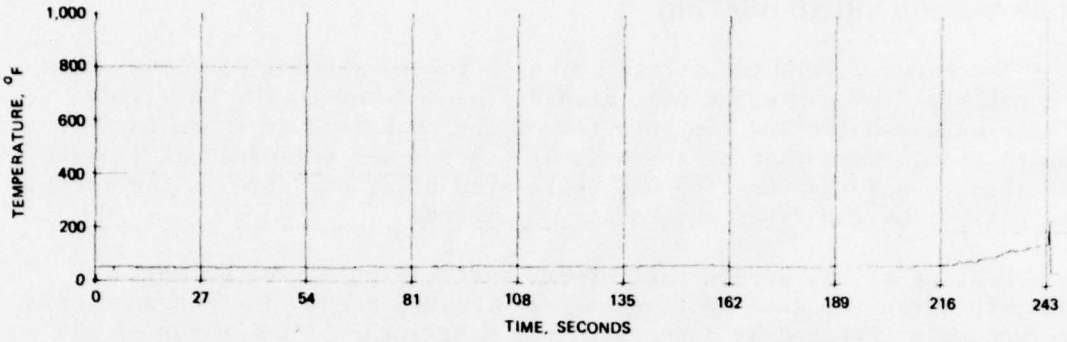

FIGURE E-14. Output of Thermocouple Attached to Screw in Wear Plate on Top of Cockpit Floor Covering About 4 Inches (10 cm) Aft of Forward Bulkhead.

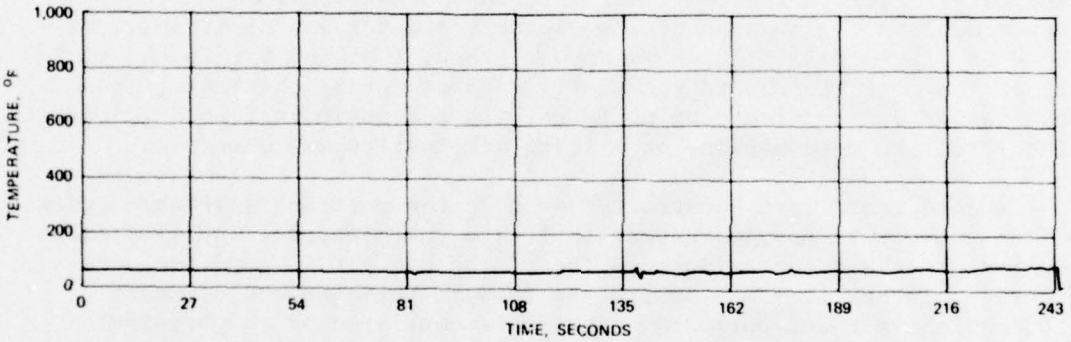

FIGURE E-15. Response of Slug Calorimeter on Cockpit Floorboard Facing Down. About 4 Inches (10 cm) From Forward Bulkhead and About 8 Inches (20 cm) Left of Centerline.

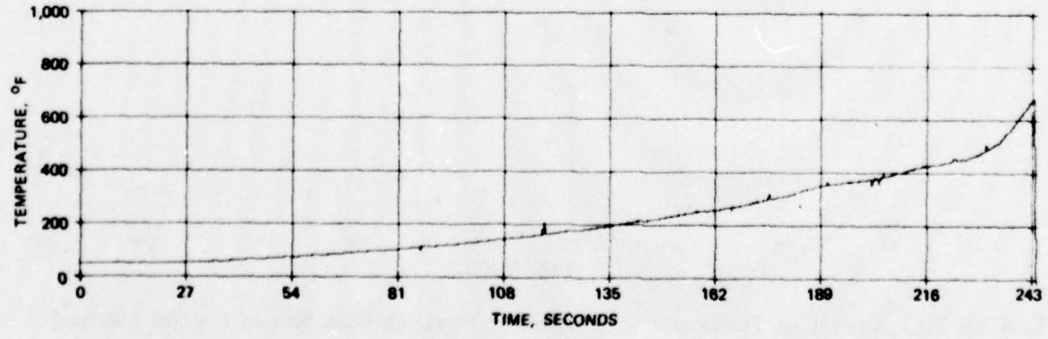

FIGURE E-16. Response of Thermocouple on Port Access Door.

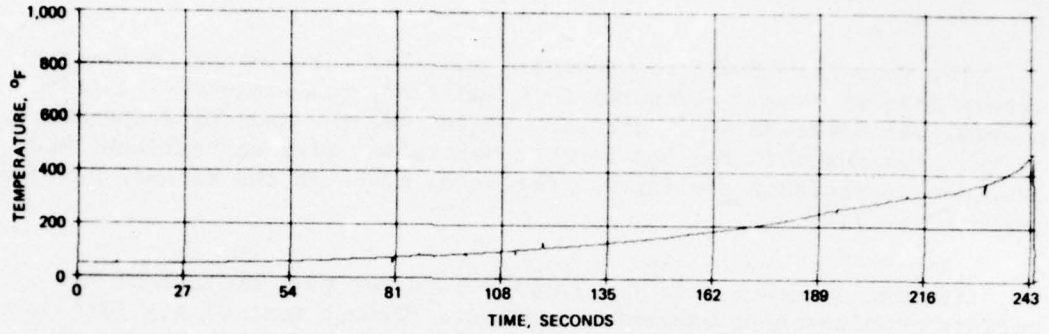

FIGURE E-17. Response of Slug Calorimeter on Port Access Door.

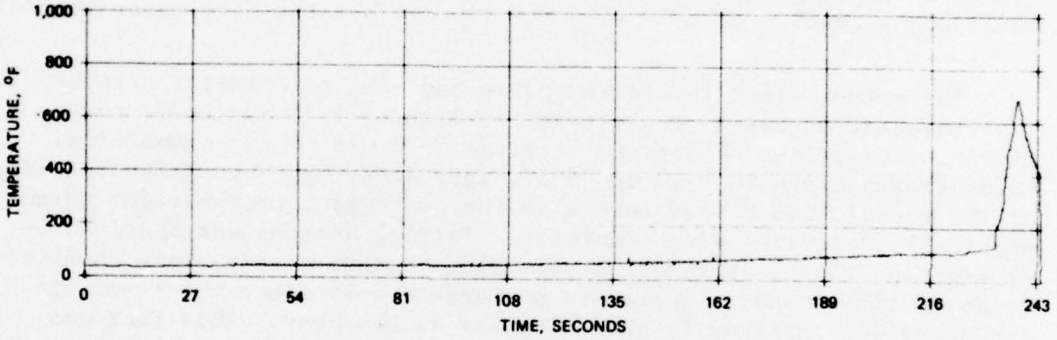

FIGURE E-18. Response of Thermocouple About 20 Inches (51 cm) Above Cockpit Floorboard in Upper Interior Corner Formed by Forward Bulkhead and Port Side.

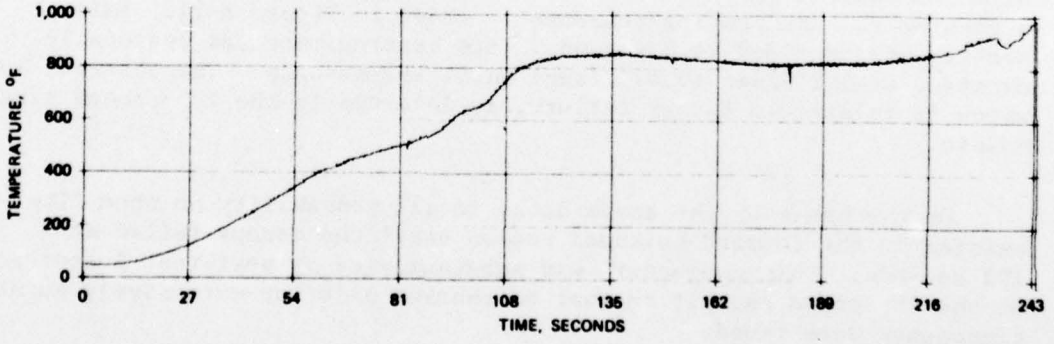

FIGURE E-19. Response of Thermocouple Attached to Starboard Access Door.

The response of the thermocouple and slug calorimeter on the port access door is shown in Figures E-16 and E-17, respectively. Initial heating was detected at 27 seconds. Note that the melting temperature of the aluminum skin was not reached before the fire was extinguished. Also, no appreciable cooling was detected, although the firemen had just put out the fire.

Further evidence that the forward interior port section of the cockpit remained near ambient temperature through most of the fire is suggested by a thermocouple located in the upper corner between the forward bulkhead and the port side approximately 20 inches (508 mm) above the floorboard. The response of that thermocouple is shown in Figure E-18. Modest heating is shown up to 232 seconds, at which time hot effluent gas caused a dramatic temperature rise that continued until 238 seconds. At this time the firemen had the fire under control.

The outputs from the thermocouple and slug calorimeter attached to the starboard access door are shown in Figures E-19 and E-20, respectively. Comparison of Figures E-19 and E-20 with their symmetrical counterparts, Figures E-16 and E-17, indicates that the starboard side of the cockpit was heated more than the port side, probably due to the previously described wind condition. Initial heating was observed at 11 seconds. The starboard fuselage skin reached steady-state conditions at about 113 seconds. There was no burn-through since the frame and stringers were apparently absorbing the excess heat. This fact was confirmed by post-test inspection. The heat flux impinging on the starboard side of the cockpit was about 0.1 BTU/ft^2-sec (1134 W/m^2) compared with about 0.01 BTU/ft^2-sec (113 W/m^2) on the port side.

A thermocouple was placed behind the instrument panel in the forward bulkhead region with a direct view of the sky through the glareshield access hole. Its heating response is shown in Figure E-21. Initial heating was recorded at 8 seconds. Its heating rate was reasonably constant at 1.2°F/sec (0.67°C/sec) until 162 seconds. The observed hump, which is related to canopy failure, is detected in the 195-second time domain.

On the basis of the above data, in all probability no open fire existed in the forward bulkhead region until the canopy failed at 192 seconds. This conjecture was substantiated by post-test inspection of the dissected cockpit in that no charred paint or extensively burned components were found.

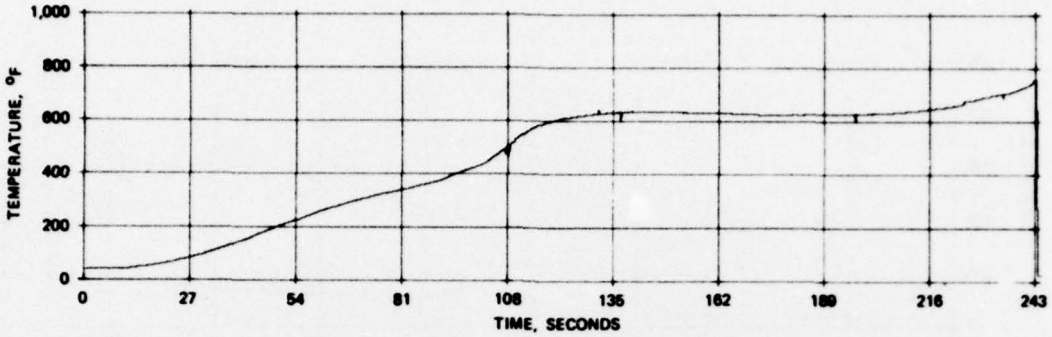

FIGURE E-20. Response of Slug Calorimeter Attached to Starboard Access Door.

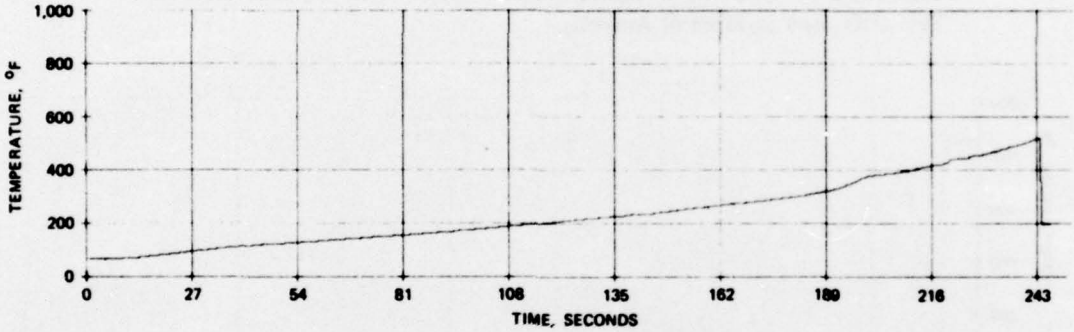

FIGURE E-21. Response of Thermocouple Placed Behind Instrument Panel Near Forward Bulkhead and With Direct View of Sky Through Glareshield Access Hole.

PORT AND STARBOARD SIDE HEATING

A thermocouple was placed 5 inches (127 mm) from each side of the cockpit in front of each armrest. The output from these two thermocouples is shown in Figures E-22 and E-23 for the port and starboard sides, respectively. Interior cockpit self-heating (material decomposition) behavior is indicated on the port side between 96 and 161 seconds; then similar response is observed between 220 seconds and the end of the test. Similarly, for the starboard side, cockpit material decomposition behavior is indicated between 104 and 135 seconds. These peculiar responses occur in the same time frame that the cockpit toxic gases exhibited unexpected "reversals." Fire was observed to occur at 231 seconds.

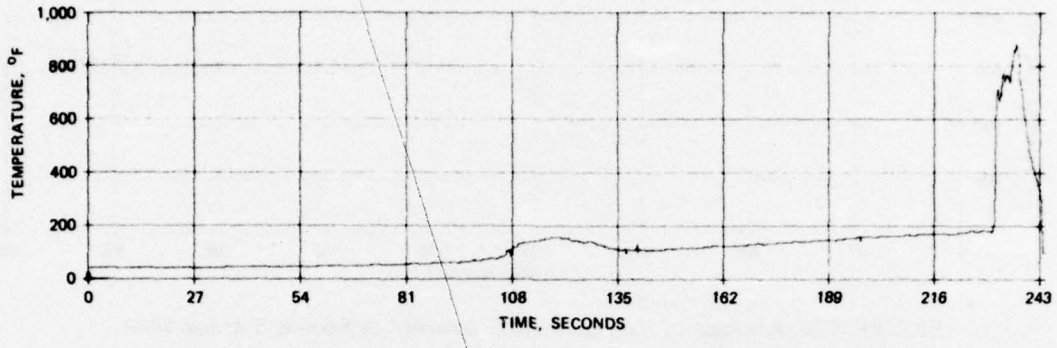

FIGURE E-22. Response of Thermocouple 5 Inches (12.7 cm) From Starboard Side of Cockpit in Front of Armrest.

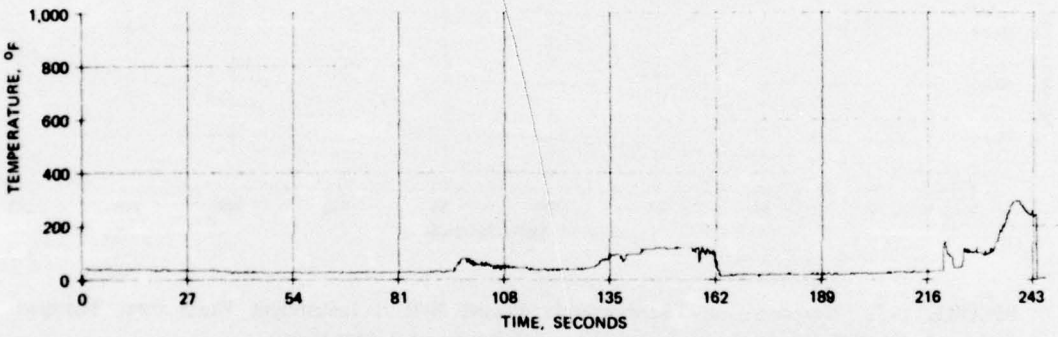

FIGURE E-23. Response of Thermocouple 5 Inches (12.7 cm) From Port Side of Cockpit in Front of Armrest.

Thermocouples were also placed adjacent to the upholstery at the elbow region on both the port and starboard sides. Their response is shown in Figures E-24 and E-25, respectively. No appreciable heating was recorded, hence it is suspected that the heat observed above was due to smoldering material forward of, rather than behind, the pilot's position.

Thermocouples were attached to both the starboard and port sides of the instrument panel facing the pilot's seat. The outputs from these thermocouples are shown in Figures E-26 and E-27, respectively. As was confirmed by post-test inspection, no appreciable heating was present until the canopy failed.

Another thermocouple was attached within the smoke tube of the smoke-measuring transducer, which was attached to the instrument panel (Figure H-6). The output from this thermocouple is shown in Figure E-28. No appreciable heat was recorded until the canopy failed.

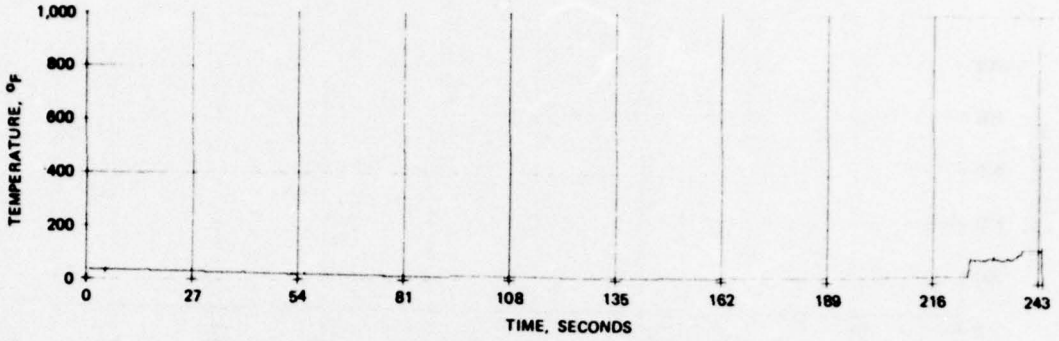

FIGURE E-24. Response of Thermocouple Adjacent to Upholstery at Elbow Region on Port Side of Cockpit.

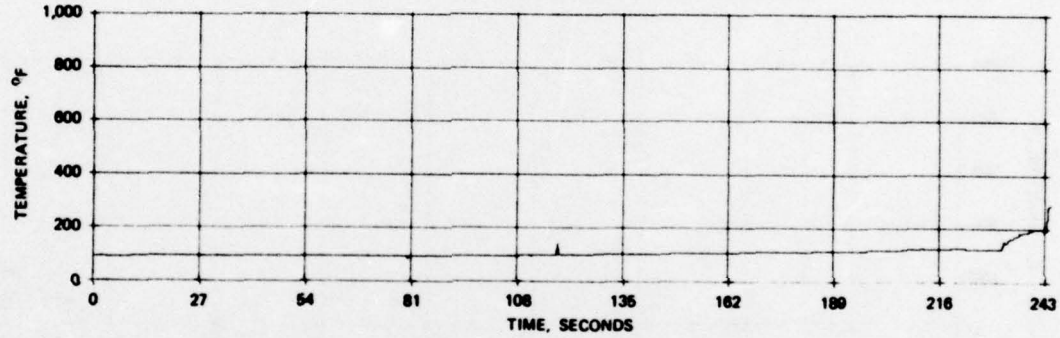

FIGURE E-25. Response of Thermocouple Adjacent to Upholstery at Elbow Region on Starboard Side of Cockpit.

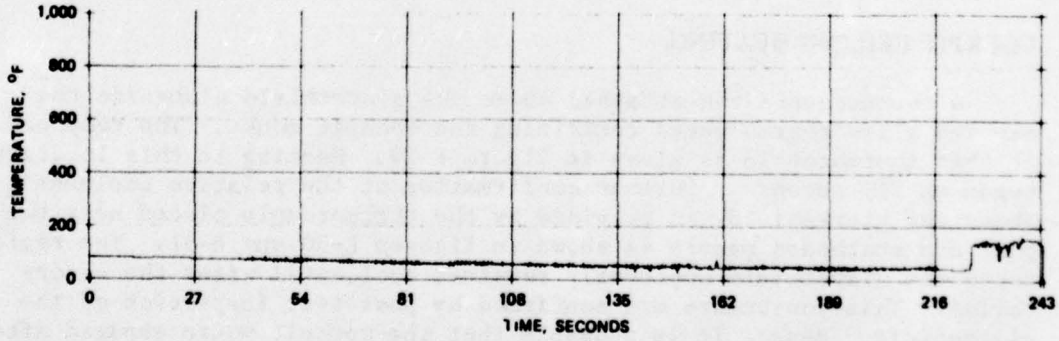

FIGURE E-26. Response of Thermocouple Attached to Starboard Side of Instrument Panel Facing Pilot's Seat.

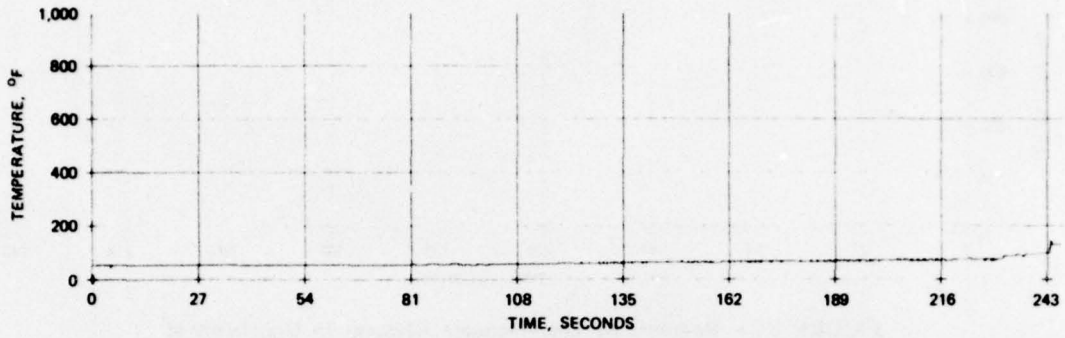

FIGURE E-27. Response of Thermocouple Attached to Port Side of Instrument Panel Facing Pilot's Seat.

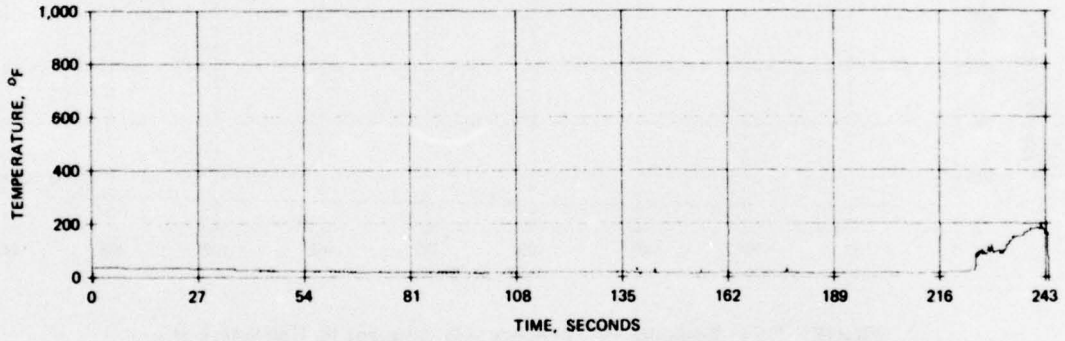

FIGURE E-28. Response of Thermocouple Attached Inside Hollow Tube of Smoke Transducer.

COCKPIT CEILING HEATING

A thermocouple was attached above the glareshield alongside the exposed glass ferris wheel containing the cockpit mouse. The response of this thermocouple is given in Figure E-29. Heating in this location began at 211 seconds. Further confirmation of the relative coolness above the glareshield was provided by the thermocouple placed near the port and starboard panels as shown in Figures E-30 and E-31. The region above the glareshield apparently remained cool until after the canopy failed. This conjecture was confirmed by post-test inspection of the glareshield. Hence, it is probable that the cockpit mouse expired after the canopy failed.

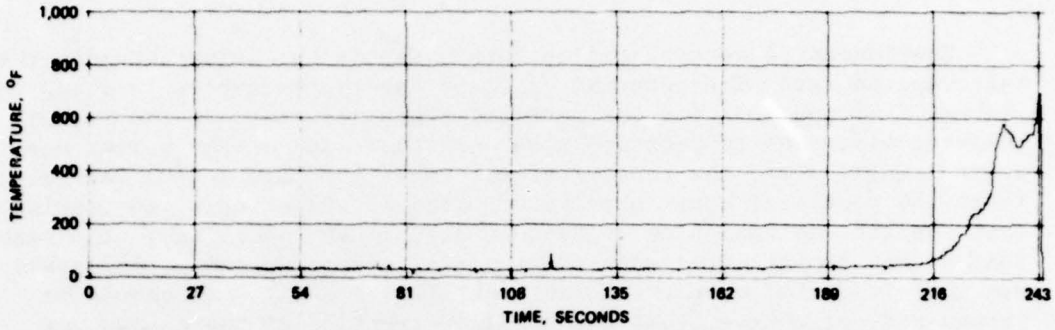

FIGURE E-29. Response of Thermocouple Attached Alongside Glass Ferris Wheel Above Glareshield.

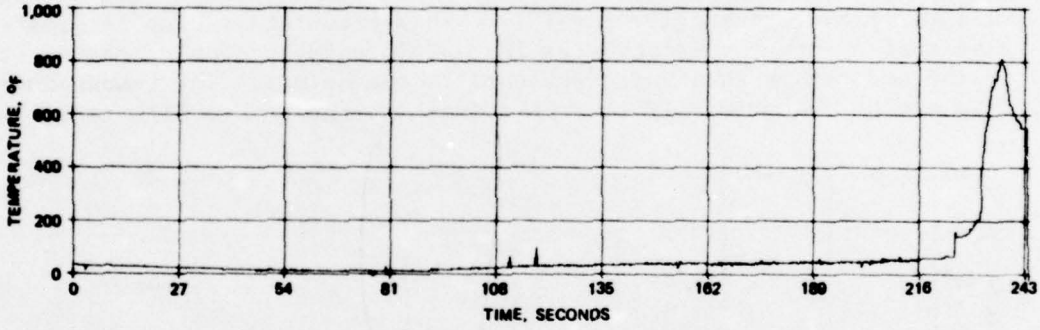

FIGURE E-30. Response of Thermocouple Placed Above Glareshield Near Port Panel.

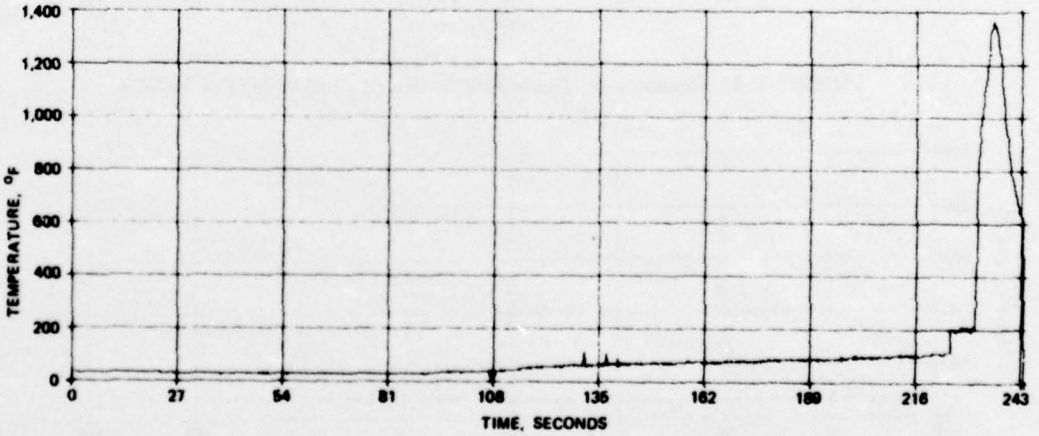

FIGURE E-31. Response of Thermocouple Placed Above Glareshield Near Starboard Panel.

Thermocouples were placed on both sides of the helmet housing the instrumented rat. The response of these two thermocouples is shown in Figures E-32 and E-33 for the port and starboard sides of the helmet, respectively. The temperature rise on either side of the helmet was nominal until after the canopy failed. Note (in Figure G-9) that significant EEG postictal rate activity occurred at 133 seconds, suggesting that the rat was beginning to sense heat through the canopy. The reason that higher temperatures were not recorded after the canopy collapsed was that it melted over the helmet (see Figure E-34). It should be recognized, of course, that the final destruction of the canopy was caused by the firefighters.

A thermocouple was also placed aft of the pilot's helmet. Its response is shown in Figure E-35. This thermocouple recorded a definite steady rise in temperature from about 27 seconds. At the time of canopy failure it had reached 127°F (51°C). This temperature rise is greater than that of other thermocouples in the vicinity, probably because it was in the air rather than being attached to the helmet. The temperature rise may be due primarily to free convection and not to fire radiation.

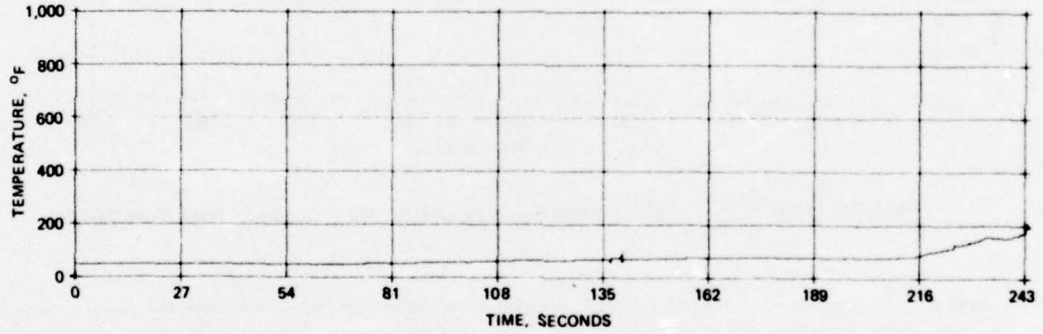

FIGURE E-32. Response of Thermocouple Placed on Port Side of Helmet.

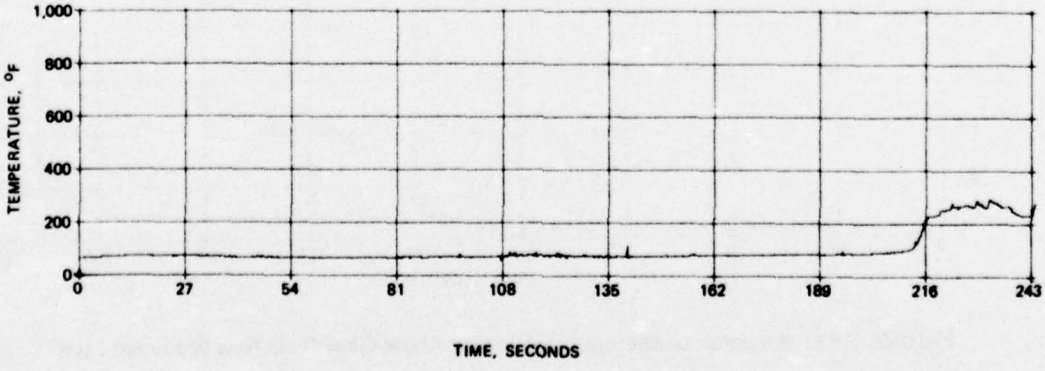

FIGURE E-33. Response of Thermocouple Placed on Starboard Side of Helmet.

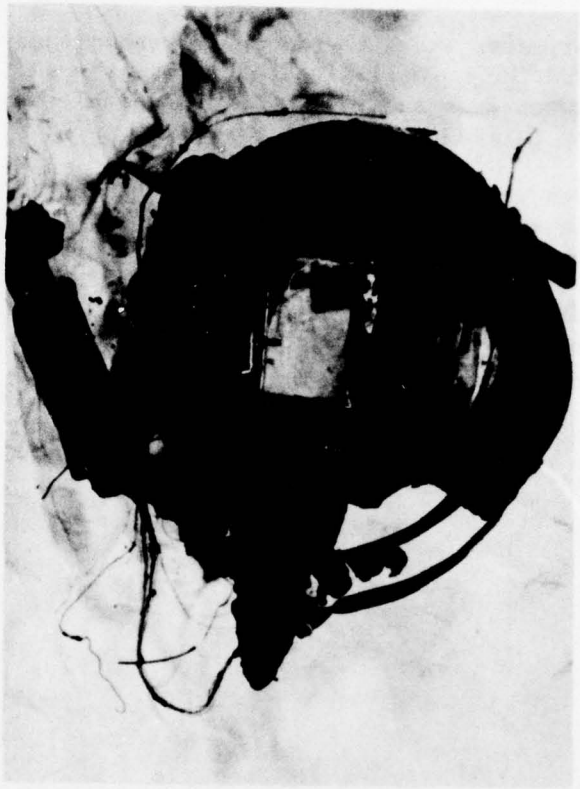

FIGURE E-34. Helmet and Bottom View of Rat After Fire. (Neg. LHL 187362)

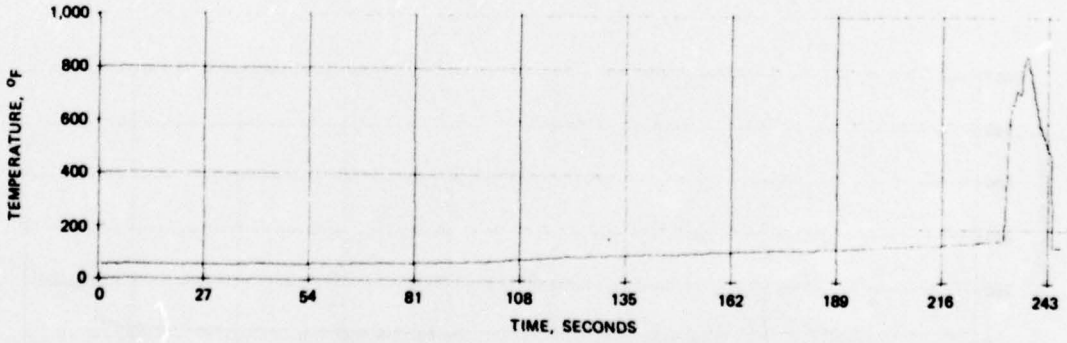

FIGURE E-35. Response of Thermocouple Placed Behind Pilot's Helmet.

A slug calorimeter and a thermocouple were placed on top of the seat frame (behind the helmet) directed toward the sky. Their outputs are shown in Figures E-36 and E-37. No appreciable heating was recorded before the canopy failed.

Thermocouples were attached to screws on the inside of the forward metal rim holding the leading edge of the canopy. The response of those thermocouples for the port, top, and outside regions are shown in Figures E-38, E-39, and E-40, respectively. Again, heating is shown not to be significant until after the canopy fractured. The relatively high heating response after the canopy failed suggests that the fire already existed forward of the pilot (manikin), as confirmed by the movie camera in the manikin, but required the top venting to propagate inside. Fire penetrated the starboard top side of the canopy first, as confirmed by the movie,[1] thus providing the required vent.

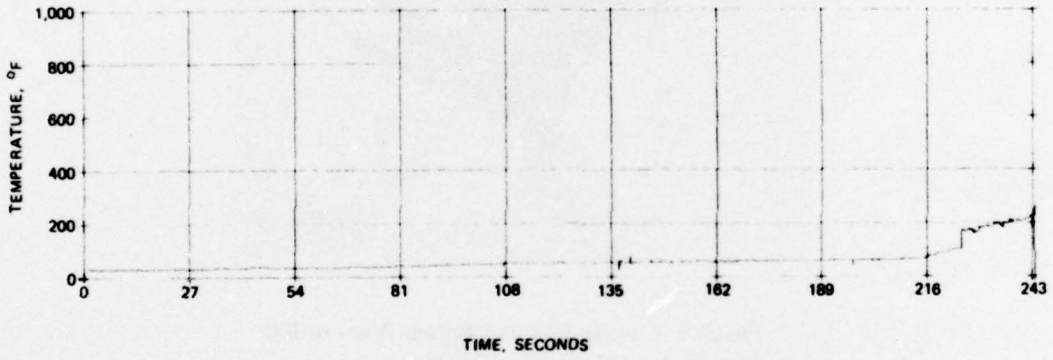

FIGURE E-36. Response of Slug Calorimeter Placed on Top of Seat Frame Behind Helmet and Directed Toward Sky.

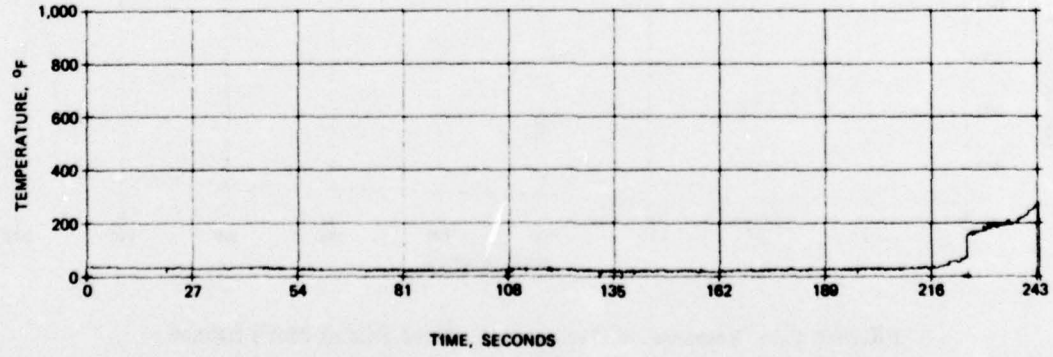

FIGURE E-37. Response of Thermocouple Placed on Top of Seat Frame Behind Helmet and Directed Toward Sky.

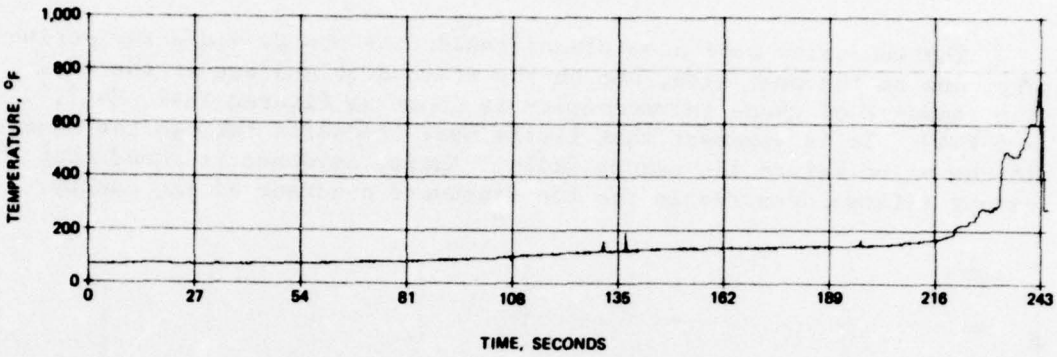

FIGURE E-38. Response of Thermocouple Attached to Screw on Inside of Metal Rim Holding Leading Edge of Canopy in Port Region.

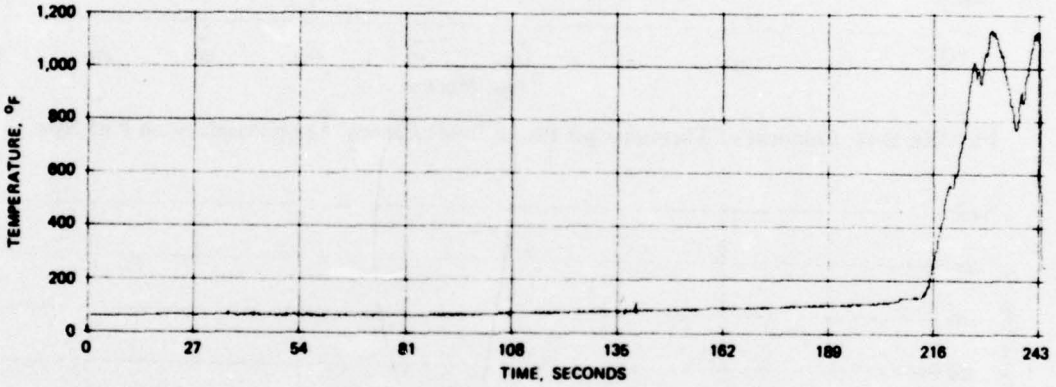

FIGURE E-39. Response of Thermocouple Attached to Screw on Inside of Metal Rim Holding Leading Edge of Canopy in Top Region.

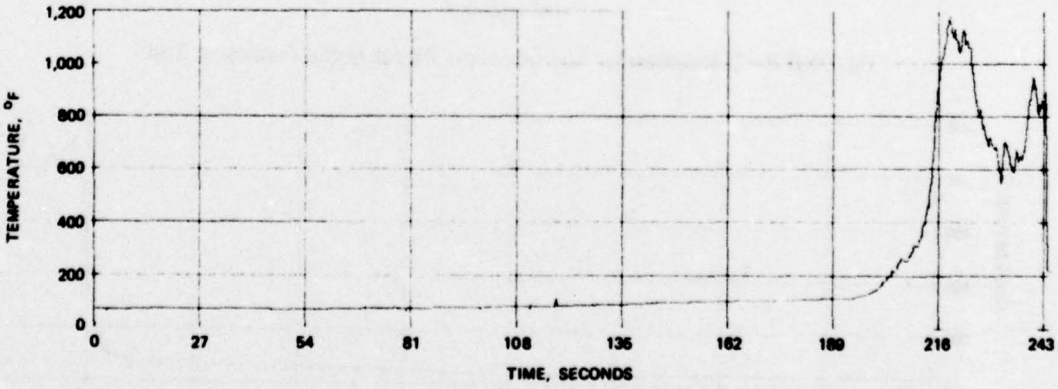

FIGURE E-40. Response of Thermocouple Attached to Screw on Inside of Metal Rim Holding Leading Edge of Canopy in Starboard Region.

Thermocouples were also placed inside the canopy along the periphery; one on the port side, one on the starboard, and one at the top. The response of these thermocouples is shown in Figures E-41, E-42, and E-43. It is apparent that little heat transmits through the canopy to the pilot before the canopy fails. Again, evidence is found that the canopy failure occurred in the top starboard quadrant of the canopy.

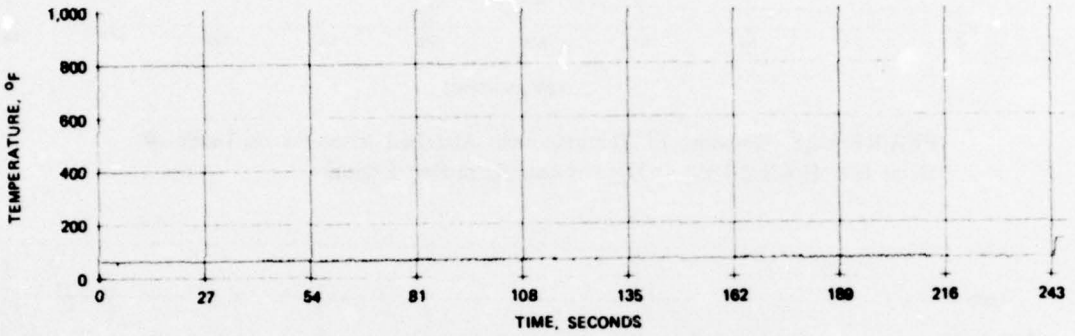

FIGURE E-41. Response of Thermocouple Placed Inside Canopy Along Periphery on Port Side.

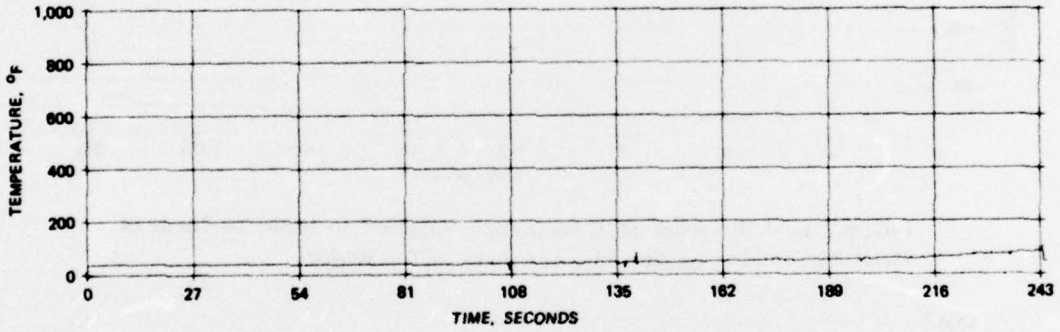

FIGURE E-42. Response of Thermocouple Placed Inside Canopy at Top.

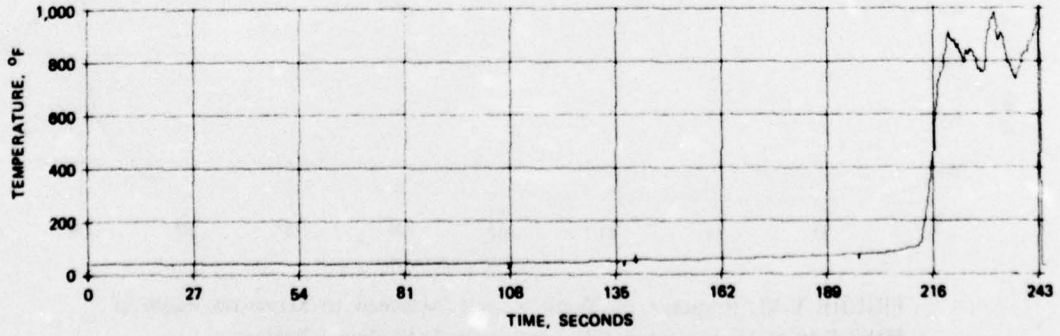

FIGURE E-43. Response of Thermocouple Placed Inside Canopy Along Periphery on Starboard Side.

COCKPIT FLOOR HEATING

The output of a slug calorimeter attached to the starboard floorboard forward of the pilot's position is shown in Figure E-44. This slug calorimeter was located 22 inches (559 mm) aft of the forward bulkhead. The data suggest no appreciable heating penetrated the forward starboard floorboard.

A thermocouple was placed on the pilot's seat above the aft floorboard. The response of this thermocouple is shown in Figure E-45. The heating begins at 59 seconds. The heating is due to fire in the wheel well eventually penetrating the floorboard and heating the seat from below. Post-test inspection revealed that the floorboard under the seat had melted and burned through. It is possible that this event contributed to or caused the anomaly in the development of toxic gases between 120 and 150 seconds that is discussed in Appendix F.

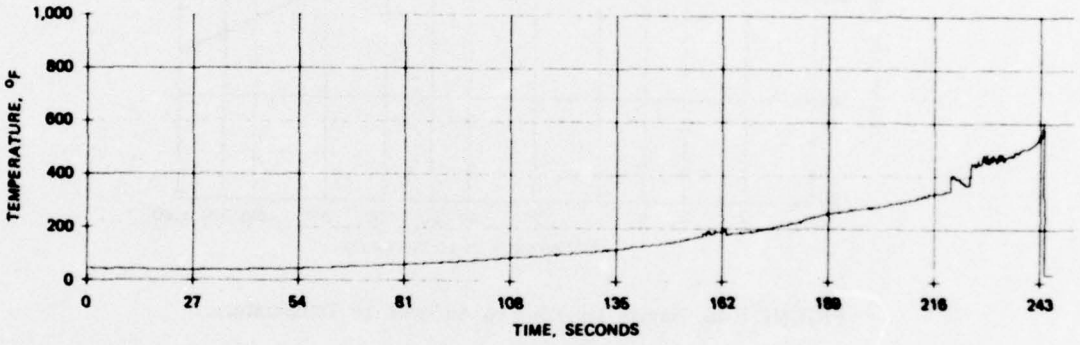

FIGURE E-44. Response of Slug Calorimeter Attached to Starboard Floorboard Forward of Pilot's Position.

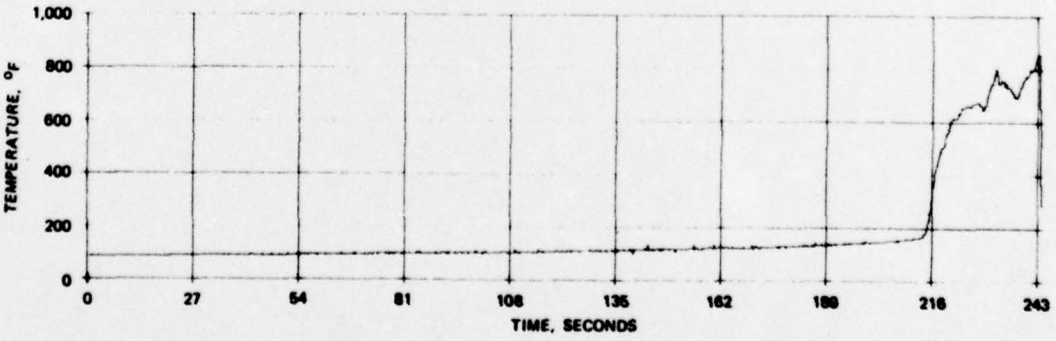

FIGURE E-45. Response of Thermocouple Placed on Pilot's Seat Above Aft Floorboard.

PILOT TOLERANCE TO AIR TEMPERATURE

The temperature data presented above indicate that this cockpit engulfed in a pool fire remained relatively cool up to the time the canopy failed. Though the measured temperatures would cause discomfort, they could readily be tolerated by a pilot, as suggested by the curve in Figure E-46, which was taken from an Army report on crash survival.[10]

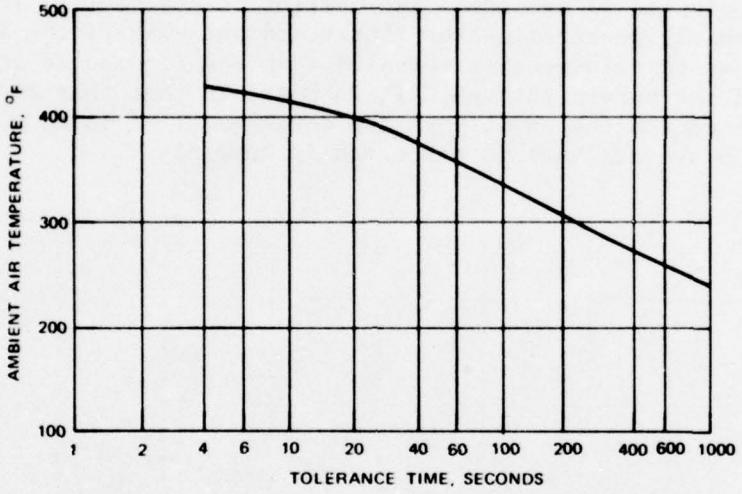

FIGURE E-46. Human Tolerance to Ambient Air Temperature.

[10] Army Air Mobility Research and Development Laboratory. *Crash Survival Design Guide.* Fort Eustis, Va., October 1971. (Tech Report 71-22, p. 373, AD 733 358, publication UNCLASSIFIED.)

Appendix F

TOXIC GAS APPARATUS AND MEASUREMENTS

Appendix F
TOXIC GAS APPARATUS AND MEASUREMENTS

One of the objectives of this study was to obtain baseline data on toxic gases in a sealed cockpit during the fire. Excluded from the cockpit were pilot's clothing, parachute, charts, and paraphernalia on the basis that, if such items burned, the cockpit would be considered uninhabitable at such time. In general, the chemical compositon of materials used in Navy cockpits are not known. Therefore, data collected from a single aged cockpit are not statistically significant, but do have value in the baseline context used in this study. In a carrier deck fire the presence of toxic gases could be a critical factor, if self-contained breathing/eye cover equipment were not available. Eye irritation, impairment of breathing, and degradation of the mental faculties could conceivably incapacitate a pilot or prevent him from functioning alertly or aiding in his own rescue (present Navy SOP is to eject and not take chances). Data from a test such as this one can be used for estimating acceptable levels of toxic gas production for specifying cockpit materials, e.g., specifying the measured baseline concentrations as acceptable or unacceptable.

Dangerous toxic effects associated with fires are usually related to the presence of materials such as chlorine, cyanide, and carbon monoxide and to the depletion of oxygen. Other noxious gases include hydrogen sulfide, sulfur dioxide, ammonia, and nitric oxide. Probably many potential toxic gases and their effects have yet to be identified. Hence the practice has been to measure the popular species, since practical measuring tools are readily available. On the basis of a literature search and interviews with persons active in fire-related toxicology, a number of methods of measuring and analyzing such gases was considered.[11] From among them, the few that seemed most appropriate to the objectives of this study were selected to obtain baseline data. It is important to note that experimental toxicity is presently advancing quickly, and hence the approach used is only indicative of the potential candidate tools and methods available.

[11] G. Longelle and C. Verdier. "Gas Sampling and Analysis in Combustion Phenomena," AGARD Vugraph No. 168, North Atlantic Treaty Organization, Advisory Group for Aerospace Research and Development. Hartford House, London, July 1973. P. 180.

The selected methods were combined into a system that is shown schematically in Figure F-1. Potential sources of inaccuracies are many, such as absorption losses to plumbing. Reasonable precautions were taken in the context of practicality. The accuracy of the approach used in this study can be surmised by the consistency of the data collected. As indicated, air was circulated from the cockpit through 1/4-inch (6-mm) stainless steel tubing to the tunnel below, where it was sampled by the various transducers. The rate of air circulation was 0.022 m^3/min. At the first station, water only was removed from the gas by means of a dehydrator (Model PD-750-12 Perma Pure Dryer, Oceanport, N.J.). Next, 10-μm and 5-μm filters were used to remove particulates. After that the gas was cooled to 65°F (18°C) by passing the tubing through a water bath. Next 0.05-liter gas samplers (Pyrex, Corning 7740) were filled for subsequent analysis. The remaining gas was then balanced for redistribution from a stainless steel manifold into a NO/NOX chemiluminescence monitor (Model AA-2, AeroChem Research Laboratory, Princeton, N.J.), a carborn dioxide infrared monitor (Model 864, Beckman Instruments, Fullerton, Calif.), repackaged chlorine and cyanide specific ion monitors (Models 94-17 and 94-06, Orion Research, Cambridge, Mass.), and two glass containers (Pyrex, Corning 7740) holding an instrumented rat and a free-running mouse on a glass treadmill. Then, after passing through a mass flowmeter and a pressure regulator, nitrogen was added to the remaining gas (about 0.001 m^3/min) and the gas was reheated to existing cockpit temperature. Finally it was returned to the cockpit. Figure F-2 is a schematic of the physical arrangement of the elements of this system. A photograph of the actual arrangment during preparation is shown in Figure F-3.

The gas sampler apparatus is shown in Figure F-4. Figure F-5 is a schematic of the timing electronics used to control 20 pairs of solenoid valves in the apparatus. Between each pair of valves is attached a 0.05-liter glass container incorporating a septum for withdrawing trapped gas. The timing electronics can be programmed to operate over intervals of between 1 and 20 seconds per channel. Only 15 of the available channels were used in this test to trap gas samples in the glass containers at ambient tunnel temperature (about 65°F or 18°C). The other five channels were used to trap gas for a separate analysis conducted by the University of Utah Flammability Research Center (UUFRC). The description of the traps used on these five channels and of the ensuing analysis of the trapped gas is given below. The 15 gas samples collected in glass (Pyrex, Corning 7740) containers were analyzed at ambient conditions by means of a gas chromatograph at NWC (Model 8500, Carle Instruments, Fullerton, Calif.). The other five samples were collected in stainless steel tubing containing trapping material developed by the Flammability Research Center. These tubes were immersed in liquid nitrogen while the gas was trapped, and the samples remained stored in liquid

nitrogen until they reached the Flammability Research Center for analysis by gas chromatograph/mass spectrometer (GC/MS). A recent journal article gives a good description of the operation of the GC/MS.[12]

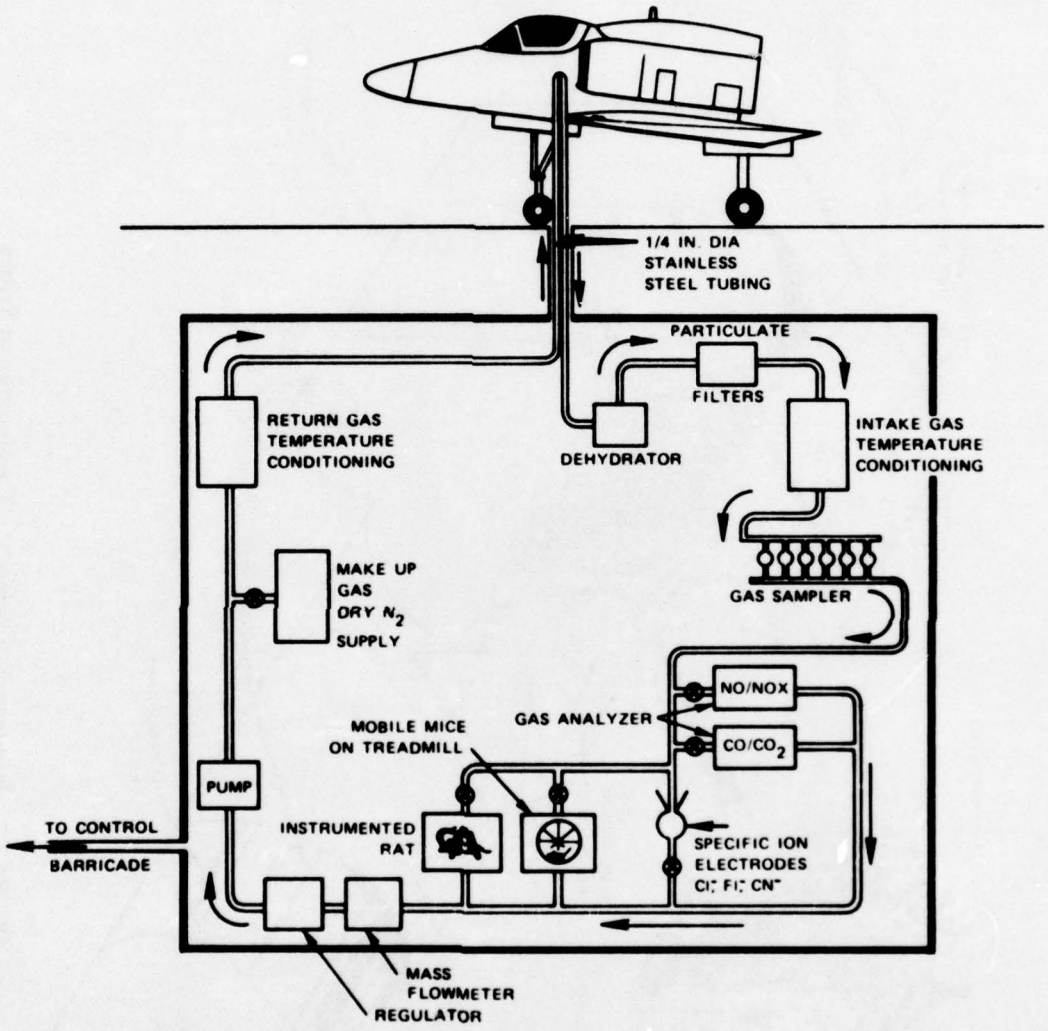

FIGURE F-1. Schematic of Gas Measurement System.

[12] S. R. Heller, et al. "Trace Organics by GC/MS," *Environmental Science and Technology*, Vol. 9 (March 1975), p. 210.

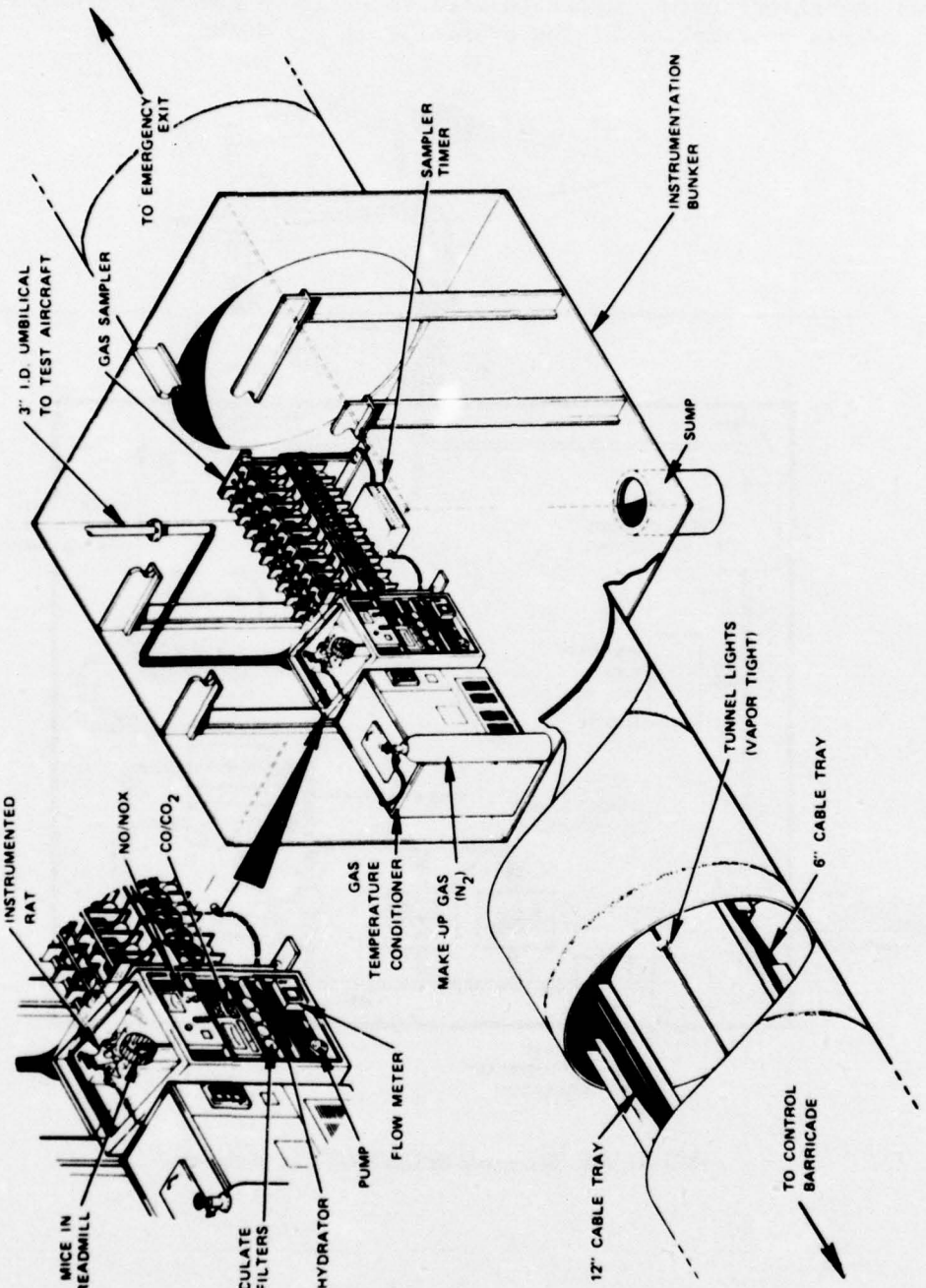

FIGURE F-2. Arrangement of Elements of Gas Measurement System.

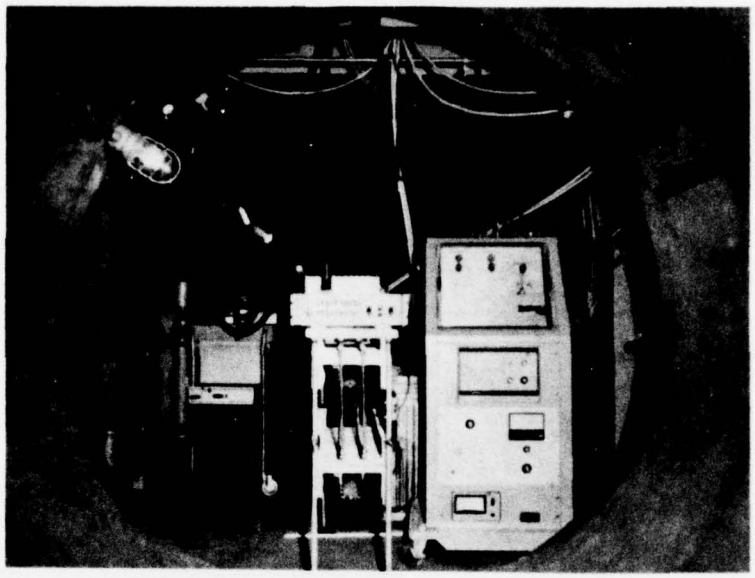

FIGURE F-3. View of Instrumentation Bunker Before Test. (Neg. LHL 186990)

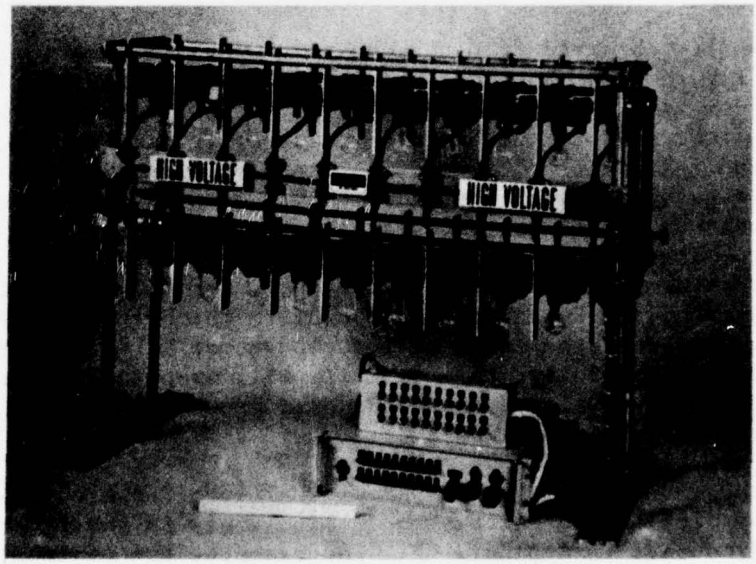

FIGURE F-4. Gas Sampling Apparatus. (Neg. LHL 192252)

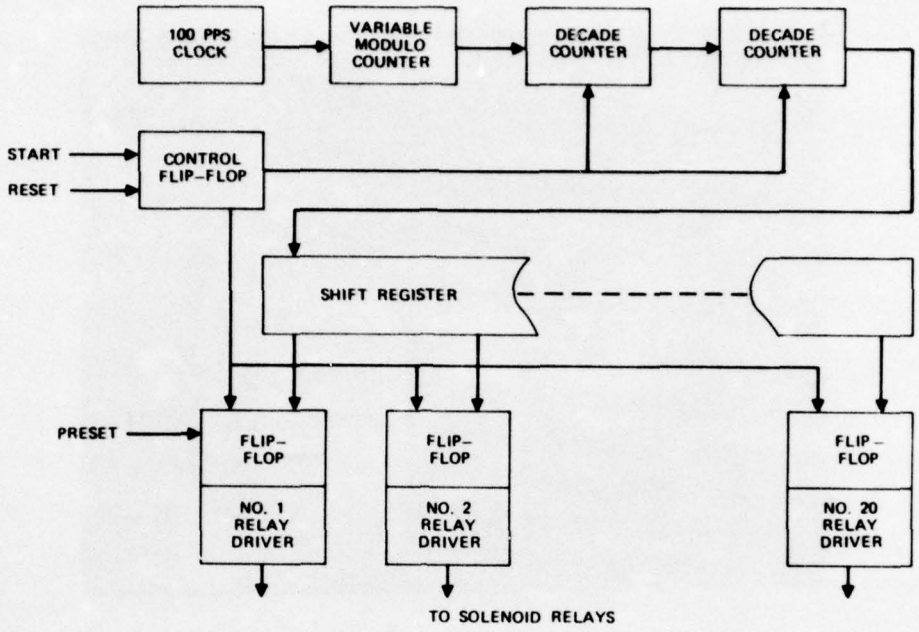

FIGURE F-5. Schematic of Timing Electronics for Gas Sampling Apparatus.

NWC GAS ANALYSIS

The results obtained from the analysis of the 15 gas samples are plotted in Figure F-6. The concentrations of oxygen, carbon dioxide, and carbon monoxide are shown, along with the concentrations of Cl^- and CN^- ions as indicated by the output from the specific ion electrodes. Note that the initial production of carbon dioxide and carbon monoxide correspond with the initial depletion of oxygen at about 55 seconds. At about 120 seconds a peculiar reversal occurs, suggesting that air entered the cockpit. Then at 150 seconds the depletion of oxygen and the production of carbon dioxide, carbon monoxide, Cl^-, and CN^- resumes. The data from the Flammability Research Center confirm the peculiar reversal (see Table F-4). However, the cause of the phenomenon is open to subjective interpretation. Hopefully, this reversal will eventually be explained by the model to be developed using the data generated in this report and in subsequent planned experiments.

That the quantitative values shown in Figure F-6 are reasonable is supported by data on the carboxyhemoglobin levels in the rat and mouse (which is discussed in Appendix G). For example, the maximum concentration of carbon monoxide measured (at 171 seconds) was about 4,400 ppm for a short period of time. Tables F-1 and F-2 suggest that the data point is reasonable. Table F-1 shows a lethal concentration for rats as 60 minutes for concentrations of 4,650 ppm, and Table F-2 shows that the

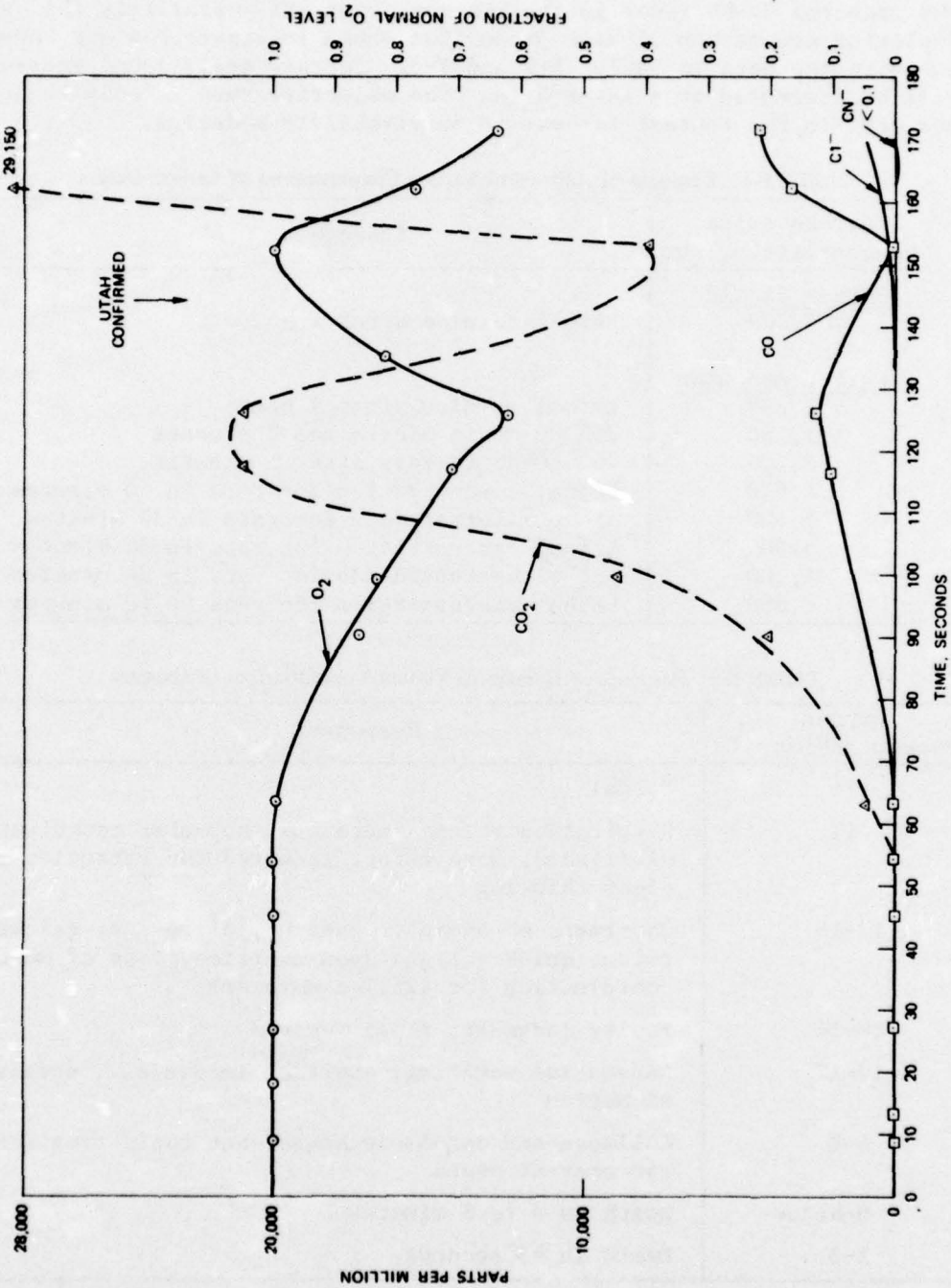

FIGURE F-6. Plot of NWC Gas Analysis.

50% CO-Hb level is reached in minutes in rats for a CO concentration of 5,000 ppm. Note that it is reported under "Animal Test Results" that the measured CO-Hb level in the rat was about 49%. Similarly the oxygen depletion and carbon dioxide production shown in Figure F-6 are consistent with the data in Tables F-2 and F-3. Further analysis of these data will be presented at a later date. The objective here is only to present the data in the context for use in survivability modeling.

TABLE F-1. Response of Animals to Various Concentrations of Carbon Oxides.

Carbon oxide concentration, ppm	Effects
Carbon dioxide	
400,000	Lethal to mice after 4 hours
Carbon monoxide	
1,250	Lethal to mice after 4 hours
1,500	25% CO-Hb in mice after 5 minutes
2,100	25% CO-Hb in rats after 5 minutes
4,670	Lethal concentration for rats in 60 minutes
5,000	Minimum lethal dose for rats in 30 minutes
5,500	Lethal concentration for rats in 30 minutes
6,100	Lethal concentration for rats in 20 minutes
8,800	Lethal concentration for rats in 10 minutes

TABLE F-2. Response of Humans to Various Concentrations of Oxygen.

Oxygen concentration, %	Response
21	Normal
17	Respiration volume increased, muscular coordination diminished, more effort required for attention and clear thinking
12-15	Shortness of breath, headache, dizziness, quickened pulse, quick fatigue upon exertion, loss of muscular coordination for skilled movements
10-14	Faulty judgment, rapid fatigue
10-12	Nausea and vomiting, exertion impossible, paralysis of motion
6-8	Collapse and unconsciousness, but rapid treatment can prevent death
6-below	Death in 6 to 8 minutes
2-3	Death in 45 seconds

TABLE F-3. Response of Humans to Various Concentrations of Carbon Dioxides.

Concentration, ppm	Symptoms
250 to 350	Normal concentration in air
900 to 5,000	No effect
5,000	TLV and MAK value
18,000	Ventilation increased by 50%
25,000	Ventilation increased by 100%
30,000	Weakly narcotic, decreasing acuity of hearing, increase in pulse and blood pressure
40,000	Ventilation increased by 300%, headache, weakness
50,000	Symptons of poisoning after 30 minutes, headache, dizziness, sweating
80,000	Dizziness, stupor, unconsciousness
90,000	Distinct dyspnea, loss of blood pressure, congestion, death within 4 hours
100,000	Headaches and dizziness
120,000	Immediate unconsciousness, death in minutes
200,000	Narcosis, immediate unconsciousness, death by suffocation

UNIVERSITY OF UTAH GAS ANALYSIS

Dr. Kent Vorhees of the UUFRC collected gaseous products in five stainless steel U-tubes containing porous polymer (proprietary item) traps from the aircraft burn. These tubes were immediately flown back to the FRC for gas chromatograph/mass spectrograph analysis. The procedure and results of the analysis are discussed in the following paragraphs.

The traps, cooled to -190°C, were connected to the interface block shown in Figure F-7. An aluminum block heated to 180°C was then placed over the U-tube, and the products were desorbed onto a 0.125-inch (3-mm) by 8-ft (2.4-m) stainless steel (Chromosorb 101) column, cooled to -20°C. The products were then separated by programming the gas chromatograph to 220°C at 10°C/min, then holding for 6 min, and finally programming to 250°C at 10°C/min. Table F-4 summarizes the GC/MS analysis of the five traps.

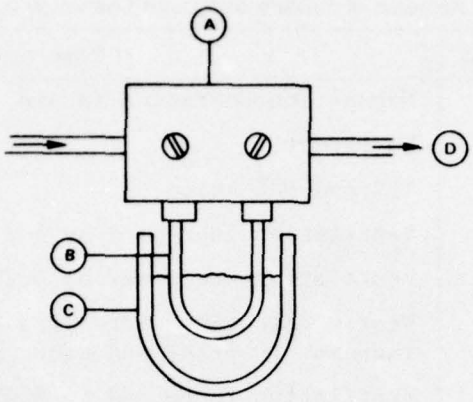

A INTERFACE HOUSING VALVES
B U-TUBE TRAP CONTAINING ABSORBING SUPPORT
C COOLANT OR HEAT SOURCE FOR ABSORPTION OR DESORPTION STEP
D EFFLUENT TO ADDITIONAL STAGES OF TRAPPING

FIGURE F-7. University of Utah Apparatus for Trapping Gases.

The values listed directly under the trap number are the electronic integrator responses. These are an indication of concentration, but cannot be used as absolute concentrations until corrected for response factors. Such correction was not incorporated into this study. However, direct comparison of the absolute concentration can be made for the same individual species present in all five traps.

The relative values in Table F-4 allow an assessment to be made in terms of the amount of materials developing as a function of time. It is clear that only Trap 5 showed the type of products expected as a consequence of combustion. The University of Utah analysts feel that the concentrations of the materials in Trap 5, plus new products, would have increased if the experiment had been allowed to go on for another couple of minutes. Indications are that the collection of samples should be timed in future tests to allow air at the final cockpit atmosphere to flow through the sampling tubes into the trapping system.

They also checked for JP-5 fuel in all traps and failed to find any of this material. One can conclude that, either because of the wind during the test or the low volatility of JP-5 fuel, none of this material reached the area of the sampling tubes.

It should be noted that the effects of the filters and dehydrator (Figure F-1), stainless steel, and glass on the removal of chemical species were not evaluated.

TABLE F-4. Summary of Analysis of Gases Produced at China Lake Burn Test.

Compound	Relative concentrations (electronic integrator responses) at listed times and traps				
	Time after ignition, sec				
	36	72	108	144	180
	Trap number[a]				
	1	2	3	4	5
Air + CO	114,003[b]	141,024	140,809	85,086	149,957
Methane (CH_4)					
Carbon dioxide (CO_2)	122	131	77	85	1,771
Ethylene (C_2H_4)	...	...	...	1	66
Acetylene (C_2H_2)	...	...	...	Tr	24
Ethane (C_2H_6)	...	...	...	...	5
NI[c]	...	25	...	...	...
NI	200[d]	10[d]	7[d]	20[d]	400[d]
Propene	...	...	...	...	500[d]
Water	4,444	30,694	3,361	3,234	14,169
NI	...	...	...	...	5
NI	...	...	...	...	5
Acetaldehyde (C_2H_4O)	Tr[e]	Tr	13	...	22
Acetone (C_3H_6O)	...	...	9	8	Tr
Benzene	...	...	...	Tr	73
NI	...	...	2	Tr	4
NI	...	...	...	...	7
Toluene	5	6	8	14	33
Xylene	...	Tr	...	Tr	Tr
Xylene + styrene + phenyl acetylene	...	Tr	...	Tr	Tr

[a] Traps were located at valves 1, 5, 10, 15, and 20 of the apparatus shown in Figure F-4.

[b] This value is the electronic integrator response.

[c] NI means not identified.

[d] Estimated by triangulation.

[e] Trace, meaning signal was observed, but was too small to activate electronic integrator.

Appendix G

ANIMAL BEHAVIOR EXPERIMENT

Appendix G

ANIMAL BEHAVIOR EXPERIMENT

The basic intent of the animal experiments was to use rats and mice as test subjects for evaluating the physiological effects produced by fire, heat, and toxic gases. Then, by using established correlations between human responses and animal responses to these various stresses, an estimate could be derived of what effects the fire would have had on a pilot in the cockpit. To obtain statistically significant data a large number of animals must be utilized. Such data were not obtained in this study and should be seriously considered in future tests.

EXPERIMENTAL SETUP

Personnel from the UUFRC furnished the rats used in this test and prepared them for the experiment.

Two rats had electrodes implanted in the head and chest so that electroencephalographic (EEG) and electrocardiographic (EKG) data could be recorded during the fire test. The method of implanting the electrodes in the skull is described in an FRC report.[13] Both rats were placed in restraining slings. One was put in the cockpit inside a pilot's helmet atop the manikin. EEG and EKG leads ran from the rat to the telemetry unit in the lower part of the manikin. From there the data were transmitted to the telemetry receiving van. Figure G-1 shows the cockpit rat in place in the helmet before it was placed in the cockpit. Behind the helmet is shown the telemetry transmitter that was later installed in the manikin. Figure G-2 shows the rat positioned in the cockpit. Note the metal tube about an inch (25 mm) in front of the nose of the rat. The input of cockpit gas for the gas sampling system described in Appendix F was at this location.

The other rat was placed in a glass container in the instrumentation bunker to serve as a control. Leads from this rat ran to recording instruments in the bunker. This system failed during the test, so no EEG and EKG records were produced for the control rat. Figure G-3 shows the control rat ready to be placed in its container for the test. Both rats were also equipped with impedance pneumograph instrumentation to record their breathing rates, but these systems also malfunctioned and, therefore, breathing rates were not recorded. The control rat was trained before the test to perform an electric shock avoidance leg flexion to provide a test of physiological functioning after the fire test. After the test, blood samples were taken from both rats to measure the carboxyhemoglobin level of the blood as an indication of the amount of toxic gases absorbed in the bloodstream.

[13] University of Utah, Flammability Research Center. *The Physiological and Toxicological Aspects of Smoke Produced During the Combustion of Polymeric Materials*, by I. N. Einhorn. Salt Lake City, Utah, UUFRC, July 1974. (Report FRC-UU-38, p. 81, publication UNCLASSIFIED.)

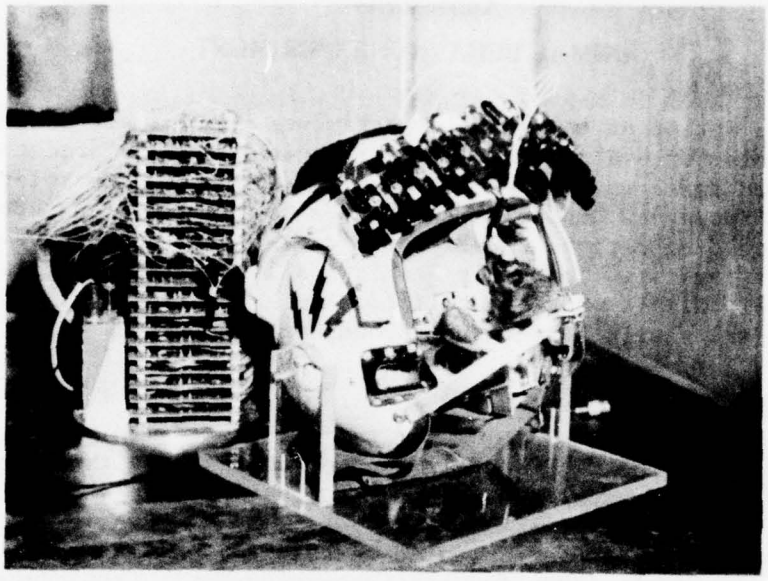

FIGURE G-1. Cockpit Rat in Helmet Before Being Put Into Cockpit. (Neg. LHL 187264)

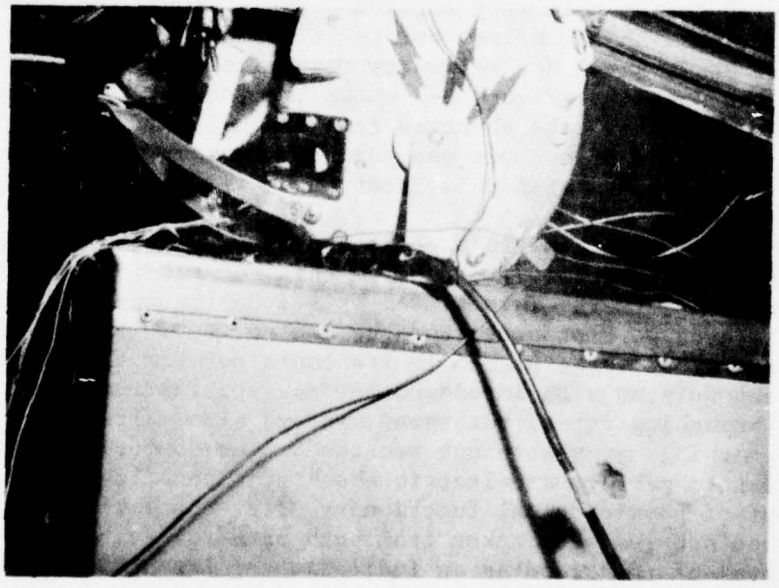

FIGURE G-2. Rat in Place in Cockpit. (Neg. LHL 187369)

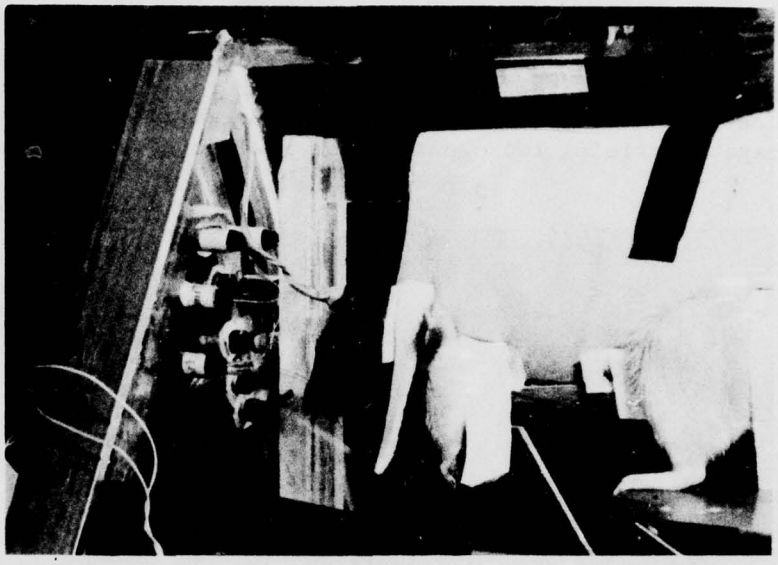

FIGURE G-3. Control Rat Ready To Be Put Into Place for Test. (Neg. LHL 187318)

A less complex animal experiment involved the use of mice on a treadmill. The purpose of this experiment was to detect toxic effects by means of the time of useful function model developed in two articles published in *Aerospace Medicine*.[14,15] Basically this method involves measuring the time a mouse can adequately function on a treadmill. The only data obtained is from a 16-mm movie camera with a telephoto lens monitoring the activity of the mouse while it is being exposed to potentially toxic gases. Two ferris wheel treadmills were constructed of glass (Pyrex, Corning 7740) as shown in Figure G-4. Glass was chosen, because it is chemically inert and optically clear. One treadmill was placed in front of the manikin camera in the cockpit in the starboard forward windshield above the eye shield (Figure G-5). The second treadmill was placed in the instrumentation bunker below the aircraft, where it was similarly monitored by a 16-mm camera with a telephoto lens.

The environmental difference between the cockpit and control mice was that the mouse in the cockpit was exposed to heat, toxic gas, and other effects of fire, whereas the mouse on the treadmill in the bunker was housed so that it could breathe only potentially toxic cockpit air that had been cooled to ambient temperature. (Note it is possible that the air loses some of its toxic components upon cooling.) A third mouse

---

[14] J. G. Gourme and P. Bartek. "Theoretical Determination of the Time of Useful Function (TUF) on Exposure to Combustions of Toxic Gases," *Aerospace Med.*, Vol. 40, No. 12 (December 1969).

[15] P. Bartek, J. G. Gourme, and H. J. Rostami. "Dynamic Analysis for Time of Useful Function (TUF) Predictions in Toxic Combustive Environments," *Aerospace Med.*, Vol. 41, No. 13 (December 1970), pp. 1392–1395.

was put into the glass container below the treadmill in the bunker. This mouse was not active during the test, because of its confined quarters, but it did breathe the same air. Figure G-6 shows the rat and mice in place in the instrumentation bunker just before the test. Above them is a cage containing two canaries for indicating air purity after the test.

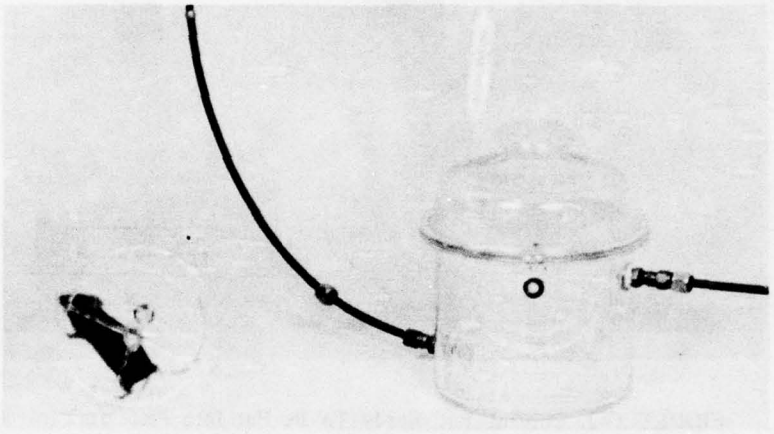

FIGURE G-4. Glass Treadmills. (Neg. LHL 186971)

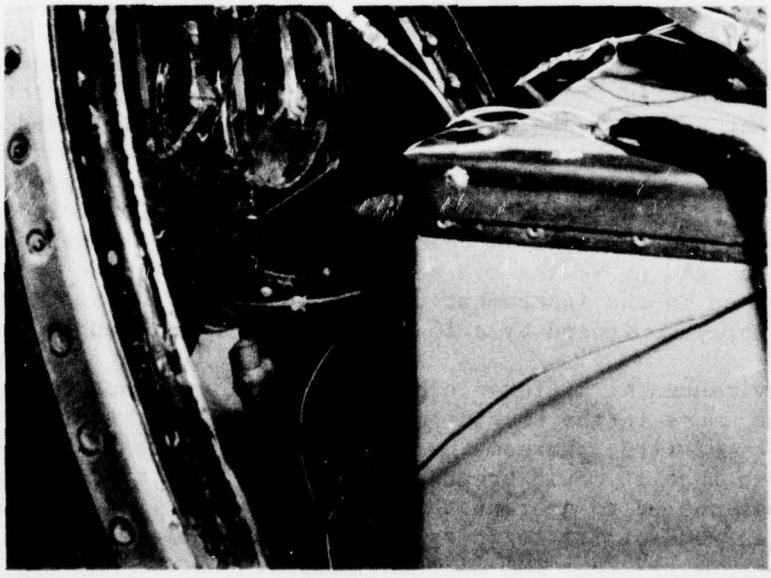

FIGURE G-5. Mouse on Treadmill in Place for Test in Cockpit. (Neg. LHL 187368)

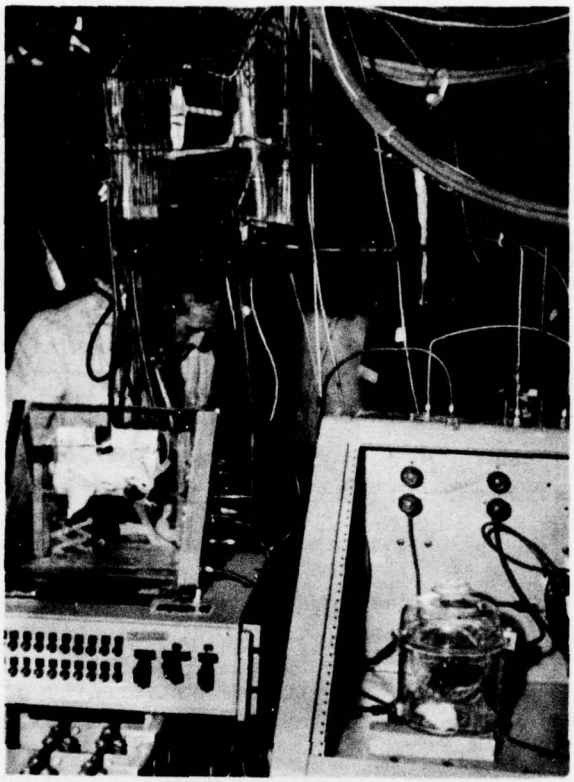

FIGURE G-6. View of Instrumentation Bunker Just Before Test, Showing Rat, Mice, and Canaries. (Neg. LHL 187321)

EXPECTED PHYSIOLOGICAL EFFECTS

Rats and mice were used in this test to give an indication of the physiological effects that would be experienced in the cockpit during the fire. Studies at the UUFRC have indicated that rats cannot survive as much thermal shock as humans can.[13] A body temperature of 42°C for extremely short durations has been established as the maximum that can be tolerated by Sprague-Dawley rats, one of the standard laboratory varieties.

Several tables from the previously mentioned FRC report are presented to show the effects of various gases on humans and the relation between human and rat response.[13] Table F-2 shows how human performance is degraded as the oxygen in the air decreases. Death will occur within a few minutes if oxygen is completely withdrawn from a confined volume. It may be seen from this table that pilot survival requires an oxygen content within the cockpit of greater than 6%.

Carbon monoxide (CO) has been thought to produce the most deaths in fires of this kind. The main action of CO after it is inhaled is to combine reversibly with hemoglobin (Hb) in the blood to form carboxyhemoglobin (CO-Hb). Table G-1 indicates the changing human reactions as CO-Hb builds up in the blood. It would appear that, for a pilot to remain functional, the CO-Hb should not be allowed to reach 50%.

TABLE G-1. Human Reactions at Various Concentrations of Carboxyhemoglobin.

CO-Hb concentration, %	Reactions
0 to 10	No signs or symptoms
10 to 20	Tightness across forehead, possible slight headache, dilation of the cutaneous blood vessels
20 to 30	Headache and throbbing in the temples
30 to 40	Severe headache, weakness, dizziness, dimness of vision, nausea, vomiting, and collapse
40 to 50	Same as above, greater possibility of collapse; syncope and increased pulse and respiratory rates
50 to 60	Syncope, increased respiratory and pulse rates, coma, intermittent convulsions, and Cheyne-Stokes respiration
60 to 70	Coma, intermittent convulsions, depressed heart action and respiratory rate, and possible death
70 to 80	Weak pulse, slow respiration leading to death within hours
80 to 90	Death in less than an hour
90 +	Death within a few minutes

The relationship between CO-Hb concentrations in man and rat is given in Table G-2. Rats inhale a larger volume of air per unit time in proportion to their body weight, hence their blood can become more rapidly saturated with CO. From this table it would appear that CO concentrations in the cockpit should not exceed 5,000 ppm during the test. Figure F-6 (p. 77) shows that about 4,400 ppm concentrations were being approached at 170 seconds into the test. Some physical impairment could be expected after 160 seconds.

TABLE G-2. Differences in CO-Hb Concentration in Blood for Rats and Men at Same CO Concentrations.

CO concentration, ppm	Time to reach given CO-Hb concentrations in rats		Time to reach given CO-Hb concentrations in man	
	20%	50%	20%	50%
10,000	in minutes	in minutes	in minutes	in minutes
5,000	in minutes	in minutes	in minutes	in minutes
2,000	in minutes	15 minutes	20 minutes	60 minutes
1,000	15 minutes	240 minutes	60 minutes	300 minutes
500	30 minutes	...	90 minutes	...
250	90 minutes	...	360 minutes	...

Hydrogen cyanide (HCN) is produced from nitrogen-containing organic compounds during pyrolysis or combustion. Table G-3 shows the relationship between HCN concentrations in air to human reactions. Concentrations above 180 ppm are considered unacceptable in the cockpit during the test. Figure F-6 shows only a negligible amount (< 1 ppm) produced during the test.

TABLE G-3. Relation of Hydrogen Cyanide Concentrations to Symptoms of Humans.

HCN concentration, ppm	Symptoms
0.2-5.0	Threshold of odor
18-36	Slight symptoms (headache) after several hours
45-54	Tolerated for 1/2 to 1 hour without difficulty
100	Fatal in 1 hour
110-135	Fatal 1/2 to 1 hour
181	Fatal after 10 minutes
280	Immediately fatal

The only other toxic gas of nominal concentration in this test was hydrogen chloride (HCl). This gas can be produced by thermal degradation of polyvinyl chloride. If HCl is inhaled, the upper respiratory tract will be severely damaged and that damage could lead to asphyxiation and death (Table G-4). From this table it would appear that the HCl concentration in the cockpit should not exceed 1,000 ppm over long periods of time. Note that this level of concentration was being approached at 170 seconds (Figure F-6).

TABLE G-4. Inhalation Effects of Hydrogen Chloride on Humans.

Hydrogen chloride concentration in air, ppm	Symptoms
1-5	Limit of odor
5-10	Mild irritation of mucous membranes
35	Irritation of throat on short exposure
50-100	Barely tolerable
1,000	Danger of lung edema after short exposure

Based on the above measurements, together with observation of the recovered animals, it would appear in the context of baseline data acquisition that toxicity is not as critical as fire penetration. It is emphasized that this tentative observation is not based on statistically significant data. Should a new canopy be developed that could withstand fire for 5 minutes, it is possible that toxicity would then become critical.

USE OF EEG AND EKG

Electroencephalography constitutes a powerful method for observing brain function. Electric potentials measured on the skull of the rat are generally assumed to originate from the cortex of the brain. Whatever the exact origin of the EEG, it is reasonable to assume that it relates in some way to the function of individual neurons.[16] The EEG is a graphic plot of voltage as a function of time. EEG voltages are in

[16] W. R. Klemm. *Animal Electroencephalography*. New York, Academic Press, 1969. Chap. 1, 2.

the microvolt range, usually about 5-75 μV in scalp records of animals. These voltages have both positive and negative polarities. EEG wave durations often range from less than 1/second to more than 100/second, depending on the recording apparatus and physiological conditions.

Interpretation of EEG waves is not an easy task because of their nondeterministic (random) nature. When Fourier techniques are used to analyze EEG waves, it is found that apparent EEG signals are composed of numerous signals of different frequencies and amplitudes. In general, the interpreter is confronted with the question of whether a signal is an inherent modulation of one frequency or whether several frequencies are compounded.[16] Visual inspection, or even mathematical analysis, does not resolve the question.

EEG voltages were recorded from the connector attached to the skull of rats, as shown in Figures G-1 and G-2. Figure G-1 shows a rat suspended within a pilot's helmet. The stack of printed circuit boards is the telemetry unit. Note the connector and lead wires on the head. Figure G-3 shows a second rat suspended in a sling. This rat was located in the instrumentation bunker beneath the A-4 during the burn test. Again note the connector and lead wires attached to its skull.

Figure G-7 shows a typical EEG response for an animal in a relaxed state. For a given animal, EEG voltages and frequencies are very consistent under consistent environmental conditions. To use the physiologists' terms, EEG signals can be generally characterized for higher animals as LVFA (during alertness) and HVSA (during relaxation or drowsiness). When an animal that is relaxed is presented with a novel or biologically significant stimulus, the cortical EEG changes from HVSA to LVSA. Such a response is often called an "arousal response." In the fully alert state the EEG amplitude is at a minimum. No dominant rhythms are present; rather, a wide spectrum of frequencies exists, usually in the range of about 15 to 30/second. Rats normally breathe at a rate of about 33 breaths/second.[17] (The breathing rate of the cockpit rat in this test, as is shown in Figure G-9, p. 98, was in the range of 35-40 breaths/second. In the relaxed or resting state, the amplitude of the EEG increases and high-amplitude spindles in the forms of bursts of 5 to 8/second begin to occur. The characteristic HVSA pattern becomes predominant during drowsiness, consisting of slow waves of 1 to 3 waves/second and higher amplitudes. The HVSA pattern also includes spindles (high-voltage bursts of four or more waves with a frequency of 6 to 12 waves/second). For animals in hammocklike slings, spindle incidence varies with the state of arousal.

[17] H. Hirschhorn. *All About Rats.* Neptune, N.J., T.F.H. Publication, 1974. P. 4.

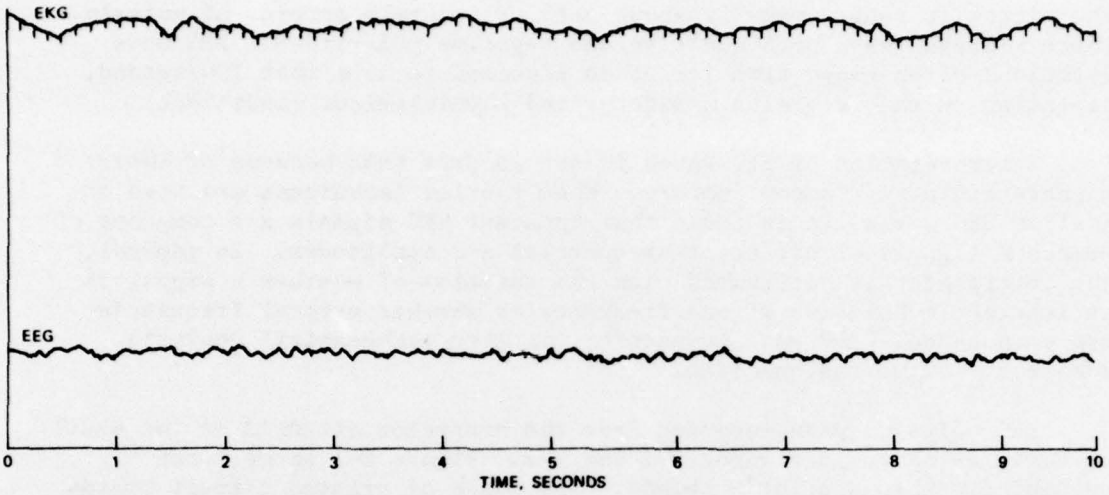

FIGURE G-7. Typical Flammability Research Center Record of EKG and EEG for Animal in Relaxed State.

Along with the EEG response, an EKG response was recorded for the cockpit rat. Two electrodes were implanted into the chest of each of the test rats; however, because of an instrumentation failure, no record of the body responses was recorded for the control rat in the instrumentation bunker. The above comments on the interpretation of the EEG generally apply also to the EKG.

ANIMAL TEST RESULTS

The results of the animal behavior experiments were derived from: inspection of the test animals after the test; blood samples taken from both rats after the test; movie coverage of both the cockpit mouse and the control mouse on treadmills during the fire (there was also some footage of an overall shot of the instrumentation bunker, including the control rat, during the fire, but it added little information that was not available otherwise); an avoidance response test of the control rat after the fire test; and observation of the control mice in the ensuing weeks after the fire.

Rats

Immediately after the fire was extinguished, the cockpit rat was examined by Dr. Steve Packham of the UUFRC. He found the rat to be alive, but with third-degree burns over the head, shoulders, forelimbs, and on the sides of hind limbs (see Figure G-8). Wires leading from the physiological monitoring electrodes were burned free of insulation, and

the externally exposed parts of the cannula on the rat were missing. A pinkish colored fluid was exuding from the nose, and the mouth and tongue were swollen shut and were dry.

The animal was immediately anesthetized with nembutal, and a heart puncture technique was used to secure a blood sample. This sample, taken 30 minutes after the end of the test, showed a 49% level of CO-Hb in the blood.

The EEG and EKG recorded from the cockpit rat are given in Figure G-9. These data cover the entire test time of 243 seconds. Data at t = -10 seconds were similar to those at t = +10 seconds. In the opinion of FRC personnel who examined them, these records are not of physiological origin. That opinion was based on the fact that frequency of the EKG signal is about 36 waves/second instead of 8. The EEG record was rejected by them on the same basis. According to the FRC personnel, any correlations of EKG and EEG records with those of other transducers was probably due to the thermal destruction of wire, leads, etc. That opinion is not shared by the author. However, it is prudent to warn other investigators of the conflicting opinions and to caution them to use the data in proper context.

Other data show that initial significant heating did not occur until from 192 to 203 seconds (see Table 1, p. 10). Hence, the thermal destruction of wires, leads, etc., could not have occurred before 192 seconds. Furthermore, the amplifier card for the rat was located inside the helmet and the electrical circuit was temperature-compensated.

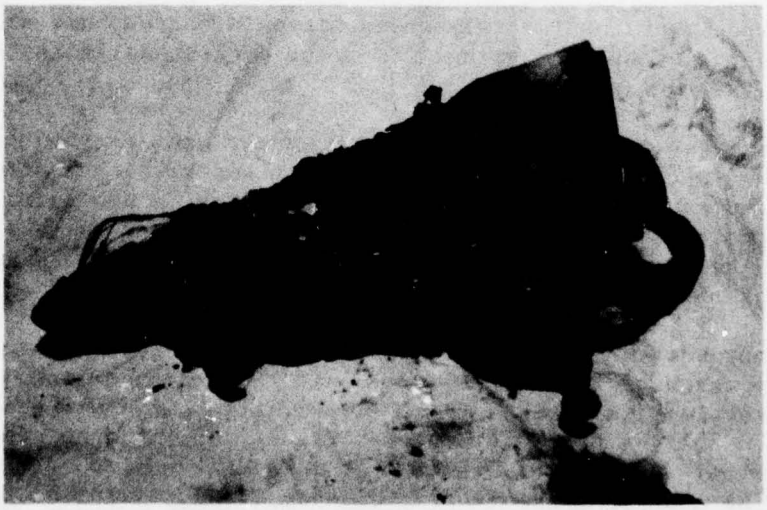

FIGURE G-8. Cockpit Rat After Fire. (Neg. LHL 187326)

The significant EEG events occurred at about 41 seconds, when both amplitude and spindle incidence decreased. At about 93 seconds, the signal amplitude and spindle incidence increased. At about 133 seconds, apparent activity of the kind that follows a sudden attack or seizure was indicated by low voltage amplitude. At about 150 seconds, animal revival was indicated. At about 161 seconds, animal hyperexcitability ended with the signal moving off scale. At about 238 seconds, EEG activity returned, suggesting that the animal was still alive.

Comments regarding the EKG records shown in Figure G-9 are similar to those given above for the EEG. At about 34 seconds, the EKG amplitude decreased and the frequency increased. At 51 seconds, the EKG amplitude increased. The reference level initiated a shift (perhaps due to animal movement). At 69 seconds, the EKG amplitude stabilized and its frequency increased. At about 93 seconds, the EKG reference increased dramatically (perhaps due to animal movement). At about 97 seconds, the EKG reference voltage peaked and started to decrease (perhaps due to the animal slowing down its movement). At about 120 seconds, the EKG reference voltage stabilized. At about 128 seconds, the reference voltage increased again. At about 133 seconds, the EKG recorded a low voltage amplitude. Animal revival occurred at about 153 seconds. From there on, the EKG is mostly off scale until the end of the test. However, at about 238 seconds the EKG returned to reference level to suggest that the animal was still alive.

It must be pointed out that the "apparent" EKG and EEG response in Figure G-9 is subjective. There is always the possibility of error due to the voltage amplification conditioning electronics, etc. It is possible that wires were connected incorrectly. On the other hand, the "apparent" response of the two independent signals corresponds very favorably with the events occurring within the cockpit as indicated by all the other transducers.

The control rat in the instrumentation bunker was observed to be still alive and functioning when personnel entered the bunker after the test. At 5 minutes after completion of the burn test, this animal was administered the electric shock flexion response test and was observed to perform the avoidance response without difficulty. From all gross observations of the animal, it appeared normal.

At 15 minutes after the completion of the fire test, a heart puncture technique was used to take two blood samples from the control rat. One of these samples indicated a 50% CO-Hb level in the blood and the other indicated 36%. A mean of these two values, 43%, is the best estimate of the actual CO-Hb level. Note that a CO-Hb level of over 65% is considered to be nearly always lethal, because of depression of respiration and the circulation.

Mice

The activity of the cockpit mouse was recorded on movie film until it could no longer be observed at 71 seconds.[1] (See Figure 1(c), p. 8.) By the time the firefighters reached the cockpit after the fire, the mouse had died in the fire.

The two mice in the instrumentation bunker survived the test with no apparent toxic effects. One of the two, a male, was subsequently mated. Both mice continued to live normally during the next 6 months of observation. Movie footage of the mouse on the treadmill in the bunker showed that the animal functioned normally while breathing the air from the cockpit.[1]

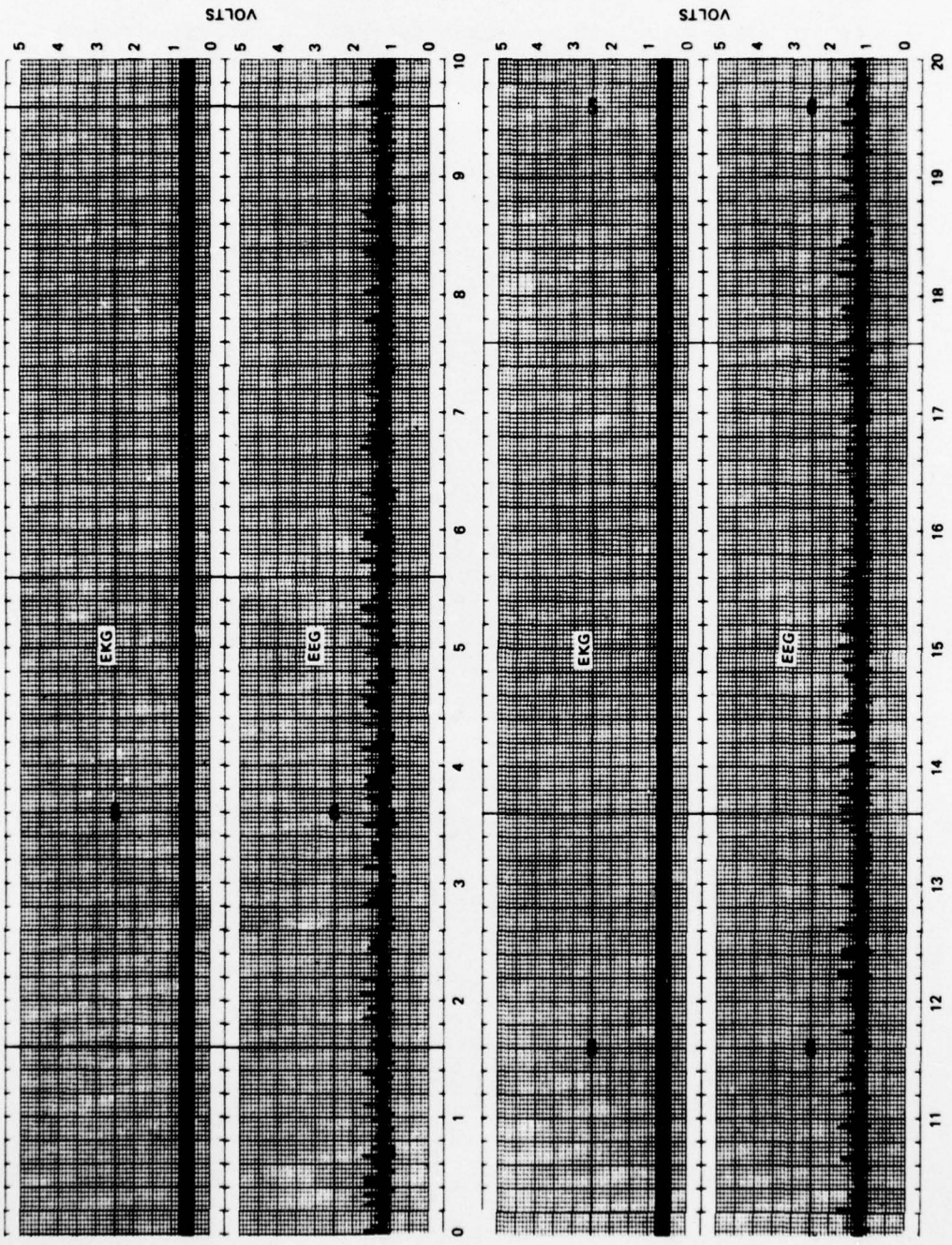

FIGURE G-9. EKG and EEG of Cockpit Rat.

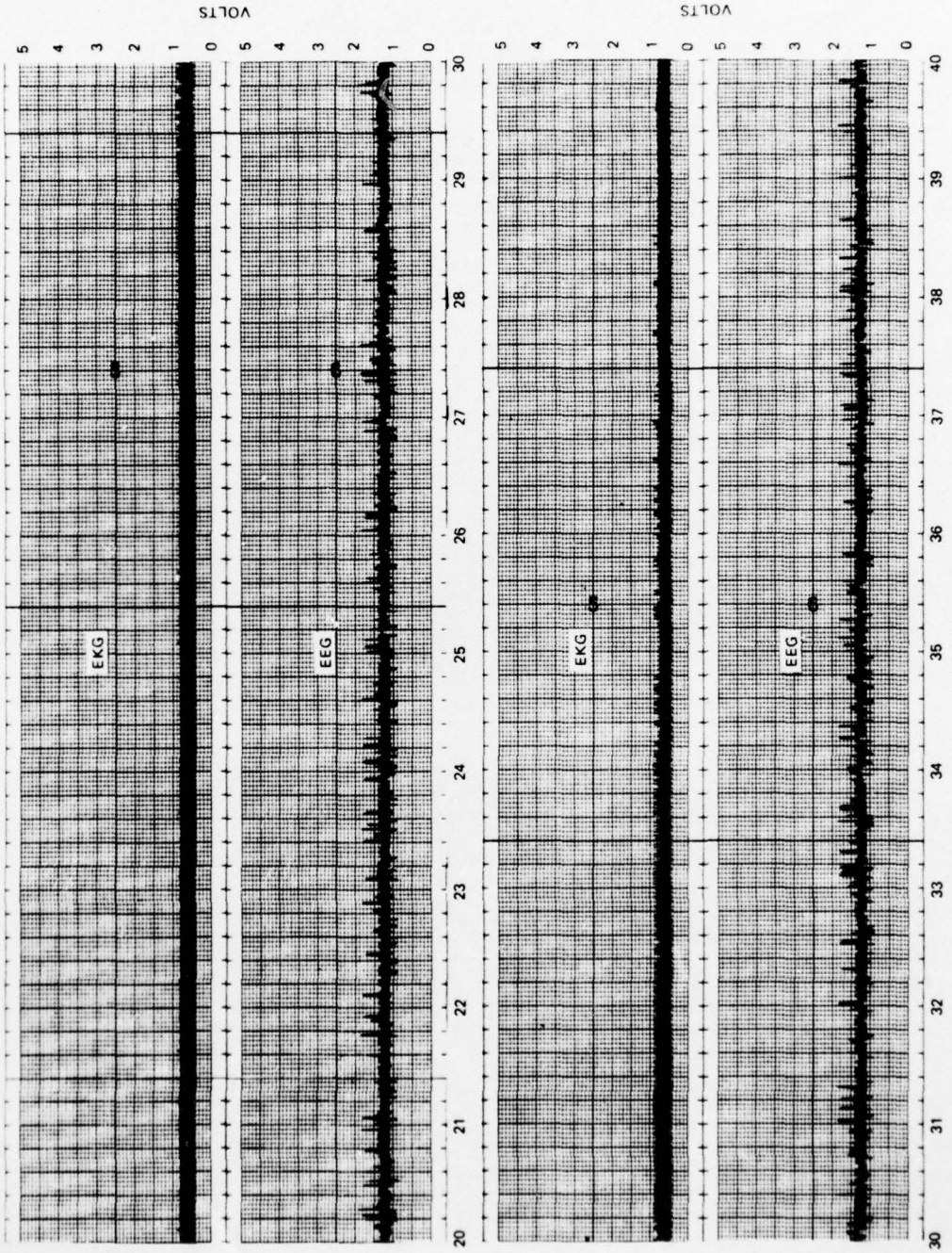

FIGURE G-9. (Contd.)

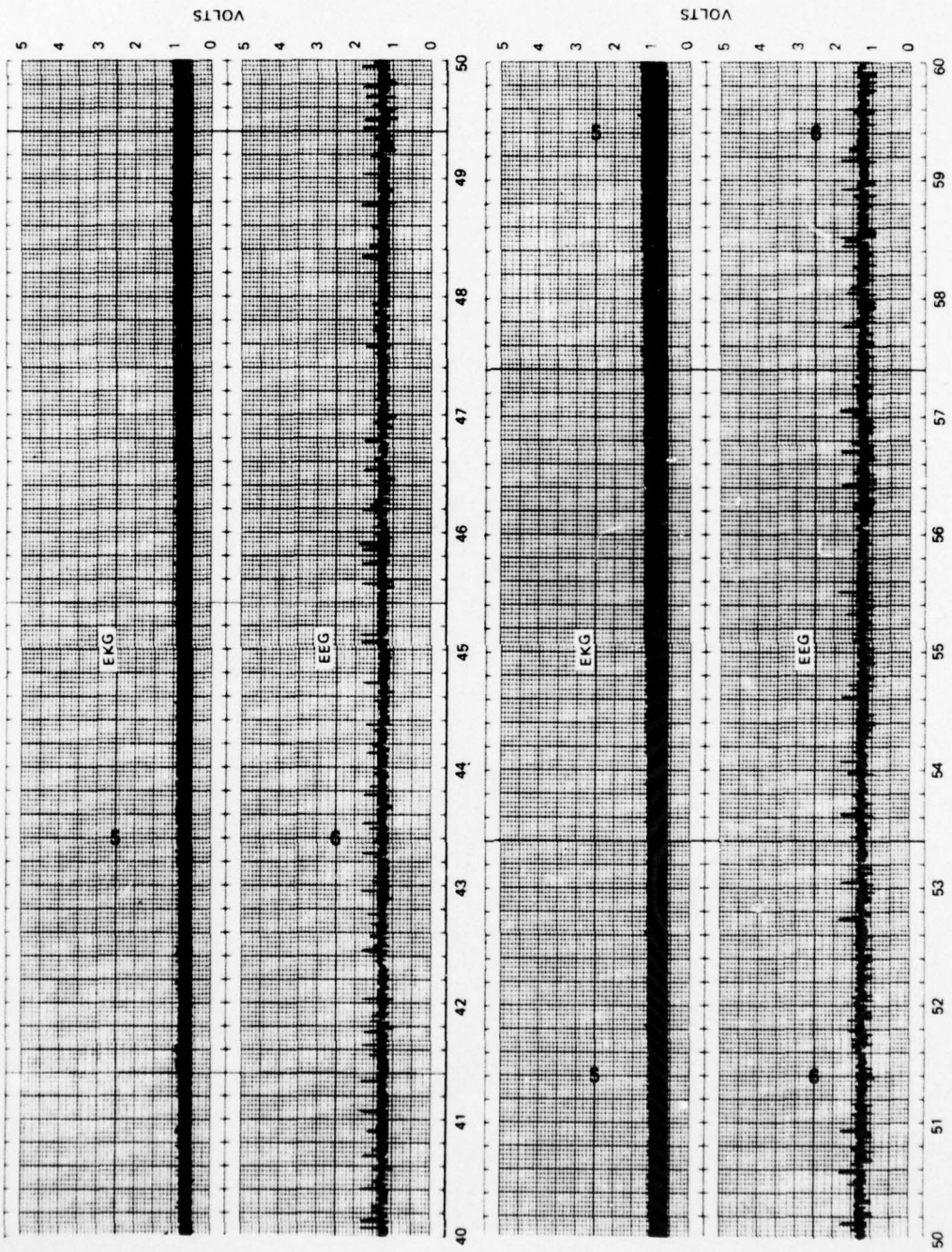

FIGURE G-9. (Contd.)

AD-A034 217 NAVAL WEAPONS CENTER CHINA LAKE CALIF F/G 1/3
BASELINE DATA FROM AN A-4 COCKPIT IN SIMULATED CARRIER DECK FIR--ETC(U)
AUG 76 A SAN MIGUEL
UNCLASSIFIED NWC-TP-5812 NL

2 OF 2
AD
A034217

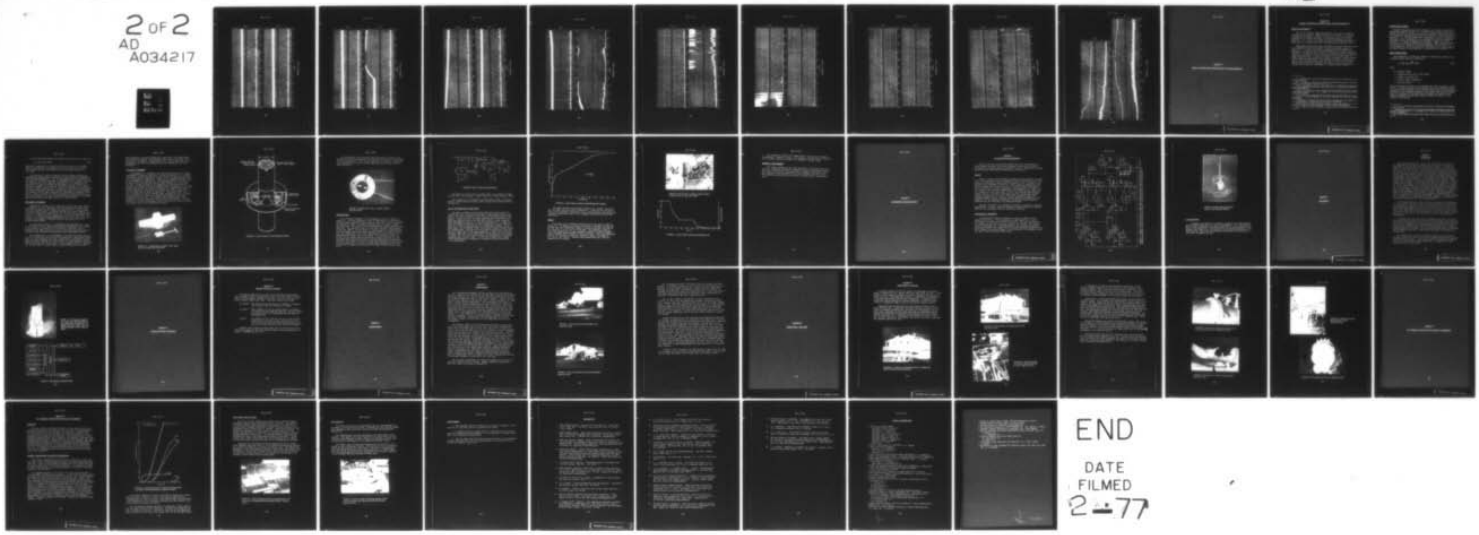

END

DATE
FILMED
2-77

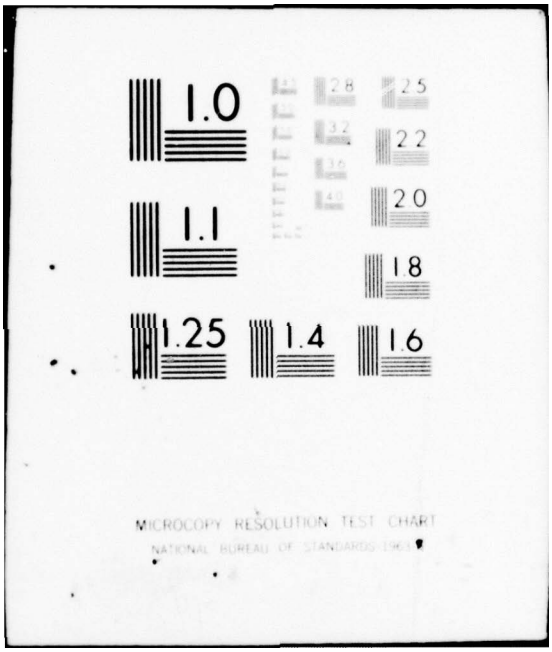
1.0
1.1
1.25
1.4
1.6
2.8
2.5
3.2
2.2
3.6
2.0
4.0
1.8
MICROCOPY RESOLUTION TEST CHART
NATIONAL BUREAU OF STANDARDS 1963

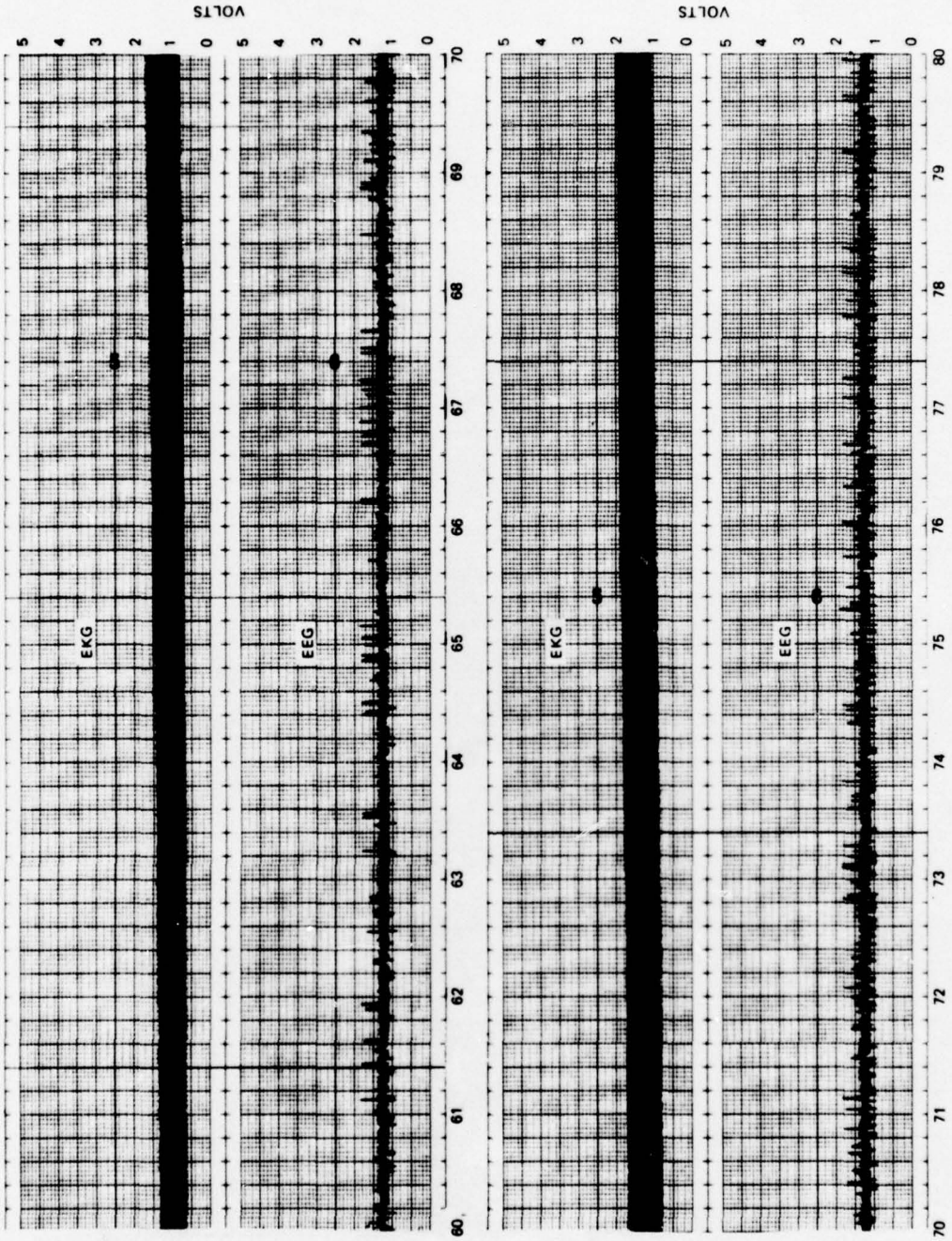

FIGURE G-9. (Contd.)

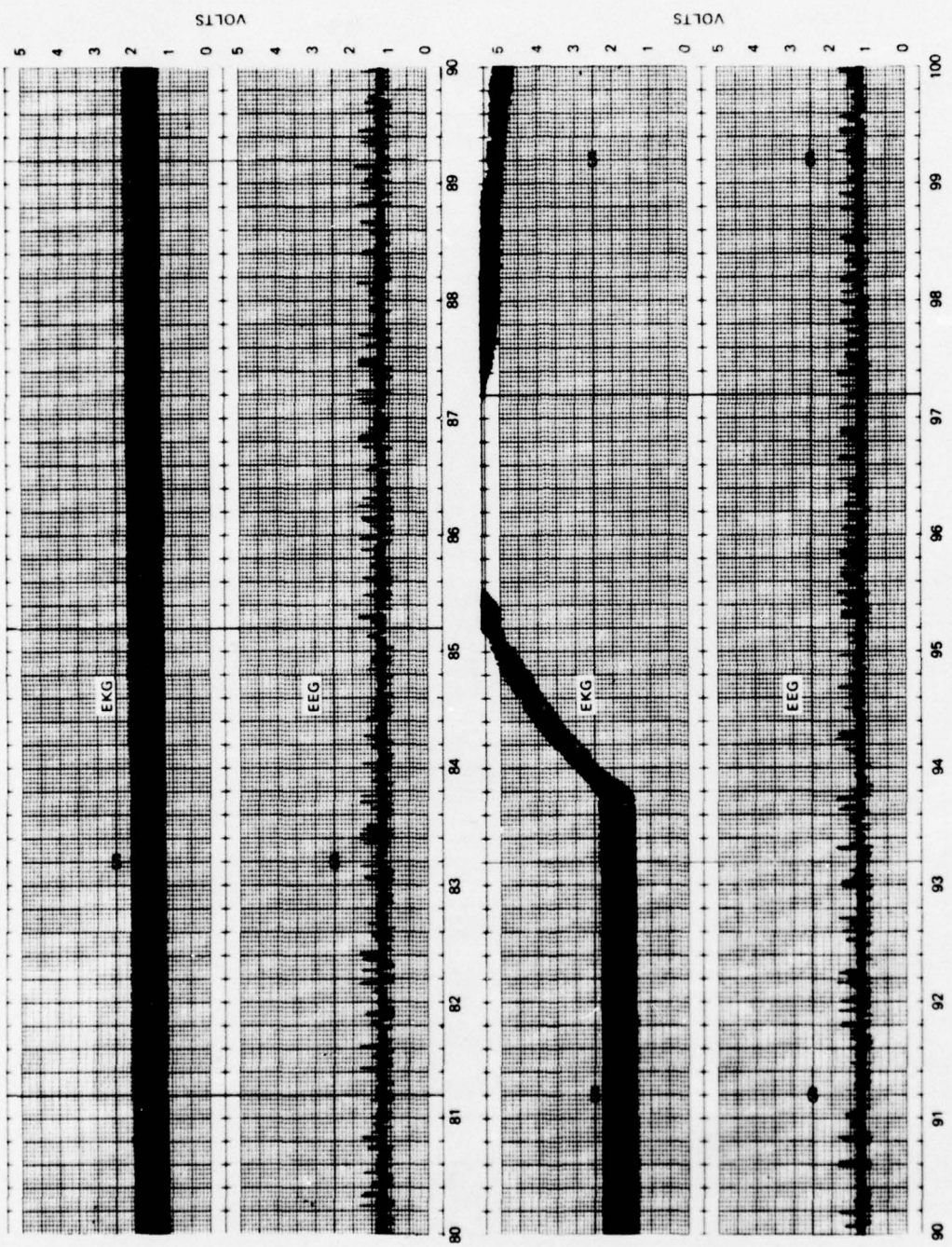

FIGURE G-9. (Contd.)

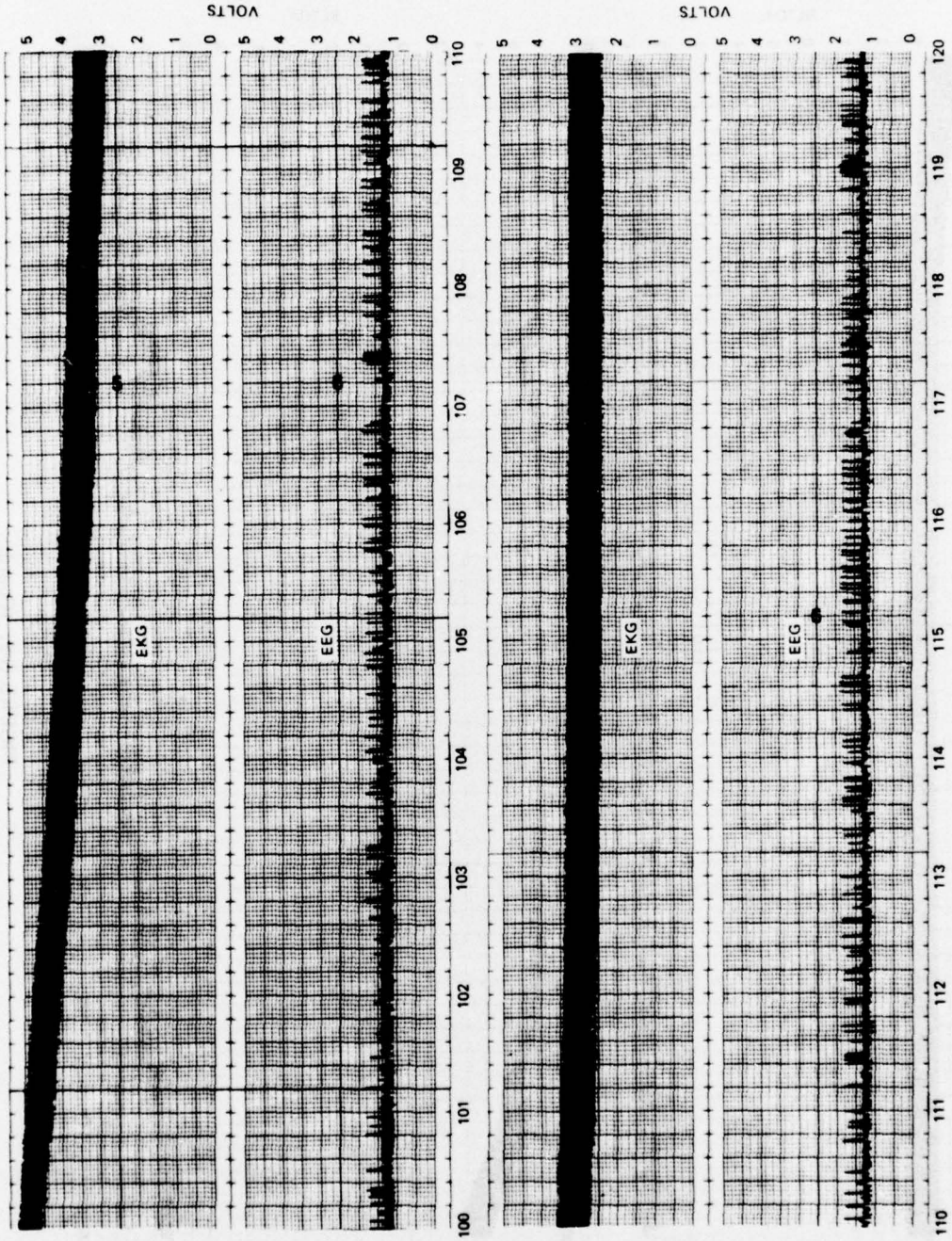

FIGURE G-9. (Contd.)

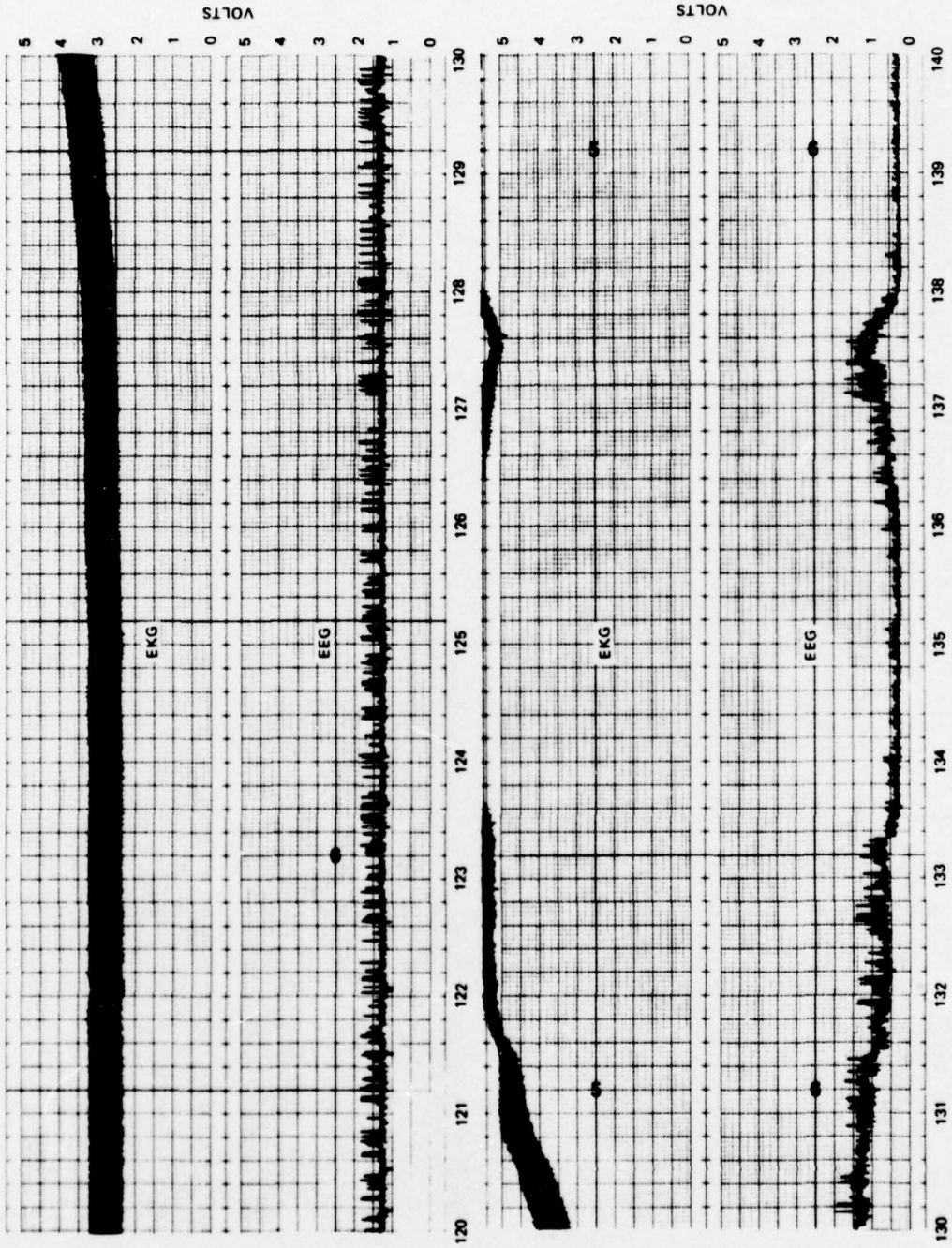

FIGURE G-9. (Contd.)

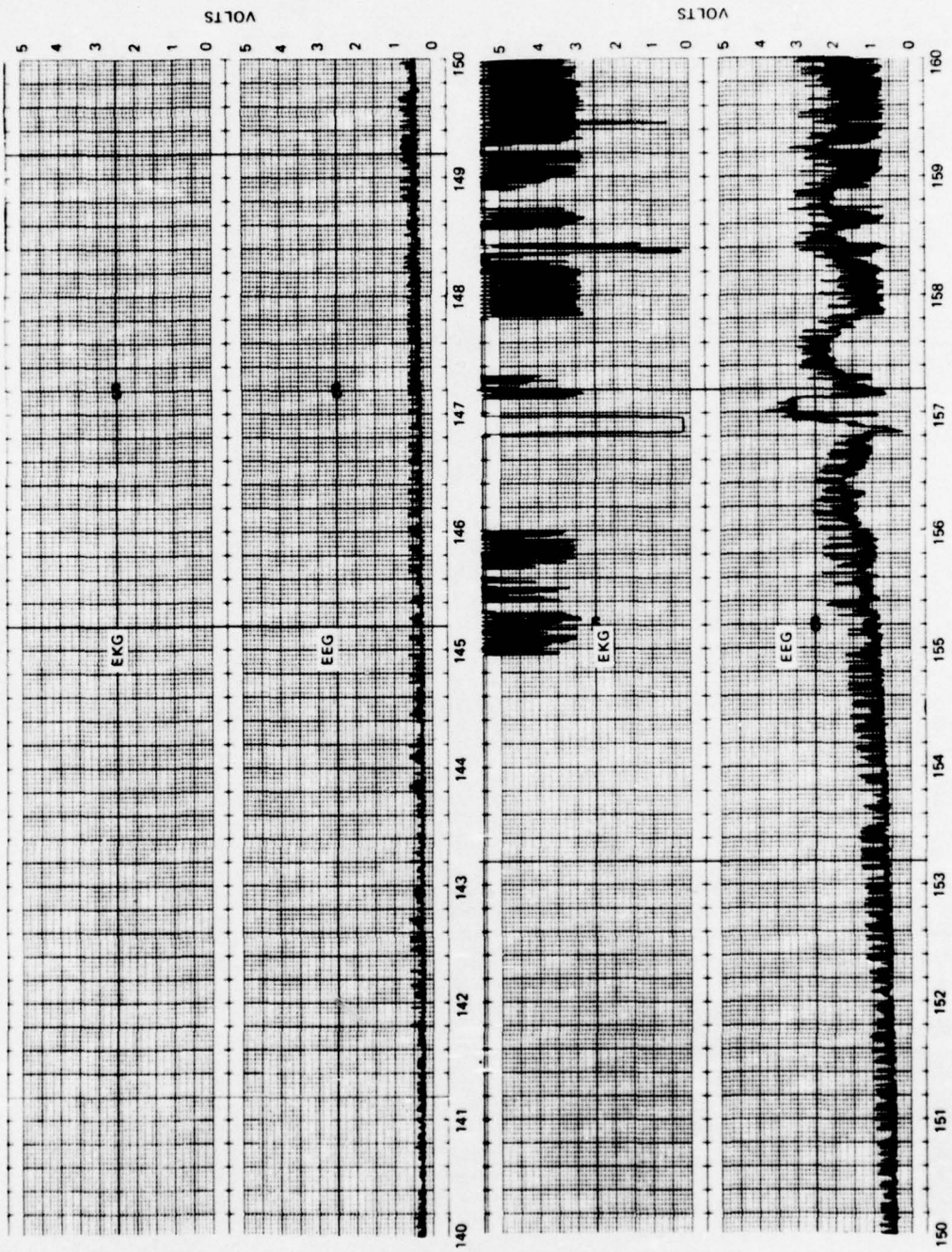

FIGURE G-9. (Contd.)

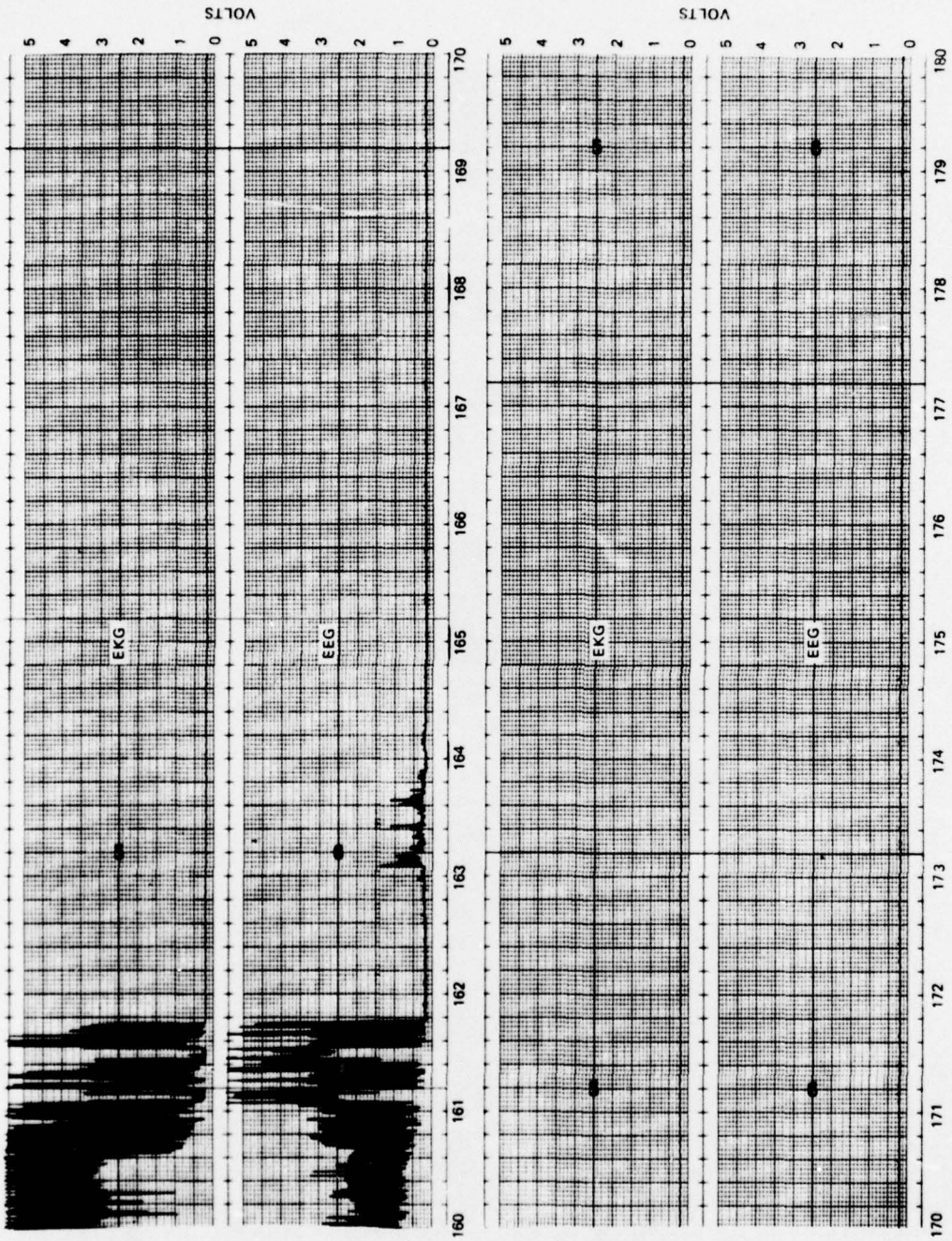

FIGURE G-9. (Contd.)

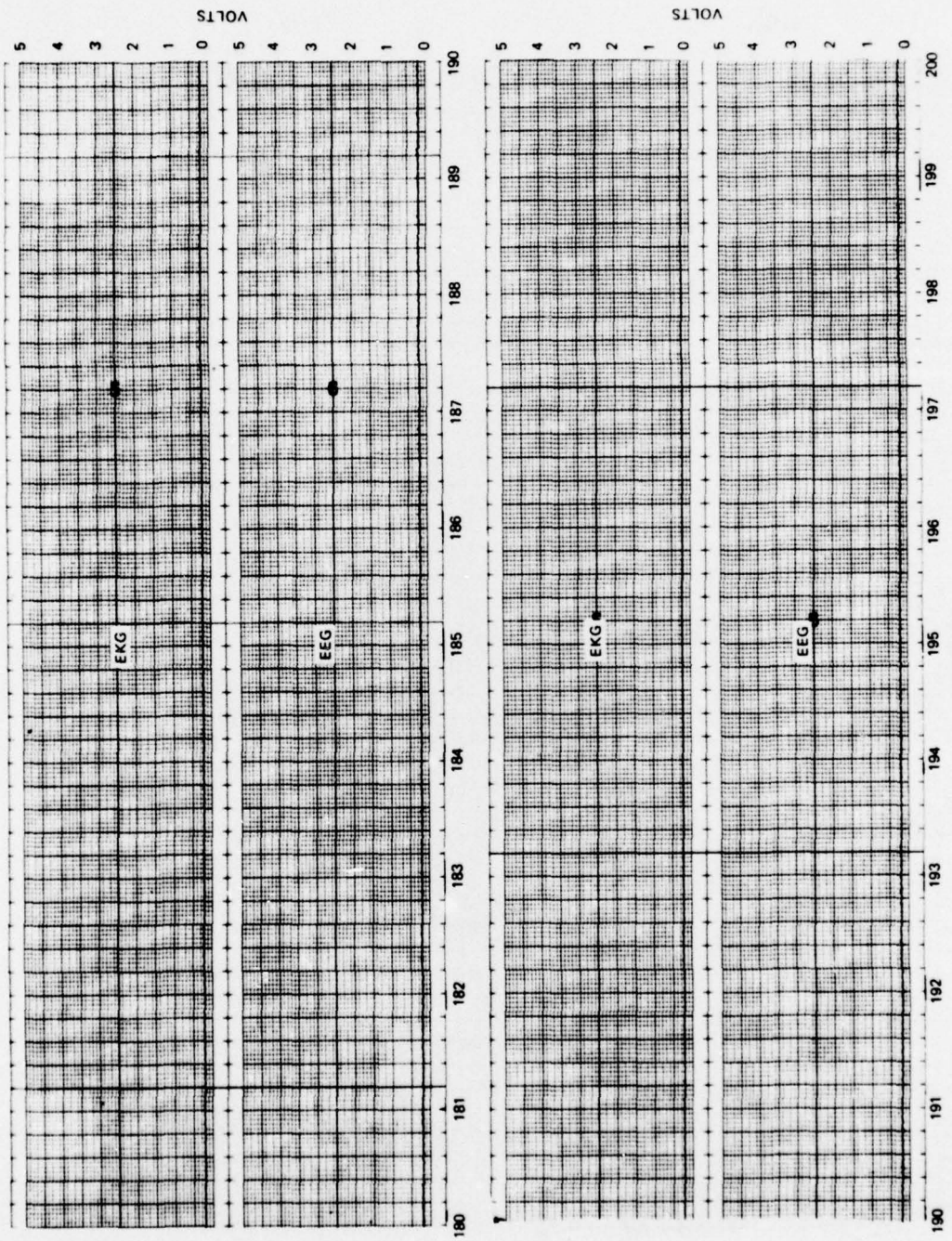

FIGURE G-9. (Contd.)

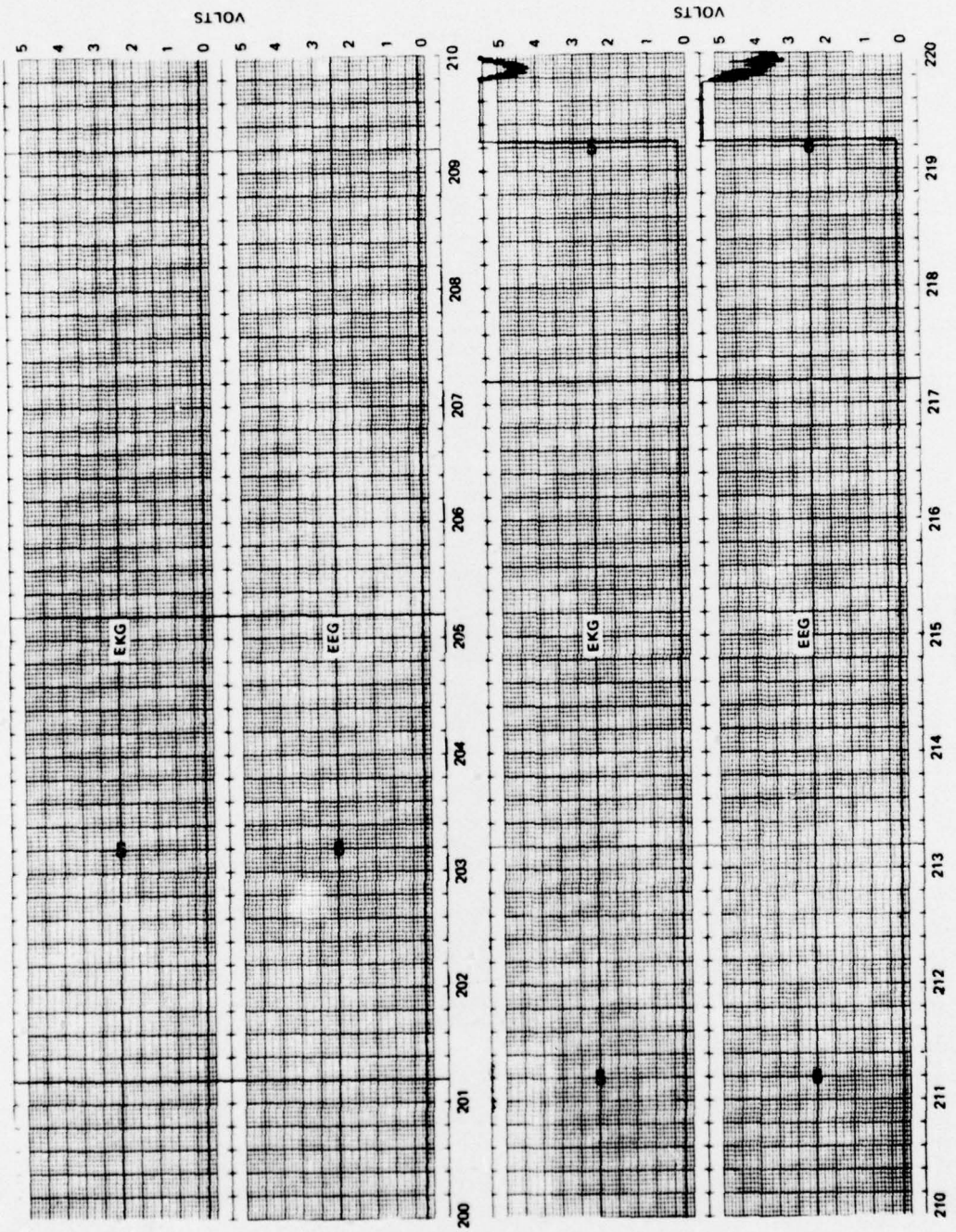

FIGURE G-9. (Contd.)

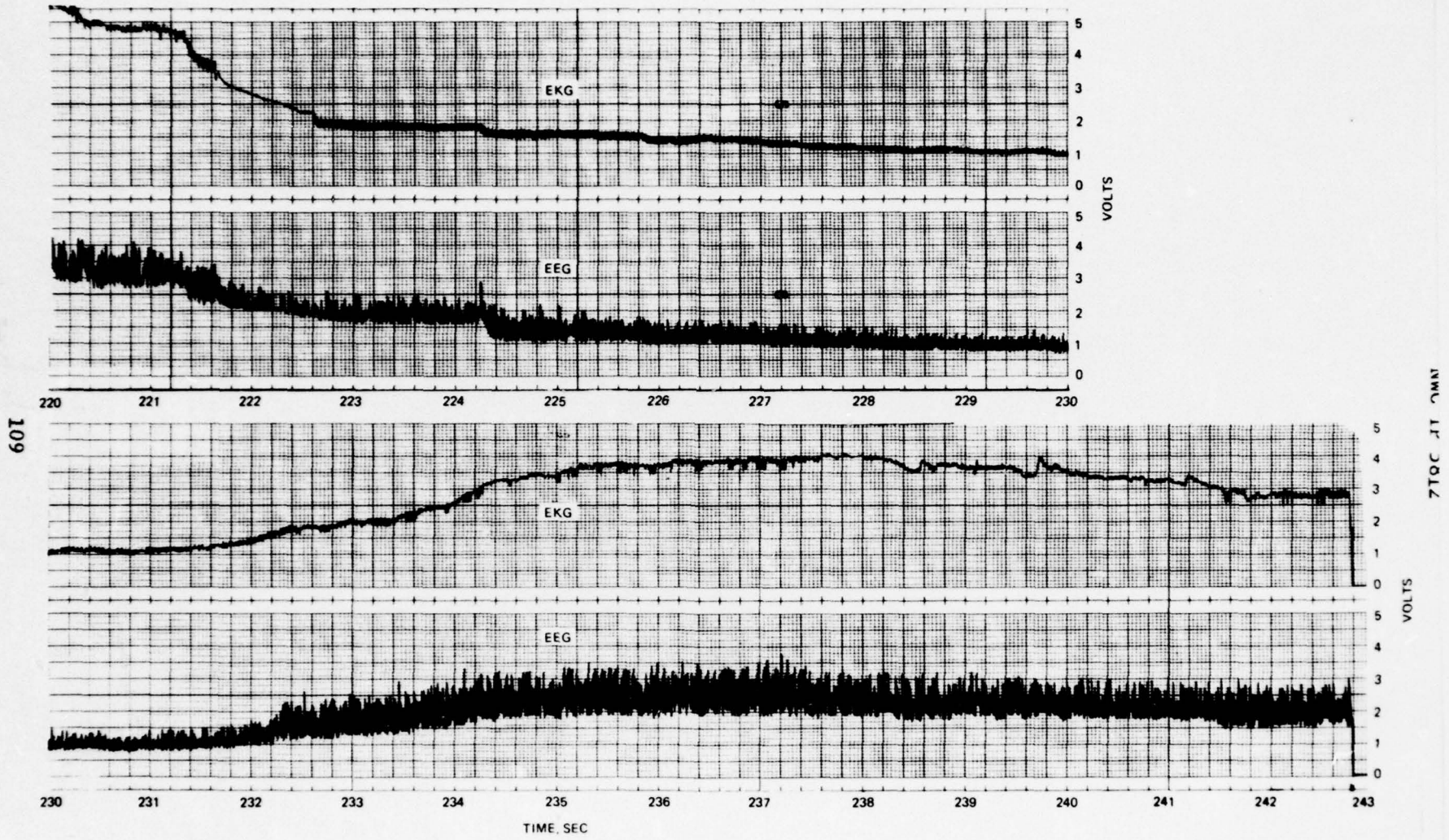

FIGURE G-9. (Contd.)

Appendix H

SMOKE TRANSDUCER CONSTRUCTION AND MEASUREMENTS

Appendix H

SMOKE TRANSDUCER CONSTRUCTION AND MEASUREMENTS

SMOKE MEASUREMENT

One of the variables measured during the test was the production of smoke in the cockpit. Smoke produced in the cockpit of a burning aircraft has a significant effect on how long a pilot can function properly[13,14,15] and is certainly a problem with respect to survivability.[13,18,19] Also it is useful to learn how the measured levels of smoke density correlate with other phenomena measured during a fire.

Smoke-measuring apparatus and techniques previously used were based on a photometric record of changes in light attenuation caused by smoke.[18,20] A problem exists in correlating such measurements with degradation of human vision and with identification of smoke-producing materials. To overcome this difficulty a transducer, which is described later, was developed. It can be calibrated in a standard smoke test chamber and then used to measure the light attenuation of smoke in burn tests outside the laboratory. The calibration permits field measurements to be correlated empirically with such factors as human vision and the kind of material producing the smoke, factors that several studies have shown can be measured in a standard smoke chamber.[19,21-25]

---

[18] J. J. Brenneman and D. A. Heine. "The Cleveland Aircraft Fire Tests," *Fire Technology*, Vol. 4, No. 1 (February 1968), pp. 5-16.

[19] D. A. Kourtides, J. A. Parker, and W. J. Gilwee. "Thermochemical Characterization of Aircraft Panel Materials," *J. Fire and Flammability*, Vol. 6 (July 1975), pp. 373-91.

[20] Air Force Aero Propulsion Laboratory. *A Smoke Detection System for Manned Spacecraft Applications*, by T. M. Trumble. Wright-Patterson Air Force Base, Ohio, AFAPL, June 1975. (Technical Report AFAPL-TR-74-97, publication UNCLASSIFIED.)

[21] Federal Aviation Administration. *Smoke Emissions from Burning Cabin Materials and the Effect on Visibility in Wide Bodied Jet Transports*, by E. L. Lopez. Washington, D.C., FAA, March 1974. (Report FAA-NA-73-155, publication UNCLASSIFIED.)

[22] American Society for Testing Materials. *Method for Measuring Smoke from Burning Materials*, by D. Gross, J. J. Loftus, and A. F. Robertson. Philadelphia, Pa., ASTM, 1967. (ASTM STP 422, pp. 166-204, publication UNCLASSIFIED.)

[23] National Bureau of Standards. *Smoke and Gases Produced by Burning Aircraft Interior Materials*, by D. Gross, et al. Washington, D.C., NBS. (Report No. NA-68-36, publication UNCLASSIFIED.)

[24] National Bureau of Standards. *Interlaboratory Evaluation of Smoke Density Chamber*, by T. G. Lee. Washington, D.C., NBS, December 1971. (NBS Technical Note 708, p. 80, publication UNCLASSIFIED.)

[25] A. F. Robertson. "Two Smoke Test Methods-A Comparison of Data," *Fire Technology* (November 1974), pp. 282-86.

Standard Smoke Chamber

Because the characterization of smoke is very complex, no universal measurement standard exists.[20,26] For some years a type of smoke test chamber developed at the National Bureau of Standards (NBS) has served as the standard for measuring the smoke characteristics of smoke-producing materials.[22,27] The NBS chamber uses a photometric sensor to measure the decrease in light transmission of a collimated vertical beam resulting from smoke; the smoke is generated by exposing a sample of a given material to a controlled radiant heating source. Smoke emission data on a wide variety of materials has been accumulated over the years.[23,28] An interlaboratory study has shown that reproducible test results can be attained for many of these materials by using this test chamber.[24,25]

Specific Optical Density

Data measured in an NBS type chamber are expressed in terms of the "specific optical density," defined as

$$D_s = \frac{V}{AL} \log_{10} \frac{100}{T} = \frac{V}{AL} D \qquad \text{(H-1)}$$

where

V = chamber volume

A = exposed surface area of test sample

L = length of optical path

T = percent light transmission

D = optical density

The specific optical density is a dimensionless light attenuation coefficient. It should vary for a given specimen and a given exposure time as a function of the thickness of the material (which affects the subsurface evolution of the combustion products), the chemical and physical properties of the material (which determine the amount and nature of smoke aerosols produced), and specimen exposure conditions (whether it is flaming or smoldering).

---

[26] C. L. Tien, et al. "Attenuation of Visible Radiation by Carbon Smoke," *Combustion Science and Technology*, Vol. 6 (1972), pp. 55–59.

[27] National Bureau of Standards. *The Smoke Density Chamber Method for Evaluating the Potential Smoke Generation of Building Materials*, by T. G. Lee. Washington, D.C., NBS, January 1973. (NBS Technical Note 757, publication UNCLASSIFIED.)

[28] C. J. Hilado. *Flammability Handbook for Plastics*. Westport, Conn., Technomic Publishing Company, 1974. Pp. 60–64.

For the NBS smoke chamber the specific optical density is given as

$$D_s = 132 \log (100/T) \qquad \text{(H-2)}$$

NBS smoke chamber data are usually reported in terms of the maximum value of D_s measured, the maximum rate of smoke accumulation over a 2-min period, and the time required for D_s to reach a value of 16 (T = 75%).

The validity of using the specific optical density concept for comparing the smoke emission properties of various materials depends on the following assumptions:[23] (1) the generated smoke is uniformly distributed; (2) the smoke generated is independent of the amount of excess air available and of any specimen edge effects; (3) coagulation and deposition of smoke is similar and independent of test sample size or the size and shape of the chamber; (4) optical density, D, is linearly related to smoke concentration; (5) human and photometric vision through light-scattering smoke aerosols, expressed in terms of optical density, are similar; and (6) smoke production is independent of material orientation. Within the limts of these assumptions the measured value of D_s for a given material can give a fairly reliable prediction of its smoke emission and, with other empirical data, of human vision.

Development of Transducer

Although the accumulation of data from the NBS type smoke chambers is valuable, its use is generally limited to applications where other data from the same type of chamber are compared to it. A few studies have shown some validity for limited scaling of NBS smoke chamber data to apply to larger test chambers.[18,21,23] The goal in the present application is to relate such test chamber data to that obtained within the cockpit of an aircraft being subjected to a burn test. This goal can be achieved by designing a transducer based on the principles of the standard smoke chamber.

It was postulated that, if a transducer were developed that could be calibrated in an NBS smoke chamber and then installed in the cockpit of an aircraft to be subjected to a burn test, then data could be gathered on the smoke production in the cockpit and these data could be correlated with laboratory data gathered from an NBS smoke chamber.

This premise led to the development of a smoke-measuring transducer for use in field burn tests such as the present one. The design requirements for this transducer were that a means must be provided to monitor light attenuation between two fixed points in a light-shielded enclosure, and the enclosure must permit smoke to pass through it freely. Moreover, the enclosure must be large enough to sample representative aircraft

smoke densities, yet small enough not to adversely affect smoke generation within the cockpit. The transducer must reject extraneous light and must not contribute to smoke production. Another important practical consideration is that the transducer be either expendable or readily repairable.

Construction of Transducer

A photograph of a transducer that was developed to meet the above requirements is shown in Figure H-1. Below the transducer is a plunger containing a neutral density filter that can be put into the transducer tube for electronic calibration. Figure H-2 is a diagram showing details of the transducer's construction. Its housing consists of a brass tube 10 inches (25.4 cm) long and with an inside diameter of 1.625 inches (4.1 cm). Around the tube at its midsection is a brass cylindrical enclosure 4.5 inches (11.4 cm) in diameter and 1.25 inches (3.2 cm) long. A light emitter and a receiver are inserted into diametrically opposite holes in the wall of the tube at its midpoint to form a 1.625-inch (4.1-cm) light path as shown in Figure H-2. The inner surface of the tube is serrated to reflect external light entering the tube. The ratio of the length of the tube to its diameter was chosen on the basis of blackbody considerations. All surfaces were anodized black. The combination of these dimensions, the serrated inner surface, the black anodization, and the narrow-angle field of view of the receiver prevents any external light from reaching the receiver.

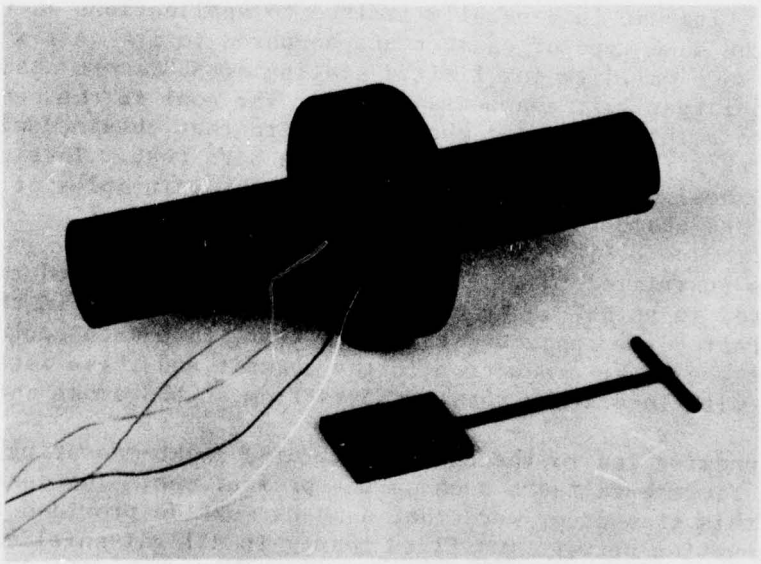

FIGURE H-1. Smoke-Measuring Transducer With Neutral Density Filter Holder. (Neg. LHL 184925)

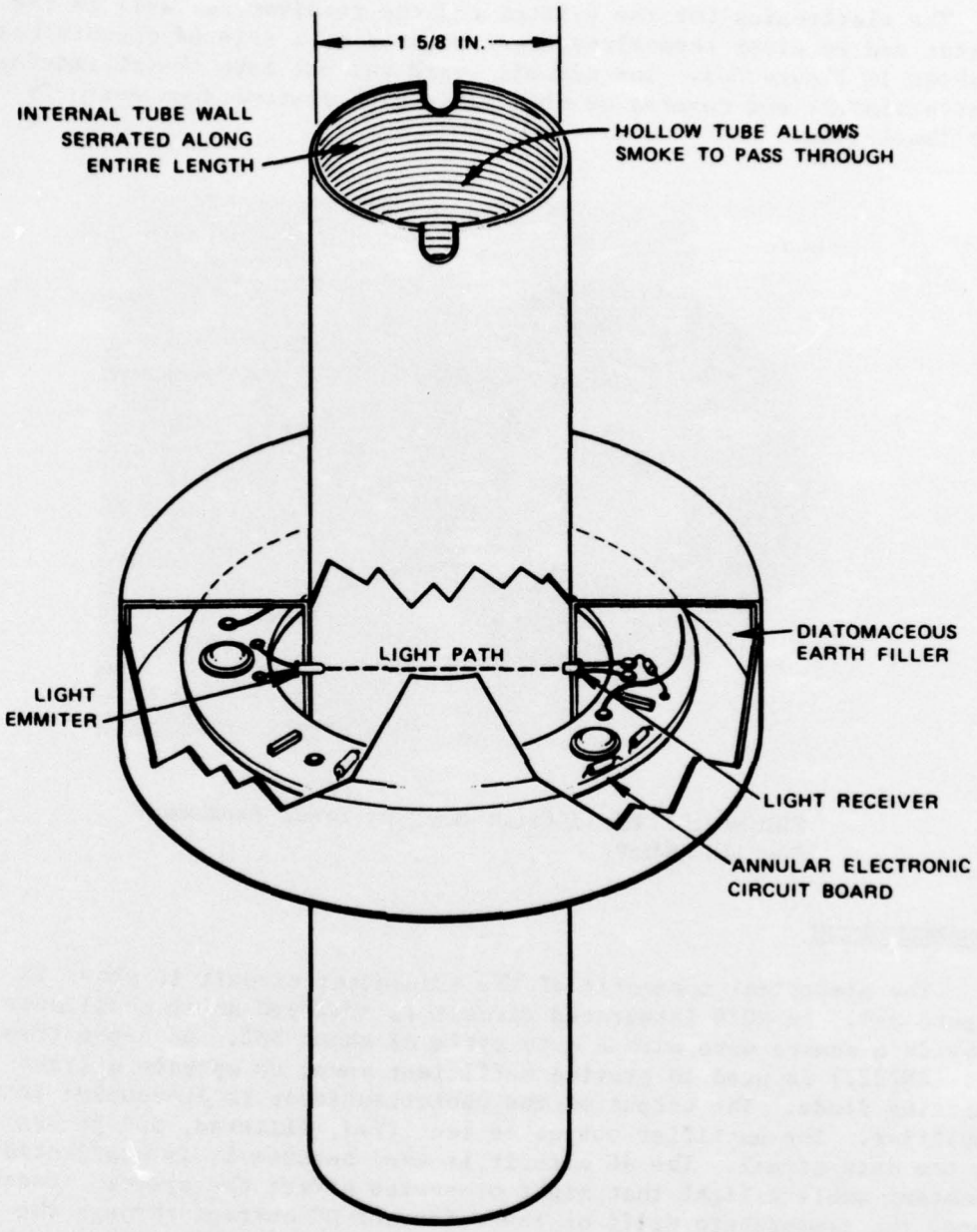

FIGURE H-2. Construction Details of Smoke-Measuring Transducer.

The electronics for the emitter and the receiver, as well as the emitter and receiver themselves, were mounted on a printed circuit board, as shown in Figure H-3. The circuit board was put into the cylindrical brass enclosure and covered on both sides with diatomaceous earth for heat insulation.

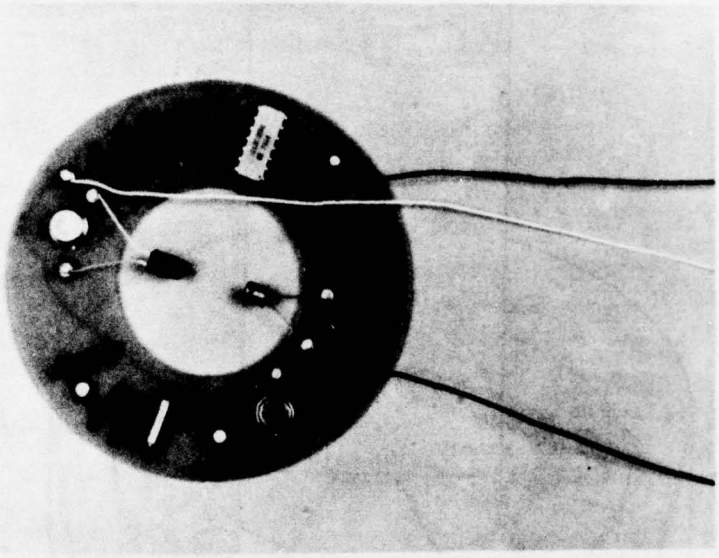

FIGURE H-3. Printed Circuit Board for Smoke Transducer (Neg. LHL 184559)

Electrical Circuit

The electrical schematic of the transducer circuit is shown in Figure H-4. An 8038 integrated circuit is employed as an oscillator to provide a square wave with a duty cycle of about 50%. An n-p-n transistor (2N2222) is used to provide sufficient power to operate a light-emitting diode. The output of the phototransistor is AC-coupled into an amplifier. The amplifier output is rectified, filtered, and presented as the data signal. The AC circuit is used because it is unaffected by constant ambient light that might otherwise affect the system. Furthermore, the temperature drift of the quiescent DC current through the phototransistor cannot affect the output. The selected resistor, the divider on the output, and the 220-kilohm collector resistor for the phototransistor can all be varied to provide sensitivity adjustment as required. The output of the ±15-V power supplies shown can be as low as 12 or as high as 18 V if needed, although some adjustment of the LED ballast may be required if the positive voltage is much different from +15 V.

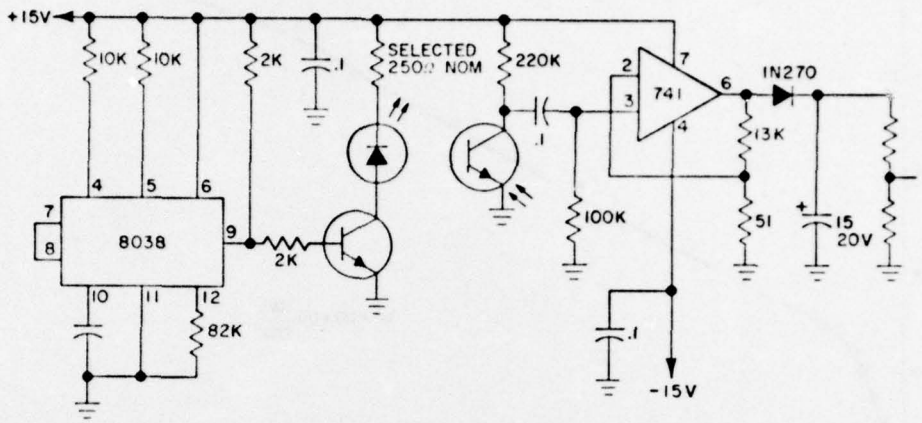

FIGURE H-4. Smoke Transducer Schematic Diagram.

The output of the circuit is proportional to the amount of light from the LED. The presence of smoke causes the output voltage to drop.

The transducer is calibrated in an NBS smoke chamber, using the specific optical density concept, before being used to measure smoke in a field test.

USE OF TRANSDUCER IN BURN TEST

The smoke transducer was used and demonstrated during the A-4 cockpit burn test to measure the change of smoke density levels with time in the region between the pilot and the instrument panel in the cockpit. Before the test the smoke transducer was calibrated at the NASA Ames Research Center in an NBS smoke chamber, using a plywood sample impregnated with salt as the "standard material." Figure H-5 gives the output voltage for the smoke transducer for three runs as a function of percent transmittance in the NBS smoke chamber. As the graph shows, the transducer output is reasonably linear between 10 and 70% transmittance. Equation H-2 can be used to obtain D_S. Note that, since the light path in the smoke transducer is much shorter than the reference light path in the NBS chamber [1.625 inches (4.1 cm) versus 36 inches (91.4 cm)], the sensitivity of the electronics of the smoke transducer must be quite high. A 1-dB drop in signal due to smoke (79.4% transmittance) corresponds to essentially total obscuration in the NBS chamber.

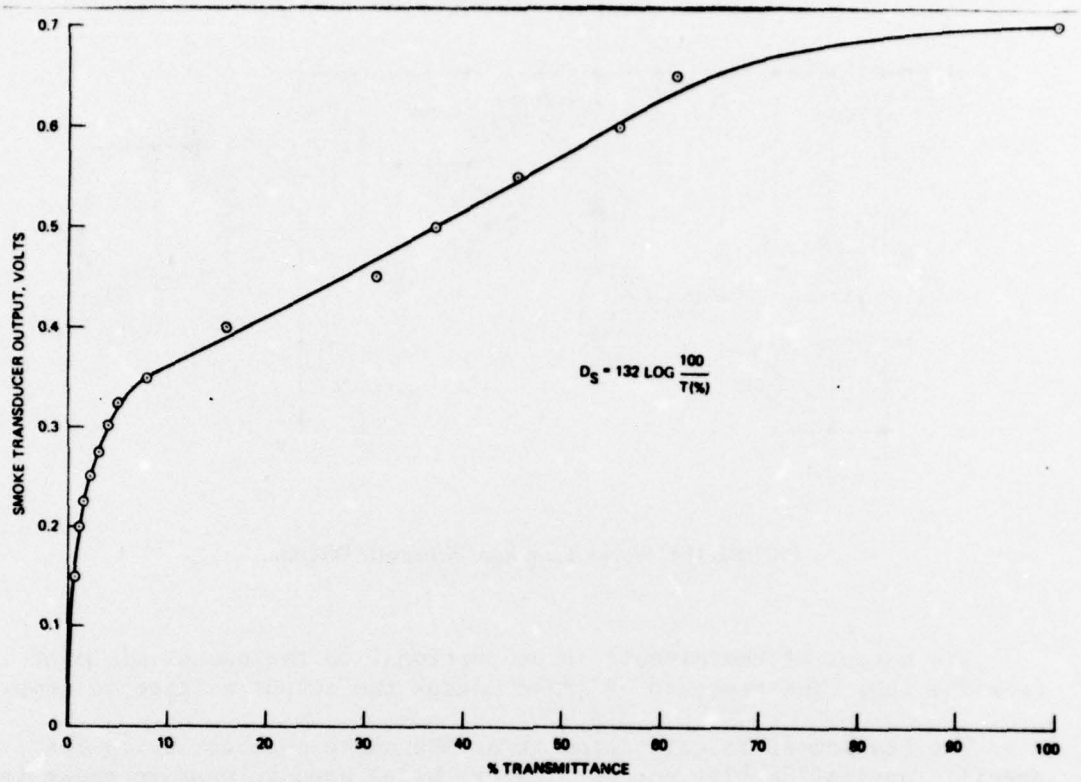

FIGURE H-5. Smoke Transducer Calibration Using NBS Chamber as Standard.

The smoke transducer was placed vertically in a holder in front of the instrument panel as shown in Figure H-6. Leads ran from the transducer to the telemetry transmitter in the cockpit manikin, and from there redundant signals were sent to the telemetry receiving van via RF and land lines.

Results

The output of the transducer during the A-4 burn test is shown in Figure H-7. No smoke was recorded until after 30 seconds into the test. At that time the transmittance began to decrease uniformly from 100 to 29% (from $D_S = 0$ to D_S -71) at 70 seconds. The materials producing this smoke apparently were then expended, because the smoke transducer output remained uniform between 70 and 120 seconds. New smoke generation began at 120 seconds, causing the transducer output to decrease to $D_S = 161$ at 140 seconds. Complete smoke obscuration ($D_S = 200$) was measured by 155 seconds.

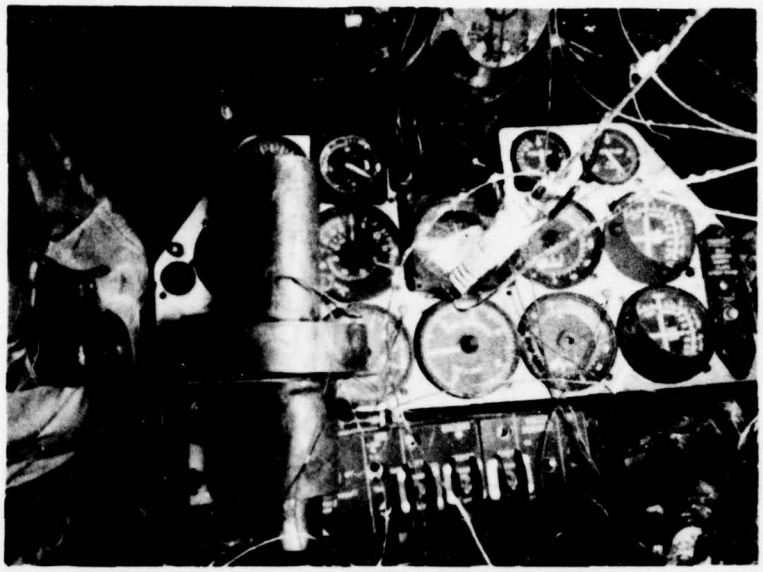

FIGURE H-6. Post-Test Photo of Smoke Transducer Mounted in Cockpit of Navy A-4. (Neg. LHL 187342)

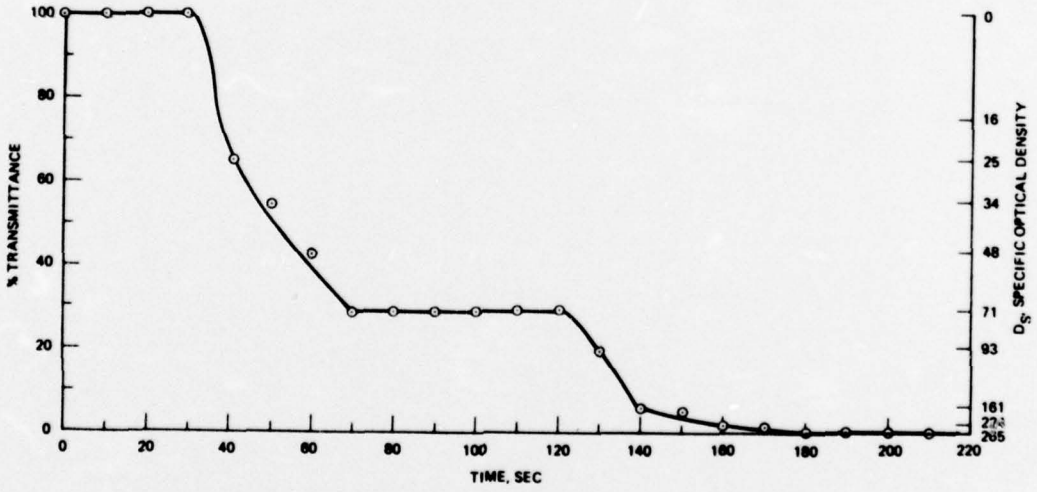

FIGURE H-7. Smoke Transducer Data Produced During Burn Test.

The transducer suffered fire damage before the fire was completely extinguished. However, because of its design, a few electronic components can be readily replaced to render the transducer operable again.

Evaluation of the Transducer

The results produced by the smoke transducer in this burn test show that this transducer represents a workable concept for measuring smoke in field test of this kind. The smoke data it produced constitute a valuable addition to the information that can be gained from a burn test. This transducer should also prove useful in other kinds of fire-related tests.

Appendix I

NO-RESPONSE MEASUREMENTS

Appendix I
NO-RESPONSE MEASUREMENTS

Three of the data acquisition systems that were instrumented produced records that were not reported because the records were either no response or minimal response throughout the test. These three systems measured sound, differential pressure, and acceleration.

SOUND

Since no record could be found of sounds recorded during an aircraft fire, it was decided to put a microphone in the A-4 cockpit to see if any unusual or significant sounds occurred during the test. Because it was expected to be expended in the fire, a fairly cheap microphone was used, but its fidelity was better than that of a normal pilot's microphone. It was connected to an audio processing card designed for the test, and the output of the card was telemetered to the receiving van. Figure I-1 is a schematic of the audio card. It has a fast-acting automatic gain control circuit to provide a listenable output no matter what sounds actually are made in the cockpit. That was necessary because the expected dynamic range of the audio signal exceeded the signal-to-noise capability of the telemetry commutator, and because nobody seemed to know how loud the sound gets in a burning airplane.

The data consisted of a lackluster recording of snapping, crackling, and popping. In short, there was nothing of significance on the record. However, that knowledge itself is useful baseline data.

DIFFERENTIAL PRESSURE

A differential pressure transducer as shown in Figure I-2 was installed on the A-4. This transducer was calibrated for ± 5 lb/in^2 (0.06 kg/m^2) to within ± 0.05 lb/in^2 (0.6 g/m^2). One side was vented to the cockpit and the other side was vented to the outside. The purpose of this measurement was to determine whether any significant pressure differences between the cockpit and the outside developed during the fire. As it turned out, none developed. It was virtually a no-response record. But again, that was useful baseline data.

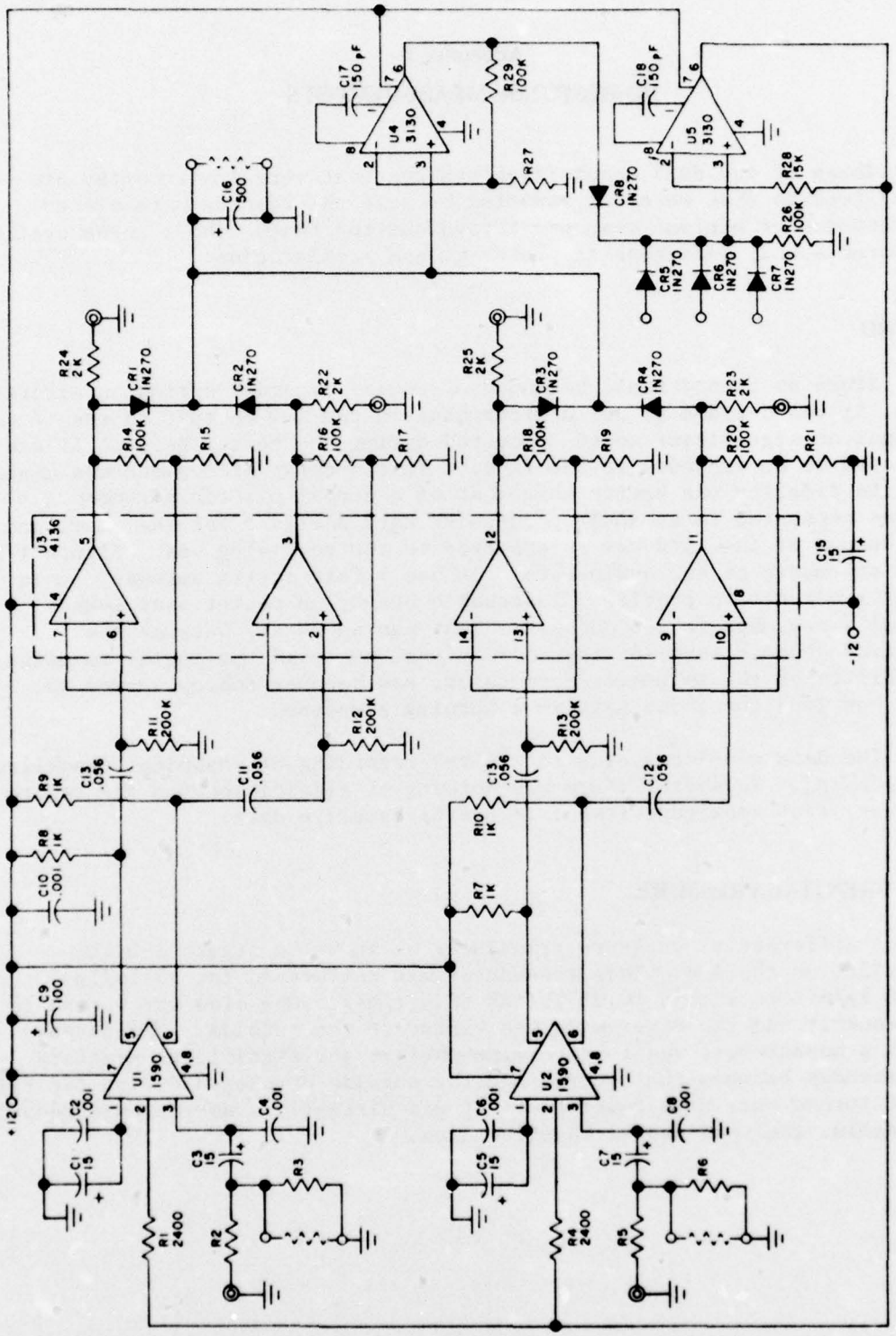

FIGURE I-1. Schematic of Audio Processing Card. Where resistor values are now shown, they were selected at the time of the test. Dashed-line resistors may be added to decrease input sensitivity or decrease release time on the AGC voltage generator.

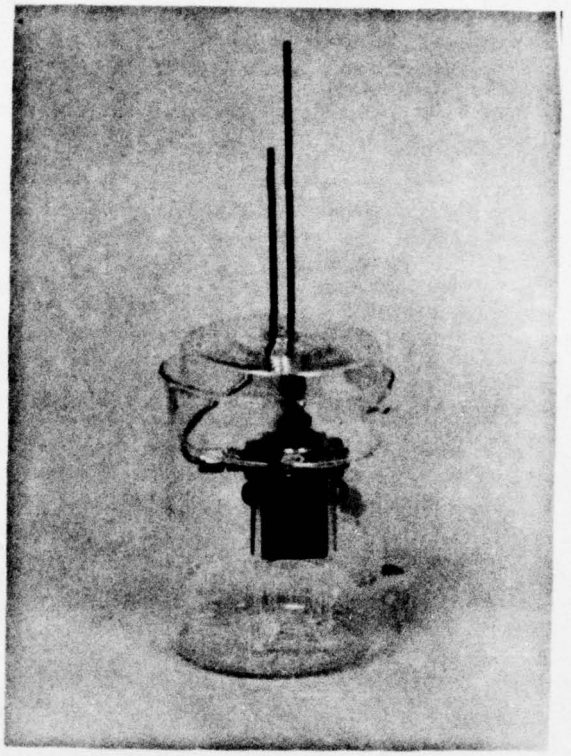

FIGURE I-2. Pressure Differential Transducer Used in A-4 Test. (Neg. LHL 186969)

ACCELERATION

To measure the effects of a possible explosion or aircraft landing gear collapse during the fire, three accelerometers (±2 *g* calibrated to ±0.01 *g*) were installed on the water jacket in the upper section of the manikin (see Figure B-2), and the data from them were telemetered to the receiving van. There was a no-response acceleration record along all three axes throughout the test.

Appendix J

TELEMETRY

Appendix J
TELEMETRY

Three data transmission systems were used in the A-4 burn test. All data gathered outside the cockpit were transmitted through the umbilical to the instrumentation bunker below ground. All data from within the cockpit were sent to the telemetry receiving van parked at the test site. Two parallel transmission systems were used to transmit the cockpit data, and the same data signals were transmitted over each system. The data signals acquired via telemetry included those from the thermocouples, slug calorimeters, directional calorimeter, microphone, strain gages, smoke transducer, accelerometers, EEG, and EKG. These signals were conveyed by leads to the manikin in the cockpit. There the signals were encoded for transmission and one set of signals was transmitted via RF by means of the transmitter shown in Figure J-1. Another set of the same signals were transmitted via land lines laid over the top of the ground. Both sets of signals were received in the telemetry van, where they were recorded on tape for processing later. Figure J-2 shows a block diagram of the telemetry system. The data acquired by means of telemetry have already been presented in Appendixes E, G, H, and I discussing the individual measurement systems. It should be noted that a comparison was made between the data received via RF and those received via land lines and they agreed within 1%.

The RF transmission was used to back up the land line transmission for two reasons. In tests of this kind fuel explosions or the cookoff of explosives (no explosives were on the aircraft for this test) often sever land lines causing a loss of data for the remainder of the test.[2] With the RF transmitter placed in the cockpit, there is a high probability that the data will be uninterrupted as long as the cockpit is intact. (During this test neither the land line nor the RF transmission was interrupted.)

A second reason for using the RF transmission was that, as far as the author and his telemetry consultants could determine, data had never before been telemetered by RF out of a fire of the magnitude of this one. It would be a valuable piece of background knowledge to learn whether there are any unforeseen obstacles, such as RF interference, to prevent acquiring data by this means. No such obstacles were found in this test. The RF telemetry data was of high quality and there was virtually no interference.

As a final note, the entire telemetry system except for the RF antenna (which may be seen on top of the transmitter in Figure J-1) was recovered after the test. It is thought that the antenna was broken by the force of the stream of light water used to extinguish the fire, rather than by the fire itself.

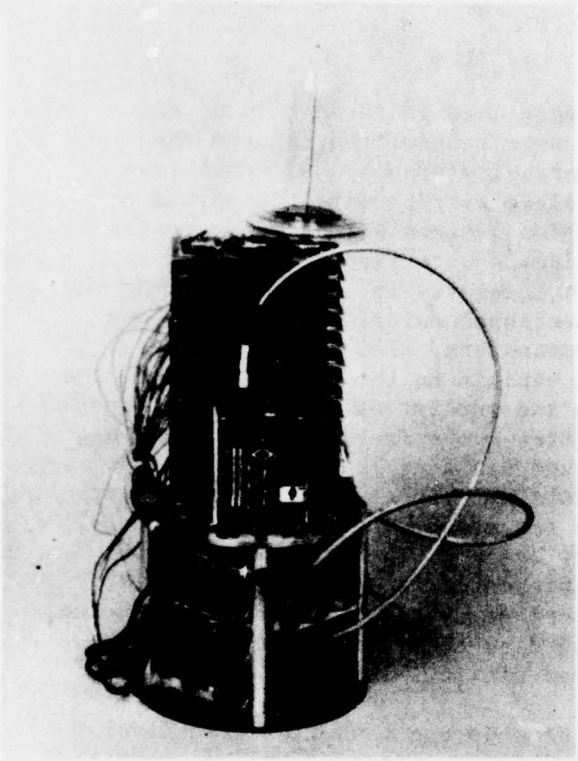

FIGURE J-1. RF Telemetry Transmitter. Item in glass cover atop the transmitter is the antenna, which was placed atop the fuselage behind the cockpit when the system was installed in the A-4. (Neg. LHL 186351)

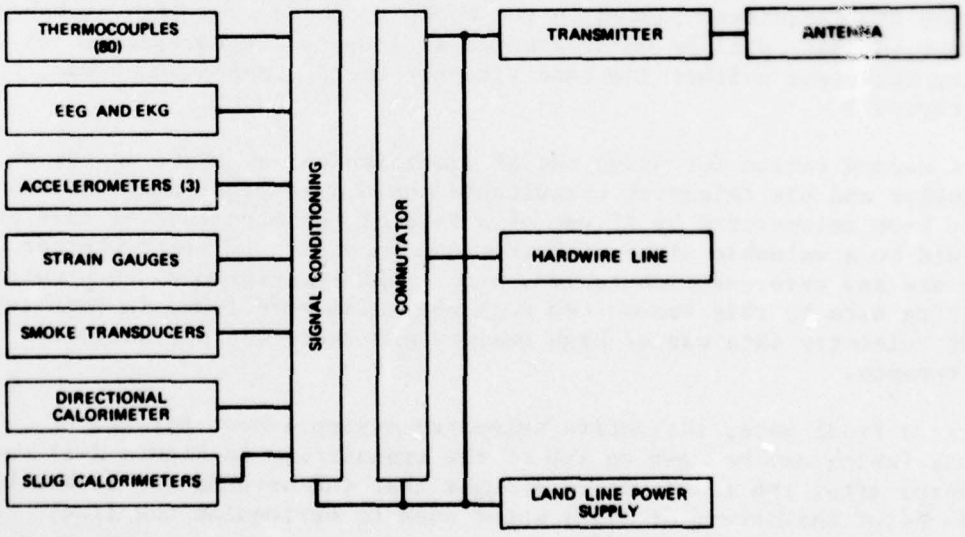

FIGURE J-2. Block Diagram of Telemetry System.

Appendix K

MOTION PICTURE COVERAGE

Appendix K
MOTION PICTURE COVERAGE

As would be expected in a study of this kind where much activity that is highly visual is taking place, one of the most valuable kinds of data is motion picture coverage of the event. For this test ten color motion picture cameras were used. They were deployed as follows:

In cockpit: One camera covered the mouse on treadmill, the generation of smoke, and the occurrence of flames.

In tunnel: Three cameras in all; one covered mouse on treadmill, one covered the gas sampling apparatus, and one covered an overall view of the instrumentation including the instrumented rat.

Outside: Six cameras in all; five were set up to cover various fixed views of the fire as part of the data for the test and one was used to record selected views for use in the color and sound movie that was later produced.[1]

Together these cameras provided visual data on the fire as well as selective footage for the movie mentioned above, which supplements this report in documenting this test.

Appendix L

FIREFIGHTING

Appendix L
FIREFIGHTING

The firefighting equipment that was on hand for extinguishing the fuel fire under the A-4 consisted of two MB-5 Navy Aircraft Fire Fighting and Rescue Vehicles that had one turret each and one MB-1 Navy Aircraft Fire Fighting and Rescue Vehicle that had two turrets. Each of the four turrets had a capacity of 250 gallons (937.5 liters) per minute of "light water" (aqueous film-forming foam). The firefighting crews stood by until the test director signaled them to put the fire out. Then they moved the three trucks in to attack the fire. One single-turret truck approached the aft of the A-4 from the port side; the two-turret truck approached the aft of the plane from the starboard side; and the other single-turret truck approached on the starboard beam of the A-4 (see Figure L-1). The combination of the wind and the terrain forced the firemen to approach the fire crosswind instead of upwind, as would have been most desirable. Nevertheless, they extinguished the blaze in 16 seconds. Figure L-2 shows the test site just after the fire was extinguished.

The two main items in the firefighting crew's plan of attack were to try to protect human life (in this case test animals representing human life) by playing light water on both sides of the cockpit area to cool it and to put the fire out as soon as possible to allow the maximum amount of test data to be retrieved from the burned aircraft. Both of these aims were achieved. Though it was expected that both the instrumented rat and the mouse on the treadmill in the cockpit would be dead by the time the fire was extinguished, the rat was still alive when removed from the cockpit. A further indication that the effort to cool the cockpit with the light water was successful is given by the records of some of the thermocouples discussed in Appendix E. The firemen began fighting the fire at 224 seconds after ignition. Three thermocouples that were on or near the canopy showed distinct temperature drops at about 225 seconds, as is indicated by Figures E-39, E-40, and E-43. Another thermocouple that was inside the cockpit behind the pilot's helmet (Figure E-35) showed a temperature drop at about 236 seconds. Also the thermocouple record in Figure E-43 shows a second drop at about 238 seconds following a buildup after the first drop.

The fire was extinguished soon enough to preserve the aircraft for post-test inspection of the damage. Damage information gained from post-test study is discussed in Appendix M.

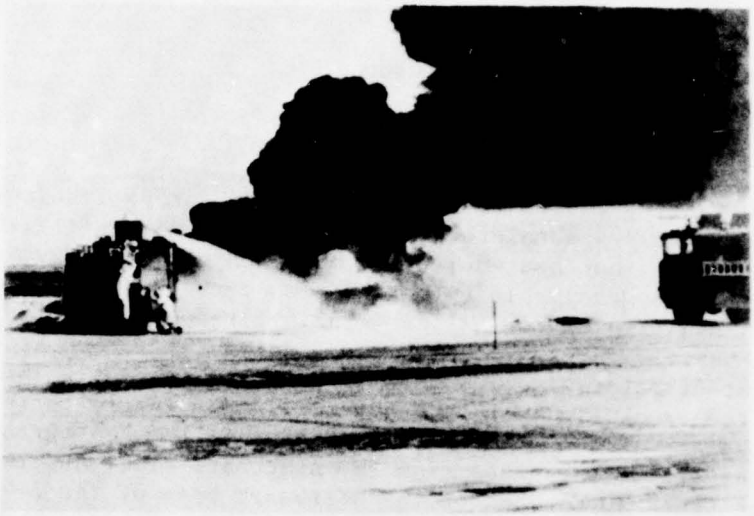

FIGURE L-1. Two of the Three Trucks Attacking A-4 Fire.
(Neg. LHL 192309)

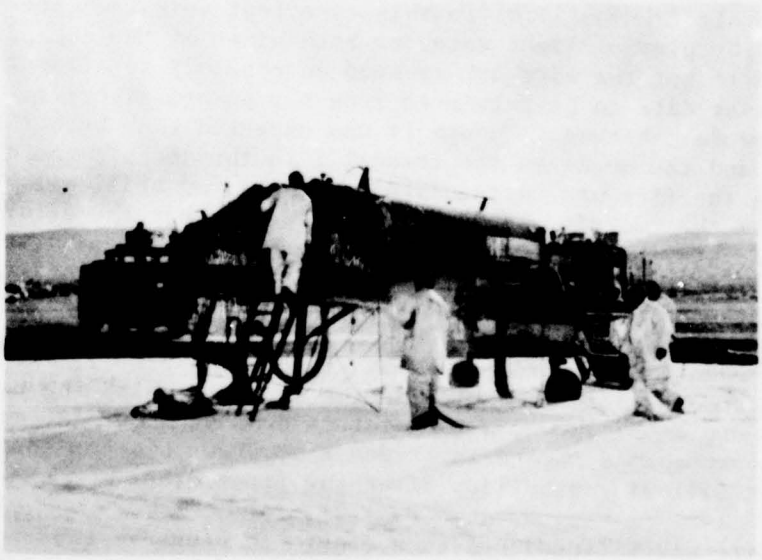

FIGURE L-2. View of Test Site Just After Fire Was Extinguished.
(Neg. LHL 187347)

The firefighting aspect of this burn test also served a secondary purpose. It provided a good live drill in which the firefighters could evaluate their techniques and look for areas of possible improvement. The movie coverage made it especially valuable for this purpose. By studying the film clips later the firemen were able to both verify their first-hand impressions and view the operation from a perspective not available to them while they were fighting the fire.

Some of the firemen's observations on their techniques are as follows. No entry into the cockpit was included in their preliminary plan. However, when they discovered that the rat in the cockpit showed signs of life, they were urged by the test personnel to use the aircraft boarding ladder to enter the cockpit after the fire was extinguished. Some time was lost in inserting the ladder guide pins into the holes provided in the fuselage. It would have been quicker and better to have used the rescue ladder from one of the fire trucks, leaning it against the fuselage.

Because the direction of the wind and the surrounding terrain made it necessary to approach the fire crosswind, the trucks had to stand off at a greater distance than they would have had they been able to approach upwind. Their nozzles had only two settings: fog and full stream. Although the optimal dispersal of the light water onto this fire would have been a fog, the stream had to be used to give the light water the necessary force to reach the cockpit and to maintain the desired direction in the wind. The results of this test and other similar experience have indicated the need for a nozzle continuously adjustable from a stream to a fog. The movie coverage of this test provided good documentation of this need. Subsequent tests were made of various light water dispersal patterns against fires of this type. The consequence was that a contract has already been negotiated to provide for a turret design that will permit a continuous adjustment from full stream to fog. The next generation of NWC firefighting and rescue vehicles will incorporate those turrets.

A total of about 350 gallons (1,300 liters) of light water was used to extinguish this fire, which is well within the capacity that is available to fight such fires on the flight deck of the large carriers.

Appendix M

STRUCTURAL ANALYSIS

Appendix M
STRUCTURAL ANALYSIS

Structural failure of the A-4 cockpit is indicated by the photos shown in Figures M-1, M-2, and M-3 that were taken after the test. These figures can be compared to Figure A-4 which illustrates the test item before the fire. The damage was caused by a combination of degradation of the material because of heat and firefighting. A listing of the significant events measured by various transducers is given in Table 1 to aid in creating an image of how the structural failure occurred.

Figures M-1 and M-2 show the port and starboard sides of the A-4 after the fire test. Significant structural failure is evident for the canopy (polymethyl methacrylate), the nose cone (fiberglass), and the sheet metal (aluminum) on both sides and under the floorboard station housing the electrical and hydraulic lines which control the aircraft, and the wheel well door. Aluminum skin not melted is buckled. Note that the fuel tank aft of the cockpit, full of JP-5 jet fuel, maintained its integrity and did not leak.

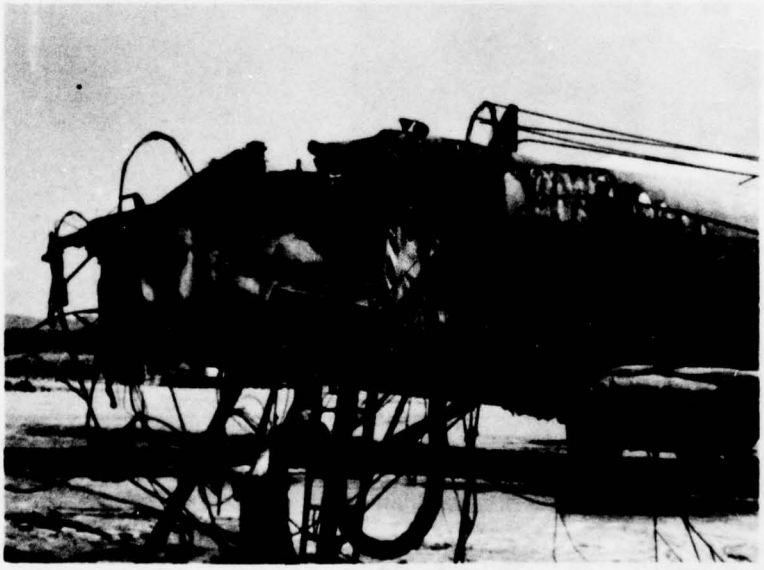

FIGURE M-1. Port Side of A-4 Aircraft After Fire Test. (Compare with Figure A-3 before fire.) (Neg. LHL 187322)

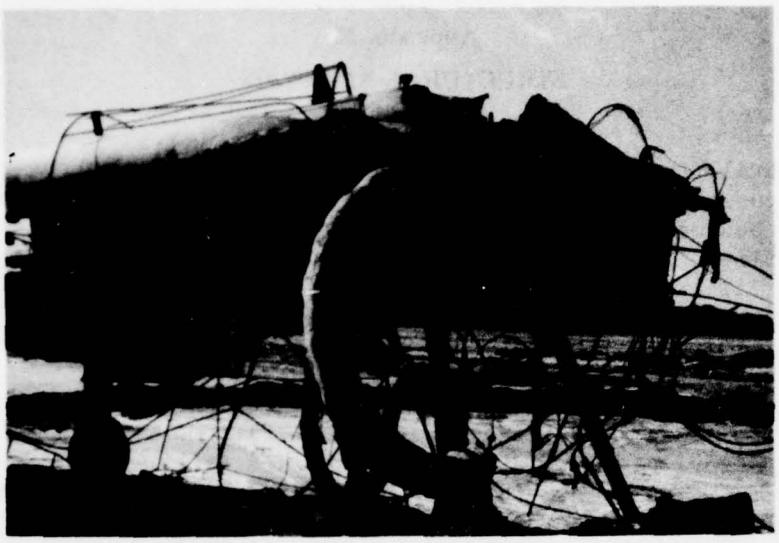

FIGURE M-2. Starboard Side of A-4 Aircraft After Fire Test. (Neg. LHL 187323)

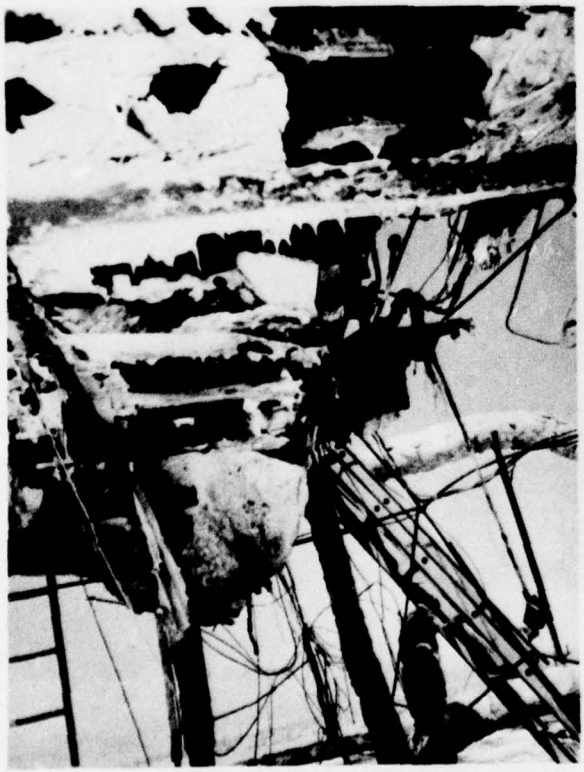

FIGURE M-3. View From Beneath A-4 Aircraft Looking Forward After Fire Test. (Neg. LHL 187345)

A combination of buckling and melting was manifested in large skin-to-stringer separation at the juncture of the floorboard and forward bulkhead. These separations could admit flames with a cross-sectional area of about 36 in^2 (232 cm^2) on either side. No other structural failures (fractures) were found on either of the two sides, the forward or aft bulkheads, or on the top (other than the canopy).

Figure M-3 is a view from beneath the aircraft from the wing root looking forward. As is evident, the understructure of the aircraft was severely melted. Flames had direct access to the fuselage rubber fuel bladder, the engine bay, the gun bays, and all hydraulic and electrical lines exposed below the cockpit floor. The aluminum flooring directly below the cockpit seat melted away with only the cross ribbing remaining. Had a parachute been included in its place under the seat, it would probably have burned with possible toxic gas and smoke generation. Of significance is the fact that the aircraft remained on its landing gear and did not collapse. Note also that the tires, immersed some 7 inches (18 cm) in water and fuel, did not blow out.

Figures M-4 and M-5 are views of the fractured canopy. The failure of the canopy is characterized by both melting and rectangular checking, apparently because of excessive thermal stresses and biaxial loading from the supports. Note the fractured funnel telemetry antenna glass enclosure. It is not known how much the light water used in firefighting contributed to the mode of failure.

Figure M-6 illustrates that the instrument panel and side panels were not significantly damaged in the fire. Carbon residue was observed on the outside of the smoke transducer and under the horizontal surfaces. Figure M-7 illustrates the significant burn damage to the pilot's helmet, which housed the instrumented rat.

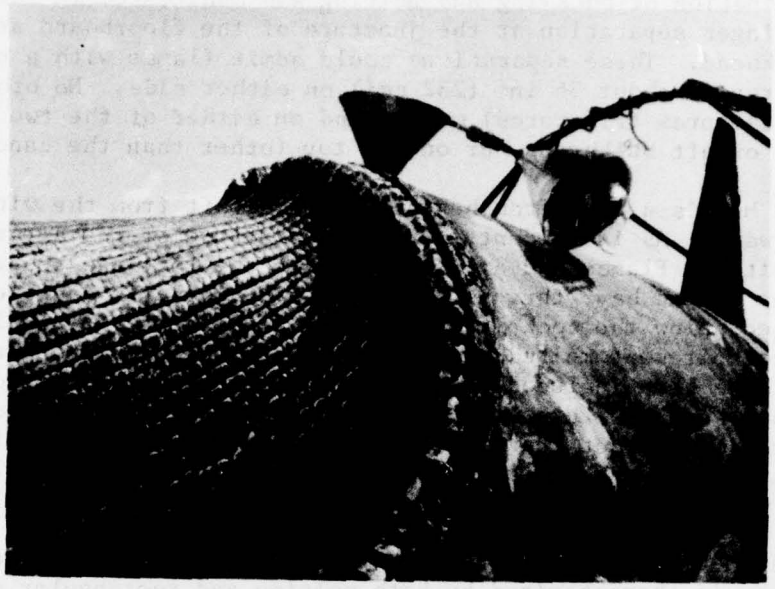

FIGURE M-4. Post-Test View of Canopy From Port Side. Note broken TM antenna on top of A-4. (Neg. LHL 187329)

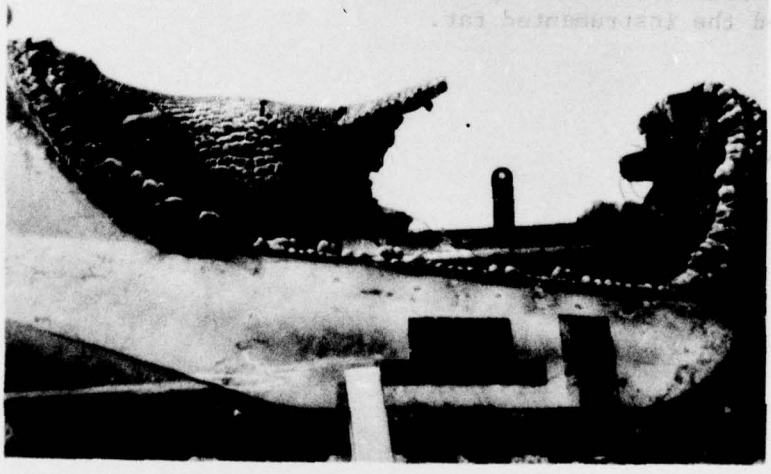

FIGURE M-5. Post-Test View of Canopy From Starboard Side. (Neg. LHL 187331)

FIGURE M-6. Instrument and Cockpit Side Panels After Fire Test. (Neg. LHL 187341)

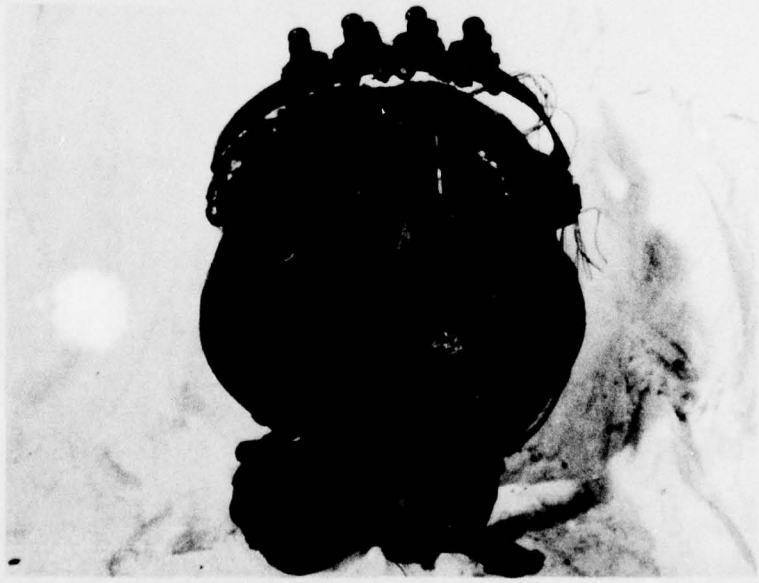

FIGURE M-7. Pilot's Helmet After Fire Test. (Neg. LHL 187324)

Appendix N

JPL THERMAL PROTECTION MATERIALS EXPERIMENT

Appendix N

JPL THERMAL PROTECTION MATERIALS EXPERIMENT

SUMMARY

Two test panels of candidate materials for aircraft cockpit fire protection were evaluated in the A-4 pool fire test by being attached to the bottom exterior of the fuselage center sections. One panel was a 12 by 12 inch (30.5 by 30.5 cm) sheet of aluminum coated with a JPL-developed fire-retardant-filled polyester. The other panel was a sheet of Palusol Fireboard which was a composite of fiberglass, wire mesh, and hydrated sodium silicate. During the pool fire test exposure, the coated aluminum panel remained attached to the fuselage and retained about 50% of the protective coating. The Palusol Fireboard, which swelled and softened during heating, fell to the ground, but was not destroyed by the fire. In summary, both materials withstood the heat of the pool fire, and are considered worthy of further evaluation under more appropriate test conditions.

THERMAL PROTECTION MATERIALS DESCRIPTION

When typical aluminum aircraft structure is exposed to a fuel pool fire, one of the first materials destroyed is the thin unsupported aluminum skin. Areas of skin backed by stringers and ribs remain intact due to the heat sink effect of the back-up material. One approach to delaying panel burn-through in critical skin areas is to provide a heat sink coating on the back side.

One candidate material selected for this test application was a fire-retardant-filled polyester applied to a 0.032-inch (0.8-mm) aluminum test panel as a 0.13-inch (3.3-mm) thick coating. The coating polyester was filled with 60% by weight sodium silicate ($Na_2SiO_3 \cdot 5H_2O$). The other material selected for test was a fire-resistant barrier material, Palusol Fireboard (BASF Wyandotte Corporation) (0.07 inch (1.8 mm) thick), which is a composite of mainly hydrated sodium silicate with small amounts of organics plus fiberglass and wire mesh. Both materials have been tested by JPL in an NBS Smoke Density Chamber for fire resistance and smoke generation at 2.5 W/cm^2 incident radiation. The results are shown in Figure N-1. Unfilled polyester is compared with filled polyester using three different candidate fillers at 65% by weight of filler. The candidate fillers shown in Figure N-1 were potassium carbonate ($KHCO_3$), trisodium phosphate (TSP) ($Na_3PO_4 \cdot 12H_2O$), and sodium silicate ($Na_2SiO_3 \cdot 5H_2O$).

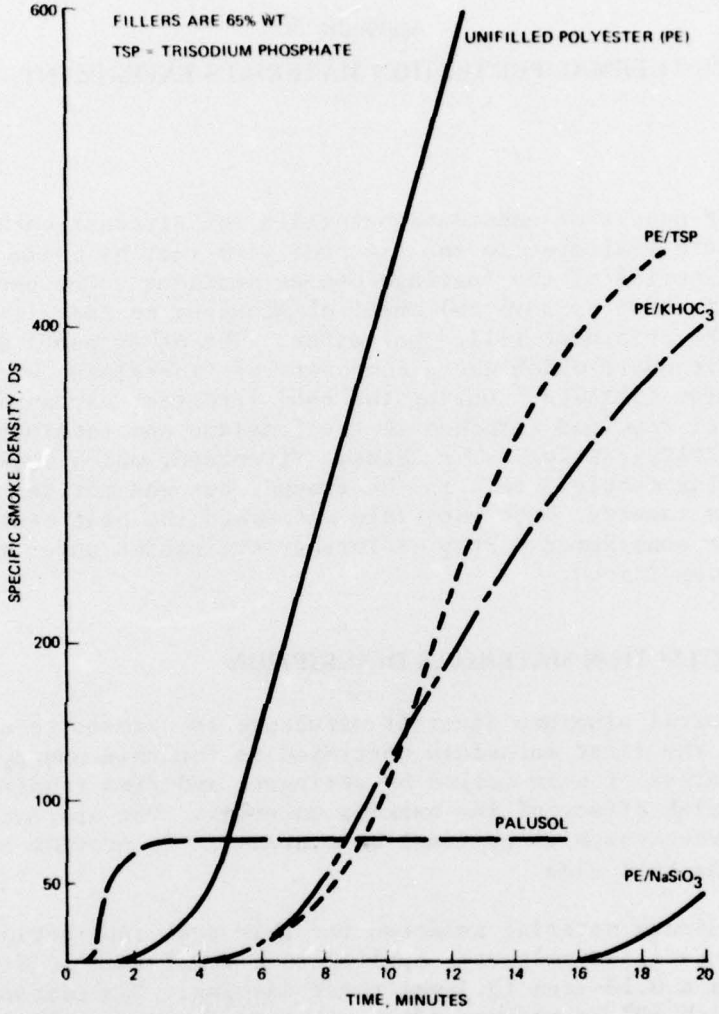

FIGURE N-1. Specific Smoke Density for "Palusol" and Polyester (Filled and Unfilled) for Non-Flaming Exposure in NBS Smoke Chamber.

The smoking tendency of Palusol, also shown in Figure N-1, shows a rapid evolution of smoke for a short time with the smoke density unchanged after the first 2 minutes. This initial smoke was attributed to the degradation of the thin epoxy film which has been applied to the Palusol sheet for moisture protection.

The outstanding candidate material, as indicated by these results, was the sodium-silicate-filled polyester. No smoke was evolved for the first 15 minutes of exposure. During this time the surface bubbled as water evolved and left a protective glassy crust on the specimen surface.

TEST PANEL INSTALLATION

Two 12- by 12-inch (305-mm) test panels of the candidate thermal protection materials were installed on the A-4 aircraft. One panel of 0.07-inch (1.8-mm) Palusol Fireboard and one panel of (0.032-inch or 0.8-mm) 2024-T3 aluminum sheet with 0.13-inch (3.3-mm) coating of fire-retardant-filled polyester (60% wt. $Na_2SiO_3 \cdot 5H_2O$) were evaluated. The panels were attached with eight screws to the exterior skin of the aircraft facing down on the bottom of the fuselage between the two main landing gear wells (Figure N-2). The filled polyester coating on the aluminum sheet was on the flame-exposed surface of the panel. Thermocouples and a surface calorimeter were located between the two panels, but data from these locations was lost due to instrumentation problems.

In application, the Palusol would be supported behind or between other materials and would serve as a fire barrier and insulating material, and would not be expected to perform a structural role. The material is designed to soften and expand on heating to seal cracks and prevent flame penetration. In this test, because of very limited time and resources, the panel was attached directly to the exterior of the fuselage to be exposed to direct flame from the burning pool.

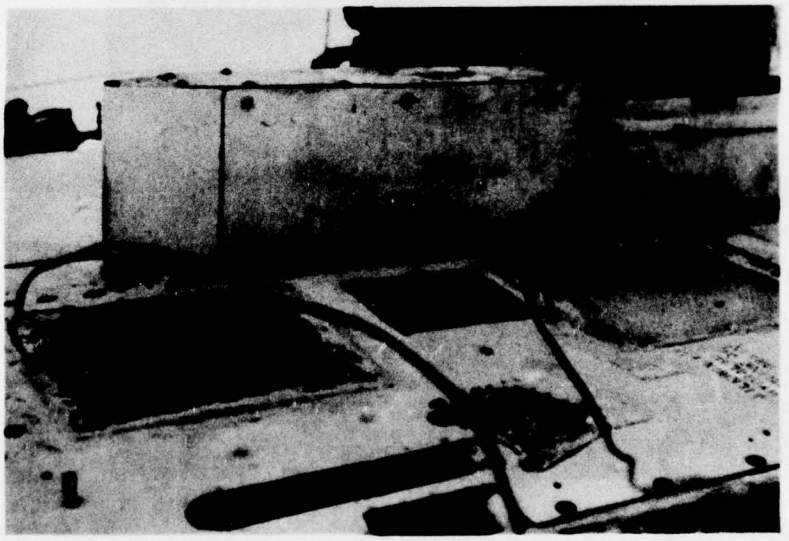

FIGURE N-2. Location of Thermal Protection Test Panels Supplied by JPL on Bottom of A-4 Fuselage Between Main Landing Gear Wells. (Neg. LHL 193173)

TEST RESULTS

The course of the pool fire development and its extinguishment are described in the body of this report. Following the fire, the two panels were examined in place and their condition recorded photographically (Figure N-3).

The aluminum panel was still attached to the bottom skin of the fuselage. The edges of the panel had melted, but about 50% of the protective coating remained in place. Much of the adjacent aircraft skin was melted away including all of the adjacent bomb rack fairing.

The Palusol panel softened and dropped from the aircraft to the ground at some time during the fire. The surface of the test panel was distorted and scorched, but still intact. The area of aluminum skin which was behind the Palusol panel was melted, but to a lesser degree than the surrounding skin areas as indicated by the relative condition of the fuselage insulation batting in these areas.

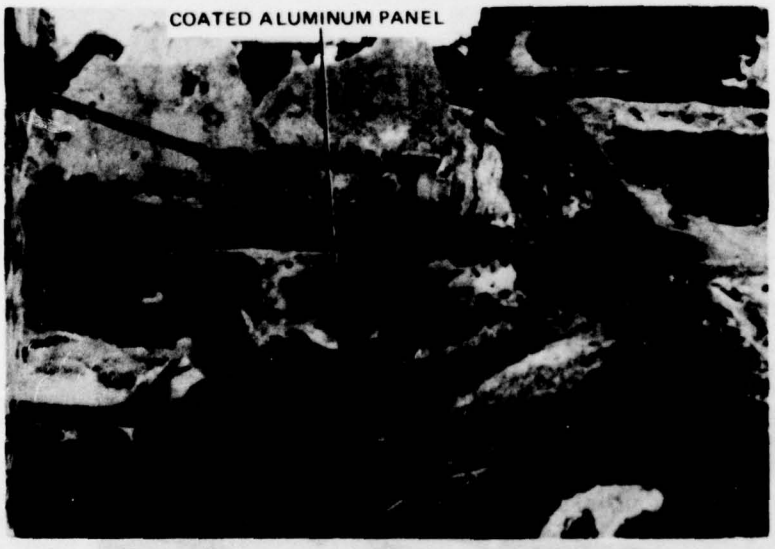

FIGURE N-3. Post-Fire Condition of JPL-Coated Aluminum Thermal Protection Test Panel After 4 Minutes of Fuel Pool Fire Exposure. (Neg. LHL 193172)

CONCLUSIONS

1. The candidate materials withstood the thermal environment of the pool fire in that they were not consumed by the flames.

2. In further testing or application of these materials, the structural and thermal barrier requirements of the components of interest would have to be considered simultaneously.

3. The low smoke- and fire-resistant characteristics of the hydrated silicate materials make them promising candidates for materials for use within the occupied cockpit area.

REFERENCES

1. Naval Weapons Center. *Aircraft Fire Survivability.* China Lake, Calif., NWC, 1976. (Technical motion picture 413, 10-1/2 min., color, sound.)

2. Naval Weapons Center. *Shrike and Sparrow Missile Baseline Cookoff Tests*, by Anthony San Miguel and P. McQuaide. China Lake, Calif., NWC, October 1974. (NWC TP 5672, publication UNCLASSIFIED.)

3. Naval Air Systems Command. *Study of Technology Requirements for the Containment of Shipboard Aviation Fire Hazard.* Washington, D.C., NAVAIR, 1972. (Exotech Report TRSR-70-15, also available from DDC as AD 884 422, publication UNCLASSIFIED.)

4. Anthony San Miguel. "Rocket Motor Design Considerations to Meet Fast Cookoff Requirements," in *JANAF Operational Serviceability and Structures and Mechanical Behavior Working Groups Combined Annual Meeting.* Silver Spring, Md., Johns Hopkins University, Applied Physics Laboratory, May 1975. Pp. 399-415. (CPIA publication 264, publication UNCLASSIFIED.)

5. G. Tichner and R. Bendler. "Thermo Man Tester," *Instruments and Controls Systems,* June 1974. Pp. 39-42.

6. Naval Ordnance Laboratory, White Oak. *A Mobile Field Laboratory for Fires of Opportunity,* by R. S. Alger and J. R. Nichols. Silver Spring, Md., NOL, 10 October 1973. P. 118. (Report No. NOLTR-73-87, publication UNCLASSIFIED.)

7. H. Grober, S. Erk, and U. Grigull. *Fundamentals of Heat Transfer.* New York, McGraw-Hill, 1961. P. 5.

8. D. J. Gaines. "Selecting Unsteady Heat Flux Sensors," *Instruments and Controls Systems,* May 1972. Pp. 80-83.

9. K. Buettner. "Effects of Extreme Heat on Man," *Amer. Med. Ass. J.,* 28 October 1950, pp. 732-38.

10. Army Air Mobility Research and Development Laboratory. *Crash Survival Design Guide.* Fort Eustis, Va., October 1971. (Tech Report 71-22, p. 373, AD 733 358, publication UNCLASSIFIED.)

11. G. Longelle and C. Verdier. "Gas Sampling and Analysis in Combustion Phenomena," AGARD Vugraph No. 168, North Atlantic Treaty Organization, Advisory Group for Aerospace Research and Development. Hartford House, London. July 1973. P. 180.

12. S. R. Heller, et al. "Trace Organics by GC/MS," *Environmental Science and Technology*, Vol. 9 (March 1975), p. 210.

13. University of Utah, Flammability Research Center. *The Physiological and Toxicological Aspects of Smoke Produced During the Combustion of Polymeric Materials*, by I. N. Einhorn. Salt Lake City, Utah, UUFRC, July 1974. (Report FRC-UU-38, p. 81, publication UNCLASSIFIED.)

14. J. G. Gourme and P. Bartek. "Theoretical Determination of the Time of Useful Function (TUF) on Exposure to Combustions of Toxic Gases," *Aerospace Med.*, Vol. 40, No. 12 (December 1969).

15. P. Bartek, J. G. Gourme, and H. J. Rostami. "Dynamic Analysis for Time of Useful Function (TUF) Predictions in Toxic Combustive Environments," *Aerospace Med.*, Vol. 41, No. 13 (December 1970), pp. 1392-1395.

16. W. R. Klemm. *Animal Electroencephalography*. New York, Academic Press, 1969, Chap. 1, 2.

17. H. Hirschhorn. *All About Rats*. Neptune, N.J., T.F.H. Publication, 1974. P. 4.

18. J. J. Brenneman and D. A. Heine. "The Cleveland Aircraft Fire Tests," *Fire Technology*, Vol. 4, No. 1 (February 1968), pp. 5-16.

19. D. A. Kourtides, J. A. Parker, and W. J. Gilwee. "Thermochemical Characterization of Aircraft Panel Materials," *J. Fire and Flammability*, Vol. 6 (July 1975), pp. 373-91.

20. Air Force Aero Propulsion Laboratory. *A Smoke Detection System for Manned Spacecraft Applications*, by T. M. Trumble. Wright-Patterson Air Force Base, Ohio, AFAPL, June 1975. (Technical Report AFAPL-TR-74-97, publication UNCLASSIFIED.)

21. Federal Aviation Administration. *Smoke Emissions from Burning Cabin Materials and the Effect on Visibility in Wide Bodied Jet Transports*, by E. L. Lopez. Washington, D.C., FAA, March 1975. (Report FAA-NA-73-155, publication UNCLASSIFIED.)

22. American Society for Testing Materials. *Method for Measuring Smoke from Burning Materials*, by D. Gross, J. J. Loftus, and A. F. Robertson. Philadelphia, Pa., ASTM, 1967. (ASTM STP 422, pp. 166-204, publication UNCLASSIFIED.)

23. National Bureau of Standards. *Smoke and Gases Produced by Burning Aircraft Interior Materials*, by D. Gross, et al. Washington, D.C., NBS. (Report No. NA-68-36, publication UNCLASSIFIED.)

24. National Bureau of Standards. *Interlaboratory Evaluation of Smoke Density Chamber*, by T. G. Lee. Washington, D.C., NBS, December 1971. (NBS Technical Note 708, p. 80, publication UNCLASSIFIED.)

25. A. F. Robertson. "Two Smoke Test Methods--A Comparison of Data," *Fire Technology* (November 1974), pp. 282-86.

26. C. L. Tien, et al. "Attenuation of Visible Radiation by Carbon Smoke," *Combustion Science and Technology*, Vol. 6 (1972), pp. 55-59.

27. National Bureau of Standards. *The Smoke Density Chamber Method for Evaluating the Potential Smoke Generation of Building Materials*, by T. G. Leè. Washington, D.C., NBS, January 1973. (NBS Technical Note 757, publication UNCLASSIFIED.)

28. C. J. Hilado. *Flammability Handbook for Plastics*. Westport, Conn., Technomic Publishing Company, 1974. Pp. 60-64.

INITIAL DISTRIBUTION

10 Naval Air Systems Command
- AIR-03PAF, CDR R. Gibson (1)
- AIR-03P3, R. H. Krida (1)
- AIR-320A, T. F. Kerns (1)
- AIR-320B, Dr. A. R. Somoroff (1)
- AIR-5204, CAPT W. Rivers (1)
- AIR-52932, Charles Bersch (1)
- AIR-5311, CDR M. J. Danrato (1)
- AIR-5323, M. Wittman (1)
- AIR-954 (2)

1 Chief of Naval Material (MAT-00F2, R. L. Darwin)

4 Naval Sea Systems Command
- SEA-0351, C. H. Pohler (1)
- SEA-065161, G. Mustin (1)
- SEA-09G32 (2)

1 Naval Facilities Engineering Command (NFAC-04D1, H. T. Anderson)

1 Naval Air Development Center, Johnsville (Code 303, Dr. E. McQuillen)

1 Naval Medical Research Institute, Bethesda (CDR L. J. Jenkins)

2 Naval Research Laboratory
- Code 5180, H. W. Carhart (1)
- Code 6183, Dr. Fred Williams (1)

1 Naval Ship Engineering Center, Hyattsville (NSEC-621, A. Marchland)

1 Naval Ship Research & Development Center, Bethesda
- Code 173.1, Richard H. Chin

1 Pacific Missile Test Center, Pt. Mugu (Code 704, C. Valley)

1 Army Mobility Research & Development Laboratory, Eustis Directorate, Ft. Eustis, Va. (SAVDL-EV-PP)

12 Defense Documentation Center

4 Federal Aviation Administration, Systems & Development Service, Washington, D. C.
- T. G. Horeff (1)
- W. McGuire (1)
- Robert McGuire (1)
- H. Branting (1)

1 National Academy of Sciences, National Research Council (Materials Advisory Board), Washington, D.C. (Dr. Robert Shane)

4 National Aeronautics & Space Administration, Washington, D.C.
- Dr. B. C. Achhammer, Head Material Sciences (1)
- John Enders, Chief, Aircraft Operations Systems Div. (1)
- Dr. Thora Halstead (1)
- W. A. McGowan (1)

1 Langley Research Center, National Aeronautics & Space Adminstration, Hampton, Va. (Albert Hall)

1 Lewis Space Center, National Aeronautics & Space Administration, St. Louis, Mo. (S. Weiss)

1 Lyndon B. Johnson Space Center, National Aeronautics & Space Administration, Houston, Texas (R. W. Bricker)
1 National Bureau of Standards, Gaithersburg, Md.
1 Jet Propulsion Laboratory, (CIT) Pasadena, Ca. (Dr. Robert F. Landel)
1 McDonnell Douglas Corporation, Long Beach, Ca. (Pete Deboby)
2 National Aviation Facilities Experimental Center, Atlantic City, N.J.
R. Russell (1)
J. C. Spurgeon (1)
2 Stanford Research Institute, Menlo Park, Ca.
Dr. Stan Martin (1)
R. Algers (1)
1 University of San Francisco, San Francisco, Ca. (Prof. Carlos J. Hilado)
1 University of Utah, Flammability Research Center, Salt Lake City, Utah (Dr. I. N. Einhorn)